Semi-quantitative immunohistochemical exploration of lung tissue remodelling in idiopathic pulmonary fibrosis

Nicola Jane Lomas

Master of Philosophy in Biomedical Engineering

March 2013

Keele University

Abstract

Aim: This thesis explores the complex cellular and biological interrelationships involved in Idiopathic Pulmonary Fibrosis (IPF) lung tissue remodelling using immunohistochemical analysis. **Methods and results:** 21 IPF and 19 control lung tissues were examined for expression and localisation of key pathogenic markers implicated in Epithelial Mesenchymal Transition (EMT), proliferation, and cell cycle within alveolar type II cells (ATII cells) and fibroblastic foci. E-cadherin was expressed in IPF and control ATII cells (mean expression score >75%). In IPF, mean expression of N-cadherin was scanty (mean expression score <10%): however 4 cases demonstrated augmented expression in ATII cells correlating to histological disease status (as reflected by number of fibroblastic foci) (Pearson correlation score 0.557). Transforming growth factor-β (TGF-β) protein expression was significantly increased in IPF ATII cells with variable expression within fibroblastic foci. The proliferation marker Ki-67 was observed within hyperplastic ATII cells but not in cells overlying foci. IPF ATII cells demonstrated variable Surfactant protein-C (SP-C). Hyperplastic ATII cells overlying fibroblastic foci expressed Cyclin D1, p53, $p21^{WAF1}$, SOCS3 and $p16^{INK4A}$. **Conclusions:** There is inconclusive evidence to support the role of EMT in the pathogenesis of IPF. Histological analysis suggests TGF-β-stimulated myofibroblasts initiate a contractile response within established fibroblastic foci leading to mechanical stress on the surrounding alveolar epithelium. My data provides evidence of potential TGF-β-mediated contact inhibition of ATII cells overlying fibroblastic foci, leading to prolonged cell stasis and subsequent senescence. This ATII cell senescence may lead to a reduction in the lung tissue remodelling capacity of IPF epithelium within the micro-niche areas surrounding fibroblastic foci. Information derived from this study may be used to develop targeted interventions aimed

at reducing the number of fibroblastic foci and therefore improving ATII cell regeneration of the alveolar epithelium. Marker expression correlation with histological disease activity may emerge as future prognostic indicators for IPF.

Contents

Chapter 2. General Methodology

Index of tables and figures

Chapter 4 Exploration of cell cycle activity and localisation in IPF lung tissue

Abbreviations list

ADSCs	Adipose-derived stem cells
α-SMA	α-smooth muscle actin
(PTEN)-Akt	Phosphatase and tensin homolog-Akt
AIP	Acute interstitial pneumonia
ANAs	Anti-nuclear antibodies
ATS	American Thoracic Society
ATI	Alveolar type I cells/type I pneumocytes
ATII	Alveolar type II cells/type II pneumocytes
BAL	Bronchoalveolar lavage
BCC	Basal cell carcinoma
BMMSC	Bone marrow mesenchymal stem cells
BOOP	Bronchiolitis obliterans organizing pneumonia
BTS	British Thoracic Society
Cdks	Cyclin-dependant kinases
cDNA	Complimentary DNA
CIS	Cytokine inducible SH2
CMV	Cytomegalovirus
COP	Cryptogenic organising pneumonia
CT	Computed tomography
CTD	Connective tissue disease
CTGF	Connective tissue growth factor

DAB	3,3'-diaminobenzidine
DAD	Diffuse aveolar damage
DcR1	Decoy receptor 1
DIP	Desquamative interstitial pneumonia
DL_{CO}	Diffusing capacity of carbon dioxide
DNA	Deoxyribonucleic acid
DR	Death receptor
E-boxes	Enhancer boxes
EBV	Epstein Barr virus
ECM	Extracellular matrix
EDTA	Ethylenediaminetetraacetic acid
EEA-1	Early endosome antigen-1
EMT	Epithelial-mesenchymal transition
EndEMT	Endothelial-mesenchymal transition
ERS	European Respiratory Society
ET-1	Endothelin-1
FCV	Forced vital capacity
GLUT-1	Glucose transport-1 protein
GOR	Gastro-oesophageal reflux
H&E	Haematoxylin and Eosin
HHV-8	Herpes Virus 8
HPV	Human papilloma virus
HRCT	High resolution computed tomography

HTA	Human Tissue Act
IFN	Interferon
IGF	Insulin-like growth factor
IHC	Immunohistochemistry
IIP	Idiopathic interstitial pneumonia
IL-8	Interleukin 8
ILD	Interstitial lung disease
IMS	Industrial methylated spirit
IPF	Idiopathic pulmonary fibrosis
JAK	Janus kinase
JPEG	Joint Photographic experts group
LIP	Lymphocytic interstitial pneumonia
LSPR	Localised surface plasma resonance
MAPK	Mitogen-activated protein kinse
MICA	Major Histocompatibility Complex class 1
MMP	Matrix metalloproteinase
MSCs	Mesenchymal stem cells
MTOR	Target of Rapomycin
NAC	N-acetylcystein
NICE	National Institute for Health and Clinical Excellence
NSIP	Non-specific interstitial pneumonia
OCT3/4	Octomer-binding transcription factor 3-4
P13K	Phosphoinositide 3-kinase

PCR	Polymerase chain reaction
PDGF	Platelet-derived growth factor
PGE2	Prostogalndin E2
RB-ILD	Respiratory bronchiolitis associated interstitial lung disease
RNA	Ribonucleic acid
RT-PCR	Reverse transcriptase polymerase chain reaction
SD	Standard deviation
Sen-β-Gal	Senescence-associated β-galatosidase
SNOMED	Systemized nomenclature of medicine
SOCS	Suppressor of cytokine signalling
SP-B	Surfactant protein B
SP-C	Surfactant protein C
STATs	Signal transducers and acivators of transcription
Tc	Technetium
TGF-β	Transforming growth factor beta
TGF-βR	Transforming growth factor beta receptor
Th	T helper cell
TIMP	Tissue inhibitors of metalloproteinases
TNF-α	Tumour necrosis factor-α
TRAIL	Tumour necrosis factor-related apoptosis-inducing ligand
Tris	2-Amino-2-hydroxymethyl-propane-1,3-diol
TTF-1	Thyroid transcription factor-1
TYK2	Tyrosine kinase-2

UIP	Ususal interstitial pneumonia
VATS	Video-assisted thorascopic surgery
VIP	Very Intense purple

Achievements

Publications

1) Idiopathic pulmonary fibrosis: immunohistochemical analysis provides fresh insights into lung tissue remodelling with implications for novel prognostic markers.

N. J. Lomas, K. L. Watts, K. M. Akram, N. R. Forsyth, M. A. Spiteri. International Journal of Clinical and Experimental Pathology (May 2012)

2) Clara cells inhibit alveolar epithelial wound repair *via* TRAIL-dependent apoptosis
K. M. Akram, **N. J. Lomas**, M. A. Spiteri, N. R. Forsyth. European Respiratory Journal (July 2012)

Conference presentations

1) **2011 European Respiratory Society Lung Science Conference, Estoril, Portugal. *ERS bursary awarded.***

Histological markers of epithelial-mesenchymal transition in IdiopathicPulmonary Fibrosis provide evidence of an alternative repair process.

N. J. Lomas, K. M. Akram, N. R. Forsyth, M. A. Spiteri.

2) **European Respiratory Society Congress 2011, Amsterdam.**

Histological markers of epithelial-mesenchymal transition in IdiopathicPulmonary Fibrosis provide evidence of an alternative repair process.

N. J. Lomas, K. M. Akram, N. R. Forsyth, M. A. Spiteri.

Awards

Institute of Biomedical Science Research Grant Award 2009, £4390.00

Acknowledgements

This research project would not have been possible without the support of many people. I wish to express my deepest gratitude to my supervisor, Professor Monica Spiteri, who offered invaluable assistance, support and guidance. Gratitude is also due to Dr Keira Watts, Dr Daniel Gey van Pittius, Dr Nicholas Forsyth, Professor Anthony Fryer and Dr Khondoker Akram, without whose knowledge and assistance this study wound not have been successful.

Special thanks also to Deborah Latham at the University Hospital of North Staffordshire for initial training in immunohistochemistry and providing access to laboratory equipment. My warmest regards are for the hard working histology staff at UHNS for their continued support and understanding that has enabled me to undertake this study during my employment within the department.

I would also like to convey thanks to Keele University and the Institute of Biomedical Science for providing the financial means to undertake this study. Thanks also go to the support staff from the Institute of Science and Technology in Medicine for assistance in the ordering of reagents, administration and clerical support (Lisa, Paula, Ann and Jeanette).

Finally I wish to express my love and gratitude to my family and partner Will for their understanding and endless support through the duration of my studies.

This thesis is dedicated to the memory of May Lomas

Chapter 1

General Introduction

1.1. Idiopathic pulmonary fibrosis

1.1.1 Definition and classification

Idiopathic pulmonary fibrosis (IPF) is a specific form of Idiopathic Interstitial Pneumonia (IIP) where the alveoli and the interstitium become damaged and scarred by as yet unidentified micro-insult/s. The main symptoms of the condition are progressive shortness of breath and a persistent cough. It is vitally important to distinguish IPF from other IIPs in order to provide an accurate prognosis and treatment plan for patients suffering from this devastating and ultimately fatal condition. Other IIP's, such as cryptogenic organising pneumonia, respond well to treatment with corticosteroids and have a greatly improved prognosis compared to those individuals with a diagnosis of IPF (Wells *et al*, 2008). A summary of the processes involved in diagnosing IIPs is seen in Figure 1.1.

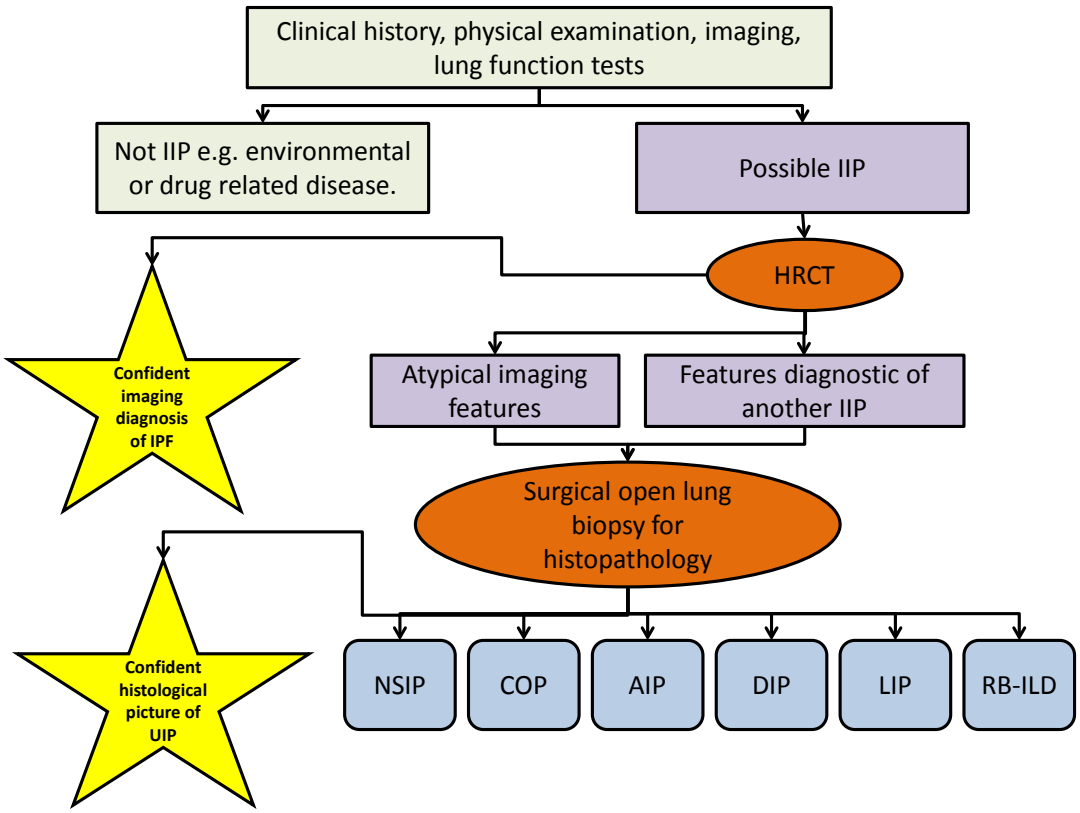

Figure 1.1 Diagnostic pathways for diagnosis of IIP. HRCT; high resolution computed tomography, NSIP; non-specific interstitial pneumonia, COP; cryptogenic organising pneumonia, AIP; acute interstitial pneumonia, DIP; Desquamative interstitial pneumonia, LIP; lymphocytic interstitial pneumonia, RB-ILD; respiratory bronchiolitis associated interstitial lung disease

Until 2001 there was no internationally recognised standard definition of IPF resulting in variable and confusing diagnostic criteria. Meetings of the British Thoracic Society, Thoracic Society of Australia and New Zealand and the Irish Thoracic Society (2008) in 2001 and the American Thoracic Society (ATS) and the European Thoracic Society (ERS) in 2011 (Raghu *et al*, 2011), examined and reviewed scientific studies into the range and overlap of ILDs in order to construct guidelines for improved differential diagnosis and management of ILDs. These collaborations amongst these societies sought to define specific

disease patterns by considering their clinical manifestations, lung tissue pathological features, and radiological characteristics. The diagnosis of IPF now requires the following as recommended by the ARS/ERS (2011);

i) Exclusion of other known causes of ILD such as environmental exposure to toxins, drug toxicity and connective tissue diseases.

ii) The presence of a pattern of usual interstitial pneumonia (UIP) on imaging and/or histology, discussed further in sections 1.1.5 and 1.1.7.

The advent of high-resolution computerized tomography (HRCT), the revised pathologic definition of IPF, and the recognition of the prognostic importance of separating IPF from other ILD patterns have profoundly changed the approach to investigating and managing the ILDs. However Maher *et al* (2007) disagree with this classification and believe that IPF and non-specific interstitial pneumonia (NSIP) should not be classed separately. They argue that a pattern of UIP and NSIP are frequently found affecting the same individuals when lung biopsy samples are taken from different sites in patients with IPF. They report that those patients with IPF on biopsy, but who are indeterminate on HRCT, have a better prognosis than those with UIP and a typical IPF appearance on HRCT. "

It was previously proposed that inflammation within the alveoli played a significant role in the development of IPF and that this inflammation led to the scarring and fibrosis seen histologicaly and radiologicaly (Keogh and Crystal, 1982). This led to the name cryptogenic fibrosing alveolitis. However, treatments which aim to reduce inflammation, such as steroids, have been ineffective in the treatment of this condition (Winterbauer *et al*, 1978, Rudd *et al*, 1981).

Current thinking is that initial damage to the epithelial cells lining the alveoli epithelium leads to an attempt, by the remaining type II pneumocytes (ATII cells), to replace the lost type I and II pneumocytes via hyperplasia and differentiation. However, this healing process becomes out of control leading to thickening and damage to the walls of the alveoli, onset of fibrosis and progressive lung parenchymal remodelling (Harari and Caminati, 2010). Since there is limited evidence to support the role of inflammation in IPF pathogenesis alternative theories include; epithelial mesenchymal transition (EMT), abnormal proliferation and apoptosis of ATII cells and fibroblasts, an imbalance of profibrotic and antifibrotic mediators and abnormal regulation of the coagulation cascade (Maher *et al*, 2007) Figure 1.7.

1.1.2 Epidemiology

There are no large scale studies on the incidence and prevalence of IPF, possibly owing to difficulty in collating information as a standardised nomenclature and diagnostic criteria were not developed until 2001. In the UK, IPF is estimated to have an incidence of 4.6 per 100,000 (Gribbin *et al*, 2006), with an annual increase of 11%. This apparent high figure could be accounted for by improvements in imaging techniques, the histological classification system of interstitial pneumonias and more accurate recording of information. Gribbin *et al* comment in their study using age/sex matched control patients this increase is not due to an aging population or an increased ascertainment of milder cases. Rates have increased progressively over time and tend to be higher in the northern and western regions of the UK (Novaratnam and Flemming 2011). IPF represents a significant health problem worldwide, with incidence rates similar to leukaemia and pancreatic cancer, and mortality rates higher than colorectal, breast and prostate cancer (American Cancer Society, 2012).

The three and five year survival percentages for patients with IPF are 57% and 43% respectively with a median survival time of 3-5 years; patients die on average 7 years prematurely (Gribbin *et al*, 2006). The crude mortality rate is around 180 per 1000 persons-years (Gribbin *et al*, 2006).

1.1.3 Risk factors

Age is the biggest risk factor for IIPs including IPF, with most cases diagnosed in individuals over the age of 60 (Alder *et al*, 2008). However, specific factors leading to the development of IPF in these individuals are yet to be determined. A number of studies have proposed risk factors detailed below;

Occupational/environmental. The incidence of IPF has been found to be higher in men than women and higher in the older population which, in a study by Gribbin *et al* (2006), was not explained by the aging population of the UK. Studies into the risk of smoking and IPF have revealed mixed results. Baumgartner *et al* (2000); Hubbard *et al* (1996) and Iwai *et al* (1994) have all found positive correlations between smoking and IPF. However a further study by Hubbard in 2000 showed only a small increase in risk of IPF for both current and former smokers which did not meet the level of statistical significance. Other risk factors include metal dust exposure (Iwai *et al* 1994; Hubbard *et al* 1996; Scott *et al* 1990, Miyake *et al*, 2005, Taskar *et al*, 2006), wood dust exposure (Hubbard *et al* 1996, Taskar *et al*, 2006), farming cattle or livestock (Scott *et al*, 1990, Taskar *et al*, 2006), stone or sand dust (Hubbard *et al* 1996, Taskar *et al*, 2006), cobalt and hard metals (Zanelli *et al*, 1994; Figueroa *et al*, 1992; Nemery *et al*, 1990). A report by Baumgartner *et al* (2000), found that examining smoking or occupational exposure alone did not produce statistically significant results; however they did find evidence of a possible interaction between smoking and

agricultural work and IPF. It may be that relevant risk factors are difficult to identify because a common environmental factor is an instigator in only a subset of susceptible individuals in the population.

Genetic. In a minority of IPF cases a familial link has been demonstrated suggesting a genetic susceptibility with autosomal dominant characteristics (Nakayama *et al*, 2007). In familial cases the gene was situated on chromosome 14q32 close to the alleles responsible for α-antitrypsin deficiency (Brambilla *et al*, 1999). In most other cases, no genetic link has been found to cause the disease; however, a range of polymorphisms have been related to IPF susceptibility, as well as its severity and progression. One such polymorphism has been reported in the Major Histocompatibility Complex class I chain (MICA). MICA was found to be upregulated in epithelial cells and fibroblasts in IPF patients, whilst the MICA receptor NKG2D was reduced on T cells (Taskar and Coultas, 2008).

Matrix metalloproteinase-1 (MMP-1) is an enzyme involved in the degradation of collagens. It has also been associated with morphogenesis, angiogenesis, tissue repair and metastasis. Ceca *et al* (2008) report that MMP-1 is strongly upregulated in IPF and that a polymorphism in the MMP-1 gene promoter proffers an increased risk for IPF especially in those individuals who smoked.

Telomere shortening has been noted in patients with both familial and sporadic pulmonary fibrosis. Mutations have been discovered in the coding regions of telomerase genes in 15% of patients with familial IPF (Tsakiri *et al*, 2007, Armanios *et al*, 2007, Alder *et al*, 2011). Telomerase is a ribonucleoprotein enzyme that adds specific DNA sequence repeats (TTAGGG) to the 3' end of chromosomes. Mutations were found in the genes encoding the protein component (TERT) and the RNA component (TERC) of the enzyme

(Cronkhite *et al*, 2008). However, telomere shortening, caused by the mutations in TERT or TERC is not specific to IPF. Patients with these mutations can develop other conditions such as NSIP, granulomatous lung disease and coal workers' pneumoconiosis (Cronkhite *et al*, 2008). These findings raise the possibility that telomerase mutations render an individual susceptible to the development of interstitial lung disease rather than being a causal factor in a specific entity.

Studies in bleomycin-induced pulmonary fibrosis in rodents have shown an increase in telomerase activity in fibroblasts, but not in differentiated myofibroblasts (Nozaki *et al*, 2000). This activity can be increased by treatment of the cells with Transforming growth factor beta (TGF-β), known to induce expression of alpha-smooth muscle actin (α-SMA) and myofibroblast differentiation. There is evidence that telomerase-expressing fibroblasts can be differentiated into myofibroblasts following stimulation by growth factors and cytokines such as TGF-β and interleukin-4 (Liu *et al*, 2006).

Gastro-oesophageal reflux. With increasing age there is a decline in oesophageal and gastric motility with increasing exposure of the oesophageal epithelium to gastric acids (Raghu and Meyer, 2012). Hiatus hernias, in which part of the upper stomach protrudes though the diaphragm into the thorax, have been reported in up to 60% of individuals over the age of 60 (Patti *et al*, 1996). These processes lead to gastro oesophageal reflux (GOR) and micro/macro-aspiration of gastric acid into the lung (Raghu and Meyer, 2012). Increased prevalence of GOR associated with IPF was first reported by Tobin *et al* in 1998. Since then the link between GOR and IPF has been reported to be as high as 87% (Raghu *et al*, 2006). However, it remains to be determined whether the aspiration of gastric acid is a causative agent of IPF (Fahim *et al*, 2011). The compounds present in the GOR responsible for lung

injury have yet to be determined but may include enzymes and bile salts (Fahim *et al*, 2011). Acute exacerbations of IPF have also been reported to be linked with GOR and aspiration (Fahim *et al*, 2010). A study by Lee *et al* (2012) examined the presence of the gastric enzyme pepsin in the bronchoalveolar lavage fluid (BAL) of IPF patients, comparing 30 patients with stable IPF and 24 patients with acute exacerbations of the disease. They report that increased pepsin in BAL fluid is associated with acute exacerbations of IPF and a decrease in pulmonary function. Although these previous studies provide convincing evidence for a link between GOR and IPF histological features of micro/macro-aspiration; alveolar haemorrhage, pulmonary oedema, and neutrophil accumulation, are rarely evident in UIP areas of IPF lung tissue samples (Raghu and Meyer, 2012). Raghu and Meyer propose that acute exacerbation of IPF may be linked to episodes of large boluses of gastric acid or that the gastric bacterium *Helicobacter pylori* is causing the damage to the alveolar epithelium. A combined statement from the BTS in collaboration with the Thoracic Society of Australia and New Zealand and the Irish Thoracic Society (2008) recommends that all symptomatic patients with IPF should be treated with proton pump inhibitors which reduce gastric acid production (Wells *et al*, 2008).

Infection. Viral infection has been implicated as an important factor in the pathogenesis of IPF and other related fibrotic lung disorders possibly through causing epithelial cell injury and promoting EMT. The latter is a process in which differentiated epithelial cells undergo transition to a mesenchymal phenotype (Sides *et al*, 2011), discussed further in section 1.2.2. Pozharaskaya *et al* (2009) demonstrated an association between the epithelial cell injury caused by chronic herpes virus infection and lung fibrosis in rodents. Other studies have proposed a link between IPF and Epstein-Barr virus (EBV)

(Mora *et al*, 2007, Sides *et al*, 2011), and Hepatitis C virus with IPF (Arase *et al*, 2008) respectively. A study of 25 patients with IPF by Tang *et al* (2003) examined viral expression and load, reporting that herpes virus-8 (HHV-8) was detected significantly more in sporadic IPF cases than the control group. However, when examining both groups for any variant of herpes virus, both had levels of viral positivity of almost 100%. For EBV, IPF and control groups had the same incidence level of around 60%. Cytomegalovirus (CMV) was found more frequently in familial IPF and less frequently in sporadic IPF cases than the control group. A more recent study by Wootton *et al* (2011) examined the sputum from 43 IPF patients using multiplex PCR, microarrays and cDNA sequencing; they observed EBV in only 2 cases and human papilloma virus (HPV) in only one case of IPF. It remains unclear from these studies what precise role is played by viruses in IPF pathogenesis. There is much controversy over viral detection methods in tissue samples, with reports claiming that molecular techniques such as PCR, direct *in situ* hybridisation and reverse transcriptase *in situ* PCR are more sensitive methods of detection of viral sequences compared to immunohistochemistry (Bhatnagar *et al*, 2012). However, others maintain that molecular techniques over-report viral presence by over-amplification of “bystander” viral sequences (Patel *et al*, 2004). These bystander sequences are levels of viral DNA that whilst present in the target tissue, are however not at a level to cause pathological derangement and clinical manifestations in the individual. This is a major challenge in proving the existence of viral involvement in IPF. For my thesis, I will conduct an immunohistochemical study on human IPF lung tissue samples, to evaluate the protein expression of selected viral markers and determine if active viral disease is present in patients with IPF. In addition, using a wide panel of markers for EMT, I will seek to ascertain if viral protein expression is localised close

to areas of EMT activity, providing for a potential link between viral instigation and disease pathogenesis in my cohort of IPF patients.

1.1.4 Clinical features

Clinically, IPF is characterised by the insidious onset of a non-productive cough, dyspnoea being present for at least 3 to 4 months, and the presence of end-inspiratory crackles. Disease progression in IPF frequently occurs through a series of rapid stepwise deteriorations. Patients are invariably at increased risk of respiratory infection, pulmonary embolism, myocardial infarctions, cerebro-vacuslar accidents and pulmonary hypertension.

The clinical diagnostic approach should include a detailed occupational history and any exposures to potential causative agents of ILD such as smoking or asbestos that may favour an alternative diffuse pulmonary lung disease, rather than IIP. The diagnostic pathway to IIP diagnosis is summarised in Figure 1.1.

Pulmonary hypertension is a common occurrence in patients with IPF (Lettieri *et al*, 2006, Nathan *et al*, 2007). This is thought to occur as a result of increased thickening around the pulmonary vessels caused by an increase in the number of fibroblasts, myofibroblasts and the deposition of collagen (Patel *et al*, 2007). The fibroblasts have been shown to produce mediators such as Interleukin 8 (IL-8) and CXC chemokines that can result in vascular remodelling (Keane *et al*, 1997). An analysis of IPF lung tissue samples revealed the expression of endothelin-1 (ET-1), a potent pulmonary vasoconstrictor and smooth-muscle cell mitogen, in the alveolar walls (Giaid *et al*, 1993). Growth factors such as TGF-β and platelet-derived growth factor (PDGF) have been implicated with both IPF and pulmonary hypertension, suggesting a possible link between their developmental pathways (Tuder *et al*, 1998).

Interstitial lung disease may be present in patients suffering from connective tissue diseases (CTD) such as rheumatoid arthritis, polymyositis/dermatomyositis, systemic sclerosis and rarely systemic lupus erythematosus (ATS/ERS statement 2011). Radiologicaly and histologicaly the conditions may be difficult to differentiate which is why a thorough clinical examination is required. Symptoms or signs suggestive of a connective tissue disease include joint pain or swelling, musculoskeletal pains, weakness and dry eyes and mouth (Strange and Highland, 2004). Immunological laboratory testing may reveal positive circulating anti-nuclear antibodies (ANAs) or rheumatoid factor. Low titres of ANAs can occur in around 10 to 20% of patients with IPF, the presence of high titres (> 1:160) would be more suggestive of the presence of a connective tissue disease (Lippmann *et al*, 1974).

1.1.5 Radiology

On chest X-ray bilateral, often asymmetric, basal reticular opacities are seen subpleuraly in the lower lobes (Figure 1.2). The detailed images obtained from HRCT scans allow for a more accurate diagnosis of IPF to be made; in the early stages of the disease sub-pleural reticular changes are seen, with further disease progression leading to the presence of ground glass opacification within areas of fibrosis. In more advanced disease, areas of honeycombing (alveolar obliteration) exist within areas of normal appearing lung (Souza *et al*, 2005, ATS/ERS statement, 2011), (Figure 1.3). A study by Rhagu *et al* (1999) sought to determine the reliability of a diagnosis of IPF from clinical information and HRCT, compared to open lung biopsy in attempt to provide evidence to negate the need for such an invasive procedure. They report that the specificity of diagnosis IPF on HTCT alone is high (90%), but the sensitivity is lower (78.5%) which may result in a diagnosis of IPF being missed in nearly one third of IPF cases. Radiological features in the differential of IPF are listed in Table 1.1.

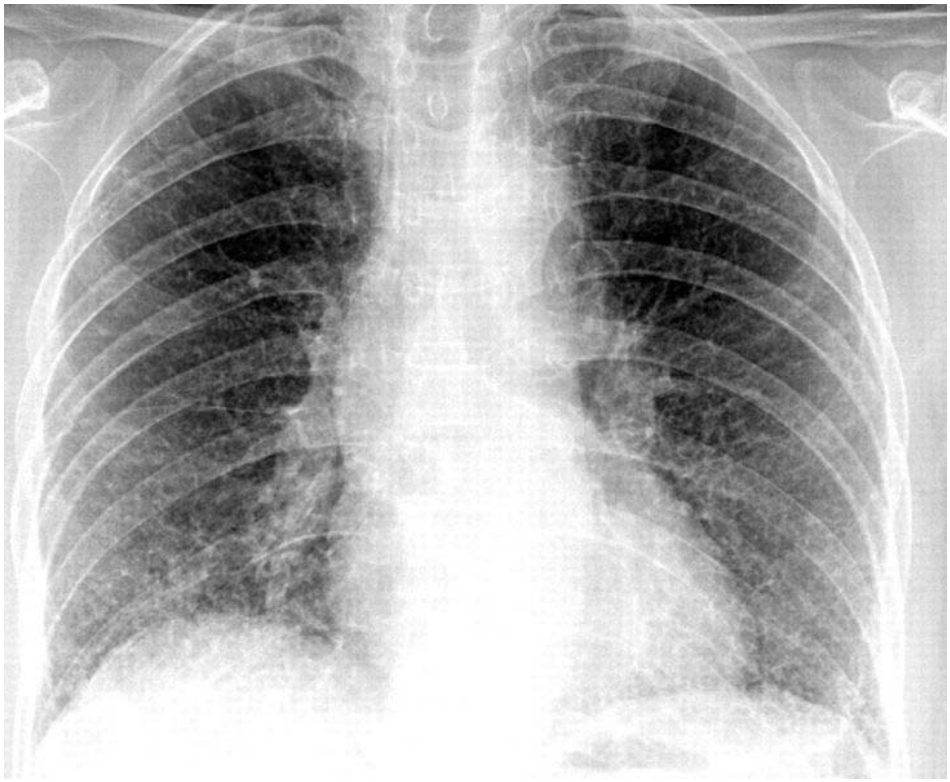

Figure 1.2 Chest X-ray showing evidence of bilateral basal fibrotic shadowing in the lower lobes of a patient with IPF (radRounds Radiology Network, 2009).

Figure 1.3. Chest CT showing honeycomb formation, a key feature of IPF. Image courtesy of Prof M. Spiteri, University Hospital of North Staffordshire.

Definite IPF	**Not IPF**
Fibrosis and distortion of lung architecture	Hyaline membranes (more likely AIP)
Sub pleural honeycombing	Marked interstitial inflammation
Patchy fibrosis of the parenchyma	Extensive ground glass opacification (more likely DIP)
Presence of fibroblastic foci	Ground glass opacification, without basal or peripheral predominance (more likely NSIP)
	middle and upper lobe lung predominance (more likely hypersensitivity pneumonitis)

Table 1.1 Radiological hallmarks of a diagnosis of IPF using HRCT. AIP; acute interstitial pneumonia, DIP; desquamative interstitial pneumonia, NSIP; non specific interstitial pneumonia.

Although Table 1.1 appears to give clear diagnostic criteria there are exceptions. Souza *et al* (2005) noted that 12% of the patients studied that had a diagnosis of UIP did in fact show predominant ground glass opacification on HRCT. The presence of diffuse ground glass opacification radiologicaly could suggest a diagnosis more favourable of non-specific interstitial pneumonia (NSIP). From observations it could be concluded that there is some overlap between the two diseases, a suggestion supported by a study by Sumikawa *et al* (2008). Out of 112 patients reviewed radiologicaly 29 cases were suggestive of an alternate diagnosis, and from this 21 had CT findings similar to NSIP, suggesting a need for histological confirmation. Maher *et al* (2007), propose that IPF and NSIP share common clinical phenotypes within a spectrum of diseases driven by a common pathogenesis. However there are no other publications in the literature supporting the concept that IPF and NSIP are the same disease. These ground glass opacifications may be the radiological

presentation of honeycomb cysts filled with secretions, diffuse alveolar damage, superadded infections or a reaction to drugs such as methotrexate or amiodarone.

HRCT has also been utilised in determining IPF disease activity and extent. A study by Muller *et al* (1987) devised a scale from 0 to 3 based on the presence and density of ground glass appearance on HRCT in 12 IPF patients, associated with increased inflammation and thickening of the alveolar walls; these radiological scores were compared to the corresponding histological lung tissue samples of the same patients. The pathologic score was significantly greater in the patients with high CT scores and is therefore an indicator of increased disease activity and extent. Further discussion of IPF disease activity assessments are detailed in section 1.1.8.

1.1.6 Lung function testing

Pulmonary function testing can provide a useful tool in monitoring physiological lung function and progression of IPF. Restricted ventilation and reduced diffusion capacity for carbon monoxide are noted (Martinez *et al*, 2006). Forced vital capacity (FCV), functional residual capacity, total lung capacity and vital capacity are all reduced (Wells *et al*, 2008).

Resting arterial blood gases may be normal initially or may reveal mild hypoxemia and respiratory alkalosis on exercise (ATS/ERS statement 2000). Patients with IPF may also have increased respiratory rates. Increasingly the 6-minute walk test is being used in IPF patients as a marker for functional exercise capacity and monitoring of disease progression (Lettieri *et al*, 2006). Blood oxygen levels are monitored during the test and a drop below 88% has been associated with an increase in mortality (Tzilas *et al*, 2009). Heart rate is also monitored during the 6-minute walk test with reports of a correlation between decreased

heart rate recovery and survival in IPF patients (Swigris *et al*, 2009); an observation supported in a large study of 822 patients by du Bois *et al* (2011).

1.1.7 Histological features

As noted in section 1.1.5, clinical history combined with HRCT findings may provide conclusive indicators to diagnose in around two thirds of patients with suspicion of IPF. The remainder require histological analysis for confirmation. Surgical lung biopsy samples for histological analysis are usually obtained using video-assisted thorascopic surgery (VATS), although some hospitals still perform open lung biopsy.

Usual interstitial pneumonia (UIP) is the term used to describe the histological picture of IPF. A major histological feature of UIP is temporal heterogeneity of fibrotic areas interspersed with areas of apparently conserved lung architecture. The presence of this temporal heterogeneity makes it is essential to obtain multiple biopsy samples from different sites and lobes of the affected lungs. Using HRCT, areas of end stage disease honeycomb formation and radiologicaly normal lung can be avoided, enabling targeting of areas of intermediate abnormality or comparatively normal lung adjacent to honeycomb lung (Wells *et al*, 2008). During VATS the tissue is stapled along the resection margin rendering this tissue unsuitable for histological examination, the remaining unstapled tissue must therefore be of a large enough size to be able to identify temporal heterogeneity, a key diagnostic feature of IPF.

Microscopic examination of lung tissue samples from IPF patients reveals evidence of type I pneumocyte (ATI) destruction with subsequent hyperplasia of type II pneumocytes (ATII cells), presumably in an attempt to regenerate the alveolar epithelial lining. The hyperplastic ATII cells can be seen throughout areas of interstitial fibrosis, including

overlying clusters of myofibroblasts termed fibroblastic foci (Figures 1.5, 1.6). The loss of alveolar architecture with aberrant lung tissue remodelling eventually forms cysts described as honeycomb change. Fibroblastic foci are another key feature seen in UIP (Figures 1.5 and 1.6) adjacent to areas of established fibrosis.

Fibroblastic foci are associated with active collagen synthesis and are found in areas of previous lung injury (Lynch *et al,* 2001). These foci have been shown to express proteoglycans (Bensadoun *et al*, 1996), the cell adhesion molecule integrin (Fukuda *et al*, 1995), vinculin, involved in the linkage of integrin to the actin cytoskeleton (Katzenstein & Myers, 1998) and tenascin, an extracellular matrix glycoprotein involved in active scar formation (Wallace *et al*, 1995). These foci consist of myofibroblasts, a specialised form of differentiated fibroblast with contractile and smooth muscle properties that can be identified by their expression of alpha-smooth muscle expression (α-SMA). The contractile properties of these cells aids in wound closure during the normal healing process. Myofibroblasts also play a role in the deposition of extracellular matrix (ECM) (Krieg *et al*, 2007) and are a source of cytokines including TGF-β which has been shown to increase collagen synthesis in cell culture studies (Flanders, 2004).

Minor secondary histological features include the presence of intra-alveolar macrophages, smooth muscle hypertrophy and eosinophil accumulation.

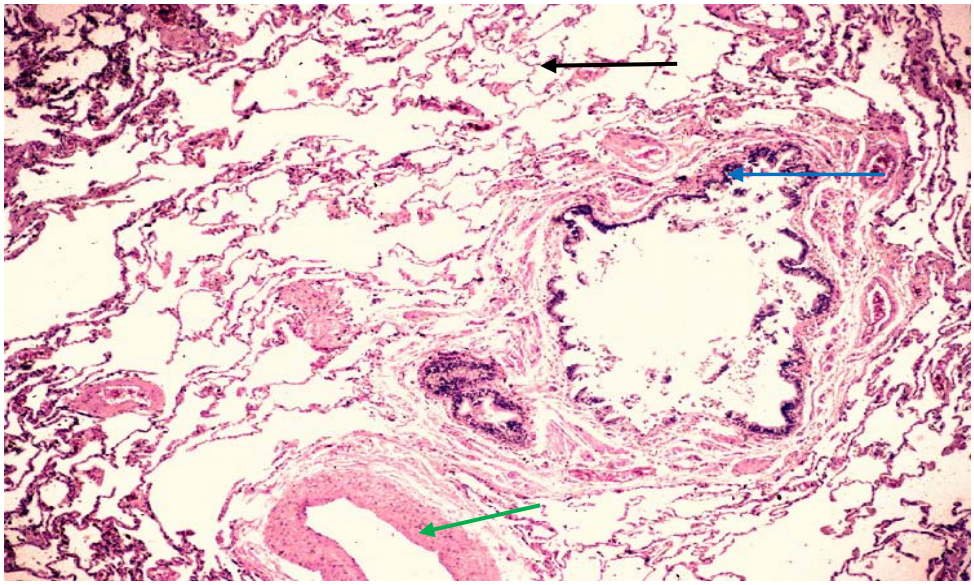

Figure 1.4. H&E stained section of normal lung tissue. The alveolar wall is composed of type I and II pneumocytes (black arrow). A bronchiole is lined by cuboidal or ciliated epithelial cells (blue arrow). A large blood vessel can be identified lined by thick muscle (green arrow). Magnification x100

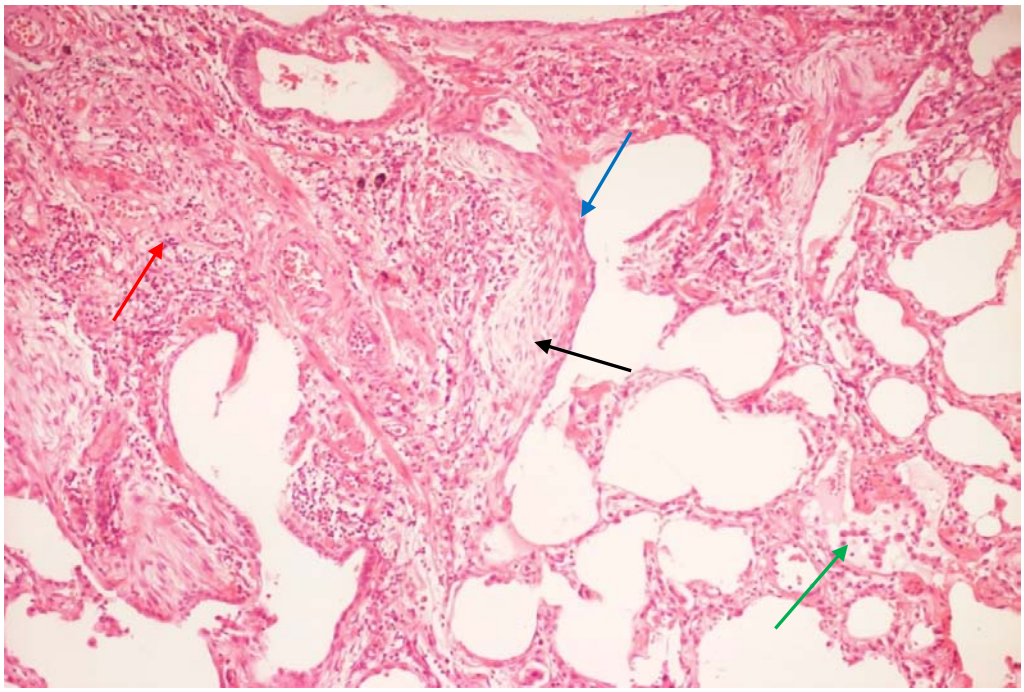

Figure 1.5. H&E stained section of IPF lung tissue with a fibroblastic foci composed of myofibroblasts centraly (black arrow). The foci is covered by hyperplastic ATII cells (blue arrow). Thickening of the alveolar walls and macrophage accumulation within the alveolar air spaces (green arrow) is also observed. Interstitial fibrosis is seen with destruction of the normal lung archetecture (red arrow). Magnification x100.

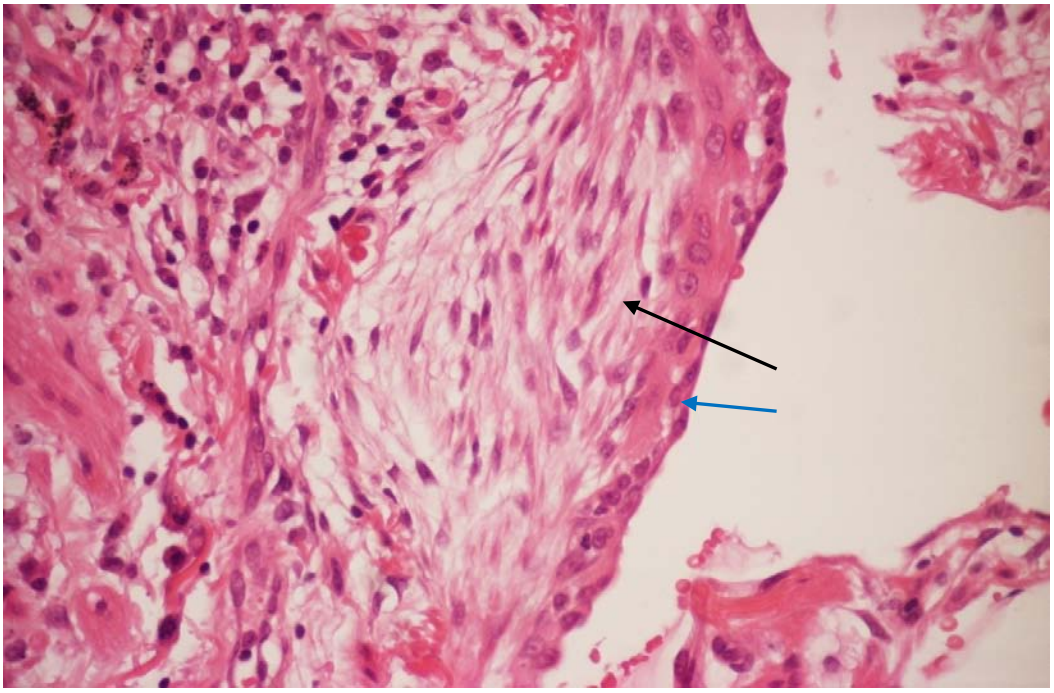

Figure 1.6. High power magnification of a fibroblastic foci (black arrow) stained H&E. Hyperplastic ATII cells are overlying the foci (Blue arrow) Magnification x400.

1.1.8 Assessing disease activity

Rather than a steady decline in lung function, IPF patients may experience sudden acute exacerbation of their symptoms. An acute exacerbation is defined by unexplained worsening of dyspnoea within 1 month, low blood oxygen levels (hypoxemia), pulmonary hypertension and increased honeycombing on HRCT lung imaging (Collard *et al*, 2007). The incidence rate of acute exacerbations of IPF is debatable with two separate studies reporting rates ranging from 9.6% (Kim *et al*, 2006) to 57% (Kubo *et al*, 2005). On lung biopsy these exacerbations are characterised by the appearance of diffuse alveolar damage (Maher *et al*, 2007). As yet there is no way of reliably predicting these acute exacerbations. An attempt was made by Titto *et al* (2006), examining the relationship between numbers of fibroblastic foci seen histologicaly with the number of acute exacerbations of the disease;

however no correlation was identified. The ability to predict which patients have more active disease would enable clinicians to provide more tailored care and monitoring for their patients.

A number of studies have reported correlations in increased disease activity and rapid disease progression with a reduction in total lung capacity, forced vital capacity, carbon monoxide diffusing capacity (Flaherty *et al*, 2003, Collard *et al*, 2003, Latsi *et al*, 2003) and with percentage of extent of disease on HRCT (Lynch *et al*, 2005). A recent study by Triantafillidau *et al* (2011) did not corroborate these findings when examining relationship between histological fibroblastic score and exercise-induced dyspnoea. They point out, however, that this may be due to their limited histological tissue sample size of 24.

More recently a study, using serum from IPF patients in lung epithelial cell cultures, examining circulating auto-antibodies to epithelial structures, has also been shown to correlate with more severe disease (Taillé *et al*, 2011). Using immunoblot analysis the circulating antibody Periplakin, a protein component of cell junctions, was discovered in the serum from 40% of IPF patients. This is a significant finding as loss of cell-cell adhesion is a key feature of EMT and leads to disruption of the alveolar wall integrity.

In addition to clinical and radiological correlations, attempts have been made to investigate the relationship between histological features and disease activity. King *et al* (2001), Nicholson *et al* (2002) and Enomoto *et al* (2006) all report that increased numbers of established fibroblastic foci in IPF lung tissue reflect an increase in disease activity. The study by King examined 87 lung samples from patients with IPF to determine a relationship between histological features and mortality. In this study King *et al* report that only

increased numbers of fibroblastic foci correlated with worse disease survival. In a further study by Nicholson *et al*, a scoring system was developed to examine correlations of histological features and disease progression and mortality in 53 IPF lung tissue samples. Nicholson devised a semi-quantitative scoring system to measure the degree of fibroblastic foci between samples and reported that increased fibroblastic foci score correlated with an increased rate of disease progression and mortality. Finally Enomoto *et al*, calculated the percentage area of fibroblastic foci in lung tissue samples from 16 patients with IPF using digital imaging techniques, and again reported an association with increase percentage area of fibroblastic foci and worse prognosis. I will use the fibroblastic foci scoring system developed by Nicholson *et al*, (described in more detail in section 2.3.5) as an indicator of disease activity. Using this scoring system I will assess whether an increased number of fibroblastic foci within IPF lung tissue samples correlates with markers of EMT, proliferation, the cell cycle and viral presence. EMT, discussed in more detail in section 1.2.2, is thought to lead to the production of myofibroblasts that constitute the fibroblastic foci and is involved in lung tissue remodelling in IPF. However, previous *in vitro* studies examining markers of EMT in IPF lug tissue samples have provided mixed results for the presence or impact of EMT in the formation of these foci (Yamada *et al*, 2008, Harada *et al*, 2010).

My thesis will explore the potential causal link between presence of EMT and increased number of fibroblastic foci by semi-quantitatively examining for expression of markers implicated as evidence of the occurrence of EMT (section 1.2.2, 3.2.2) and their correlation to the number of fibroblastic foci. Furthermore, by expanding this analysis to include a detailed examination of proliferation, apoptotic and cell cycle markers (section

1.2.3, 4.2.2), and their correlation to fibroblastic foci, this thesis will capture whether altered ATII cell turnover is linked with increasing presence of fibroblastic foci.

1.1.9 Treatment

At present there is no effective drug treatment for IPF patients, which is why there is a pressing need to understand the aetiology and pathogenesis of this devastating condition. Pharmaceutical interventions were intended to improve symptoms and slow disease progression, yet most are associated with significant side effects such as weight gain, high blood pressure and osteoporosis (ATS/ERS joint statement, 2000). The use of steroids in combination with immunosuppressant drugs used to be standard therapy for IPF patients. However, only around 12-15% of patients demonstrated improvement in lung function tests or on radiological lung imaging (Turner-Warwick *et al*, 1980). Recent studies have questioned the use of corticosteroids for the treatment of IPF reporting a greater risk of an adverse reaction from drug treatment compared to any benefit to the patient (Nagai *et al*, 1999; Flaherty *et al*, 2001; Collard *et al*, 2004; Hunninghake, 2005). The BTS do not recommend the use of high dose steroids, such as Prednisolone, alone in proven IPF cases. However there is literature evidence for combining Prednisolone with the immunosuppressant drug Azathioprine with some benefit in a small number of patients (Winterbauer *et al*, 1978); however this is an older study that has been superseded with more recent observations of negligible benefit in general in IPF. This also holds true for other drug combinations with corticosteroids such as azathioprine and a precursor to the antioxidant molecule glutathione, Acetylcystine (Cantin *et al*, 1989, Behr *et al*, 1997).

The most recent clinical trial for IPF therapy involved the use of three separate anti-inflammatory and anti-fibrotic agents; N-acetylcysteine (NAC), Prednisolone and

azathioprine (PANTHER study). The triple therapy arm of this study was discontinued as a result of serious adverse events and increased morbidity without any evidence of clinical improvement in their condition (McGrath and Millar, 2012). The adverse effects are thought to be a result of the immunosuppressant azathioprine. It is known clinically that elderly patients are more susceptible to adverse effects, such as respiratory infections, when taking this drug (Wells *et al*, 2012). However one arm of the study, examining the effect of the anti-oxidant NAC alone, is continuing with results expected to be published in 2013.

The drug Pirfenidone has anti-inflammatory, antifibrotic and antioxidant properties and has been shown to be effective in reducing morbidity in IPF patients (Noble *et al*, 2011). Pirfenidone works by down-regulating inflammatory cytokines such as tumour necrosis factor-α (TNF-α) and TGF-β. The National Institute for Health and Clinical Excellence (NICE) is expected to make its recommendations on the use of the drug in the UK in April 2013. Trial assessment of the drug's efficacy was based on results of the 6 minute walk test which resulted in an increase in blood oxygen saturation in patients tested (Azuma *et al*, 2005), and change in percentage predicted forced vital capacity (FVC) (Noble *et al*, 2011). However, side effects of the drug included abnormal liver function, gastrooesophageal reflux, vomiting and dyspepsia**.**

The use of long term oxygen therapy in IPF is recommended for patients with clinically significant resting hypoxemia (ATS/ERS/JRS/PLAT statement 2011). However evidence for its use is limited to two indirect studies examining the benefit of oxygen therapy in chronic obstructive pulmonary disease (Nocturnal Oxygen Therapy Trial Group, 1980) and chronic bronchitis and emphysema (Medical Research Council Working Party, 1981). Lung transplantation is considered as the only current 'cure' for IPF; with quoted 5-

year survival rates of 50 to 56% (Masra *et al*, 2007, Keating *et al*, 2009). It is unclear if the survival benefit is different in single-versus double-lung transplant recipients (Thabut *et al*, 2009).

Evolving treatments currently being trialled include mesenchymal stem cell therapy. Mesenchymal stem cells have been shown to inhibit fibrosis in studies on liver fibrosis, and are able to differentiate into lung epithelial cells in murine models of bleomycin-induced pulmonary fibrosis (Moodley *et al*, 2009, Kajstura *et al*, 2011). In the study by Moodley, mesenchymal stem cells were injected into areas of injured lung only. This resulted in suppression of the growth factor TGF-β and TNF-α; both implicated in the pathogenesis of IPF. The role of TGF-β is discussed further in section 1.2. In contrast an upregulation was noted of the enzyme matrix metalloprotease-2 (MMP-2) in the stem cell injected areas. MMP-2 is involved in the degradation of extracellular matrix including collagen, observed histologicaly in IPF lung tissue samples (Massova *et al*, 1998). In the separate study by Kajstura, human lung stem cells were injected into damaged mice lungs. Upon histological and analysis of the transcription factors such as thyroid transcription factor (TTF-1), octamer-binding transcription factor 3-4 (OCT3/4) and homebox transcription factor (Nanog), it was found that the human lung stem cells formed integrated human bronchioles, alveoli, and pulmonary vessels. This integration of stem cells forming normal functioning alveolar epithelium is of particular interest in IPF where it has the potential to be targeted to the areas of alveolar damage whilst sparing the existing normal functioning lung tissue. Trials of mesenchymal stem cells (MSCs) for the treatment of IPF are still in their infancy with only preliminary reports in a small study sample. The study by Tzouvelekis *et al* (2011), performed lipoaspiration on 14 IPF patients to isolate and label adipose-derived stem cells (ADSCs). These Technetium (Tc)-99 labelled ADSCs were endobronchially infused into both

lower lobes of the lungs. No significant adverse reactions, such as infection or acute exacerbations of the disease occurred 6 months post infusion. Although there have been no significant improvements in FVC or diffusing capacity for carbon dioxide (DLCO) in the study group to date, a marginal improvement in the 6 minute walk test was reported (Tzouvelekis *et al*, 2011). My study will investigate whether the "spared areas" of IPF lung are functioning normally compared to the control group, identifying which target markers show variation in expression between conserved and diseased areas of IPF lung. This will identify variations in molecular pathways such as cell cycle regulation, senescence or EMT within specific cell types which could be targeted for drug or gene therapy using MSCs directed at the affected areas. This targeted therapy has the benefit of maximising the drug efficacy whilst limiting systemic toxicity.

1.2 Pathogenesis

1.2.1 Current concepts

The pathogenesis of IPF is a failure or imbalance in a number of molecular pathways involved in fibrogenesis, apoptosis and proliferation that eventually leads to the loss of alveolar epithelial cells and the accumulation of activated fibroblasts/myofibroblasts, summarised in Figure 1.7. More recently specific molecular pathways have been identified such as the GSK-3β/β-catenin pathway (Caraci *et al*, 2008), and the WNT/β-catenin signalling pathway (Königshoff *et al*, 2009). The study by Königshoff identified an increase in the WNT/β-catenin signalling leading to alveolar epithelial cell dysplasia and abnormal epithelial differentiation in IPF lung tissue samples. The WNT signalling pathway, known to drive epithelial cell hyperplasia, effects a number of target molecules implicated in IPF such

as MMPs, the cell cycle regulator Cyclin D1 and TGF-β (Königshoff *et al*, 2009). My study investigates the interaction of Cyclin D1, TGF-β and collagen I, levels of which are regulated by MMPs, in IPF lung tissue samples.

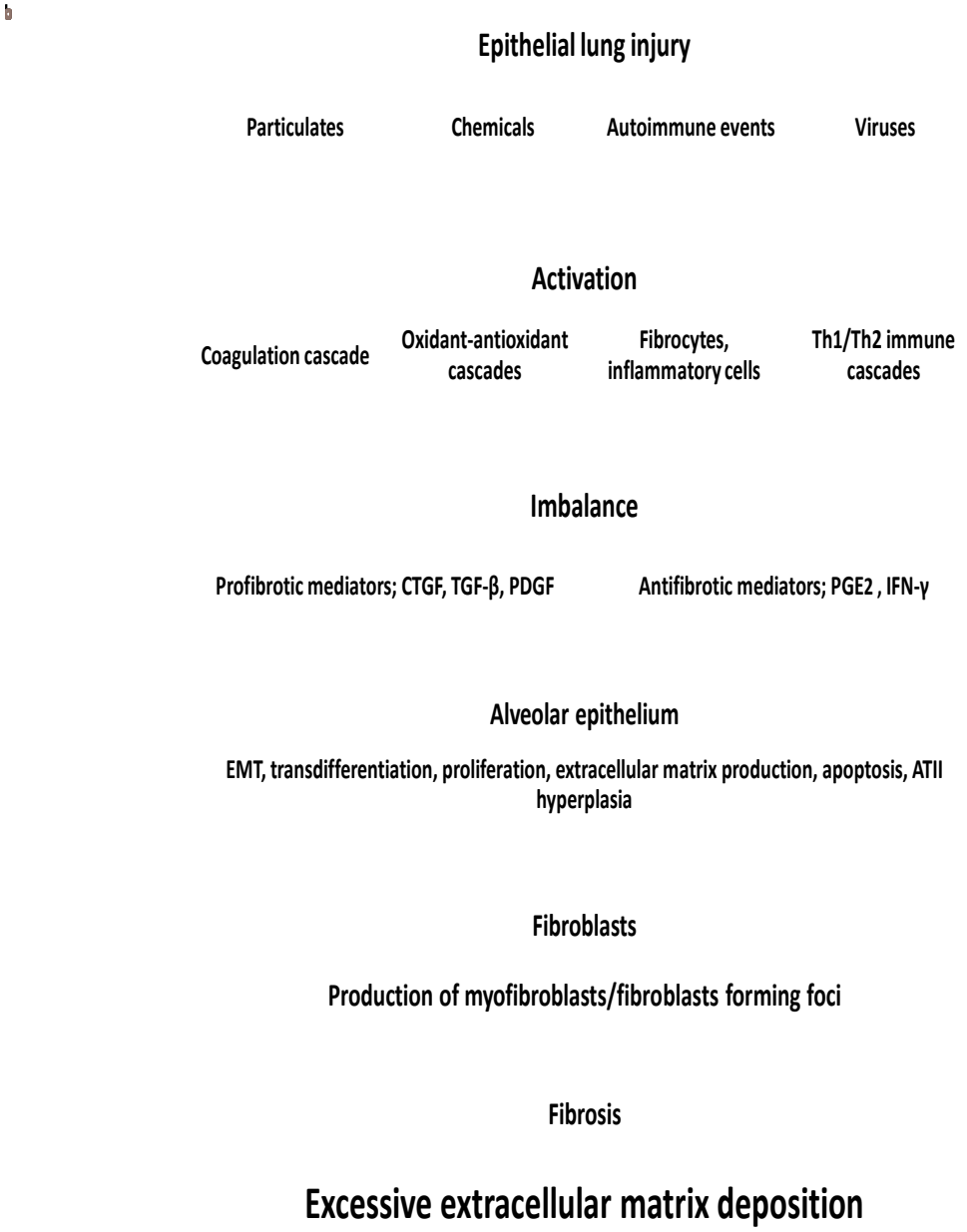

Figure 1.7. Diagrammatic representation of the possible pathways involved in the development of IPF, adapted from Maher *et al* (2007). ***CTGF; connective tissue growth factor, TGF-β; transforming growth factor beta, PDGF; platelet derived growth factor, Th; T helper cell, PGE2; prostaglandin E2, IFN; interferon, ATII; alveolar type II pneumocyte.***

Initial injury to the alveolar epithelium may have many causes such as chemical, viral or bacterial infections, or it may be idiopathic. The lung epithelial repair mechanism instigated immediately following injury is similar no matter what the initial insult may be. Histologicaly the first response to be seen is the influx of an acute inflammatory exudate into the pulmonary parenchyma and alveolar space (Crosby and Waters, 2010). Subsequently epithelial progenitor cells migrate to the sites of injury to bridge the gap in the damaged epithelium. These cells then proliferate and differentiate into the alveolar cells destroyed by the initial insult. In the lung there are two main progenitor cells; Clara cells in the bronchiolar epithelium (Strip and Reynolds, 2008) and ATII cells in the alveoli (Evans *et al*, 1975, Mason and Williams, 1977). In IPF it is proposed that ATII cell hyperplasia is an attempt to repair the epithelium damaged by an unknown insult (Katzenstein and Myers, 1998). Injury to the lung epithelium results in damage to the alveolar basement membrane allowing infiltration of fibroblasts, endothelial cells and macrophages. Activation of these fibroblasts by TGF-β leads to the generation of contractile, α-SMA-expressing cells called myofibroblasts, considered to be a key factor in IPF pathogenesis (Eickelberg and Laurent, 2010), and forming the fibroblastic foci observed histologicaly. TGF-β is also involved in initiating epithelial mesenchymal transition and the transformation of circulating fibrocytes into myofibroblasts, discussed further in section 1.2.2 (Figure 1.8) (Crosby and Water, 2010). ATII cells proliferate and aggregate over the fibroblastic foci before attempting to differentiate into type I pneumocytes which have been lost through the initial epithelial insult (Katzenstein and Myers, 1998) (Figure 1.8). The importance and proposed dysregulation of the balance between proliferation and apoptosis of cells involved in IPF lung tissue remodelling is discussed further in section 1.2.3.

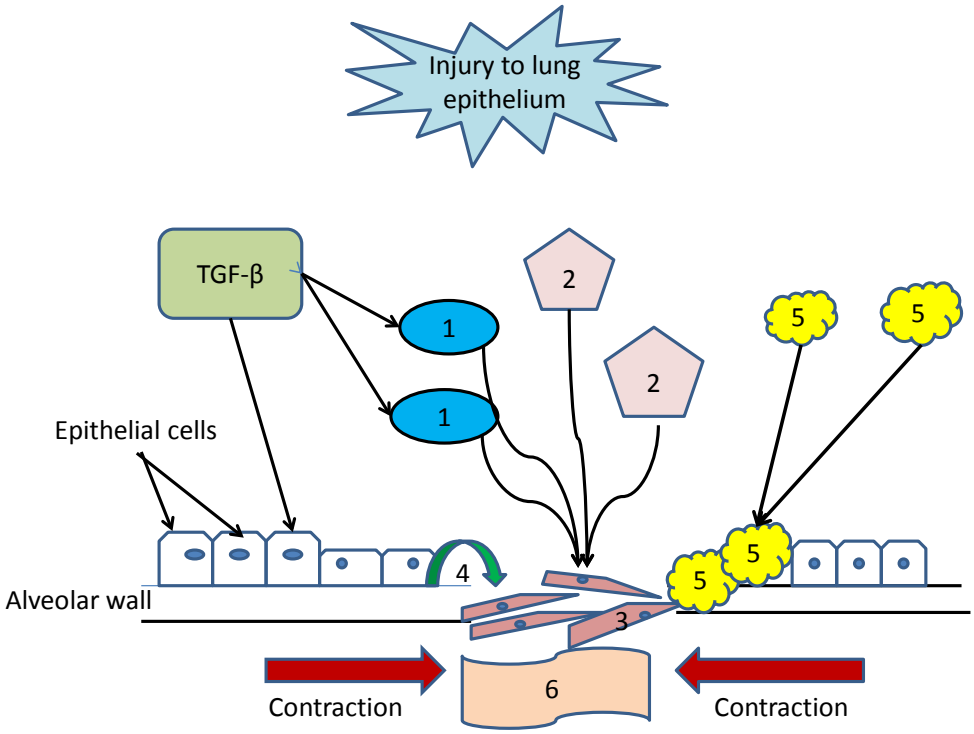

Figure 1.8 Processes involved in alveolar epithelium repair following injury. TGF-β promotes the transformation of (1) residential fibroblasts and (2) circulating fibrocytes into (3) myofibroblasts which constitute the fibroblastic foci. TGF-β may also be responsible for the transformation of the ATII cells into the myofibroblasts (4) via a process called epithelial mesenchymal transition (EMT). Mesenchymal stem cells (5) may also be recruited to the site of injury in an attempt to repair the alveolar epithelium. Myofibroblasts contract to close the wound but also secrete collagen (6) into the extracellular matrix upon stimulation by TGF-β.

Under ideal conditions the initiator of damage is removed by the acute inflammatory response, resulting in either the regeneration of the original cell type or, more commonly, by the formation of a scar. The process of scar formation begins with macrophages removing the inflammatory exudate via phagocytosis. This is followed by the growth of fibroblasts and myofibroblasts bridging the wound and the production of collagen III.

Myofibroblasts within this collagen matrix contract to draw together the wound edges (Hardy, 1989). Once the wound is closed fibroblasts cease to divide, becoming fibrocytes, and the collagen III is replaced via degradation, by MMPs, and secretion of collagen type I (Quan *et al*, 2004). MMPs are produced by fibroblasts, macrophages, some epithelial cells and neutrophils. After tissue injury initially both collagens I and III accumulate, eventually just type I predominates, due to greater resistance to metalloproteinase digestion (Stevens and Lowe, 2000). Expression of collagen I can therefore indicate an advanced/chronic level of fibrosis on histological examination. Evidence suggests that in IPF there is either abnormal MMP activation or an imbalance between MMPs and tissue inhibitor of matrix metalloproteinases (TIMP) (Bhattacharyya *et al*, 2007), (Figure 1.9).

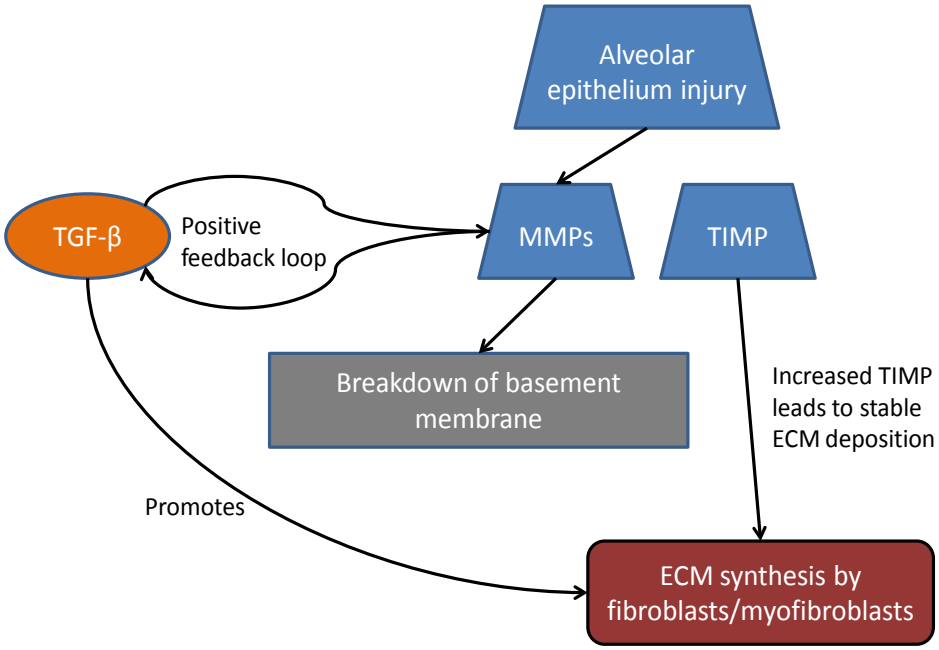

Figure 1.9 The role of matrix metalloproteinases in the pathogenesis of IPF. Injury to alveolar epithelium leads to the production of MMPs which breaks down the alveolar basement membrane and can stimulate the activation of latent TGF-β. TGF-β released by the fibroblastic foci and ATII cells stimulates further release of MMPs from ATII cells and promotes ECM synthesis. Increased TIMP overrides MMP function leading to stable ECM deposition.

Under certain circumstances, such as persistent stimulation via the initial inciting stimulus, repair mechanisms can be hindered or exaggerated leading to continued tissue damage and/or excessive scar formation, which may be the case in IPF. Long-standing interstitial fibrosis eventually results in cystic air spaces separated by areas of fibrosis termed “honeycomb lung”; this tissue remodelling is irreversible (Arakawa and Honma, 2011).

1.2.2 Epithelial mesenchymal transition

One proposed mechanism in the pathogenesis of IPF is EMT (Willis *et al*, 2005). EMT is a biological process in which polarised epithelial cells undergo morphological changes to assume a mesenchymal phenotype (Hay, 1998).This process repairs damaged tissue via the production of fibroblasts and ECM, and has been associated with fibrosis in other organs such as the liver and kidney (Kim *et al*, 2006, Willis and Borak, 2004, Potenta, *et al* 2008, Zeisberg *et al* 2007). EMT has been characterised by the switch from epithelial (E-cadherin) to mesenchymal (N-cadherin) calcium-ion-dependent adhesion accompanied by the gain of mesenchymal markers such as α-SMA (De Wever *et al* 2004). During the process of EMT cells become more motile, invasive and gain resistance to apoptosis (Willis and Borak, 2007). α-SMA is considered to be one of the key markers of EMT, being expressed by a subset of activated fibroblasts called myofibroblasts. These myofibroblasts are present in the early phase of acute lung injury, which are thought to be a source of pro-fibrogenic and matrix deposition. Myofibroblasts facilitate wound healing by contraction and provide scaffolding for type II pneumocytes by secretion of extracellular matrix proteins. If myofibroblast activation is excessive or persists for too long then fibrosis results. α-SMA is involved in cell motility, cell division, vesicle and organelle movement, cell signalling, and the establishment and maintenance of cell junctions and cell shape. Smad-mediated pathways have been shown to activate TGF-β (Mehra and Wrana, 2002) which induces the α-SMA target gene along with collagen and connective tissue growth factor shown to be involved in the pathogenesis of IPF (Inoue *et al*, 2005, Kim *et al*, 2009).

A number of transcription and growth factors have also been implicated in the pathogenesis of IPF and as drivers of EMT. The transcription factor Twist, not normally

expressed in healthy human adult lung, promotes proliferation and differentiation of cells and is proposed to drive both EMT (Pozhaeskaya *et al*, 2009) and EndMT (Potenta *et al*, 2008, Zeisberg *et al*[a], 2007, Zeisberg *et al*[b], 2007). Overexpression of Twist results in increased N-cadherin expression, which in turn leads to E-cadherin down-regulation. Hypoxia or mechanical stresses are known to turn on Twist expression (Sun *et al*, 2009). The growth factor TGF-β is implicated in mediating fibrotic tissue remodelling and the inhibition of ATII cell proliferation (Bartram *et al*, 2004), and has been reported, *in vitro*, to differentiate cultured fibroblasts to α-SMA expressing myofibroblasts (Desmouliere *et al*, 1993). TGF-β has also been reported to be an inducer of EMT (Willis *et al*, 2005) in cultured alveolar epithelial cells through Snail1, Snail2 and Smad-mediated pathways. In addition collagen I, which accumulates in the lungs of IPF patients, has also been shown to promote EMT in lung cancer cells via associated TGF-β signalling (Shintani *et al*, 2008).

It is hypothesised that hyperplastic ATII cells, and/or lung endothelial cells in IPF, transform via EMT/EndMT to produce the fibroblastic foci observed in IPF (Harada *et al*, 2010). However many of these above-mentioned studies have hypothesised the role of EMT in IPF based on extrapolations from cell culture and animal studies using only one or two markers to determine the presence of EMT. Yamada *et al* (2008) examined the role of EMT in human IPF lung tissue samples. Their study used florescent dual-immunohistochemistry to detect the expression of E-cadherin and α-SMA in the lung tissue samples from 15 patients with histologicaly confirmed IPF and compared their findings to those from 8 control lung tissue samples. Consistent expression of E-cadherin was found with no double positive cells for E-cadherin and α-SMA identified in IPF lung tissue raising the possibility that EMT does not occur in IPF lung. However the investigators did caution that the process

of EMT is transient and it may be that the length of time co-expression of epithelial and mesenchymal markers occurs may be too short to be detected in formalin fixed lung tissue samples. Conversely an immunohistochemical study by Harada *et al* (2010) examined the lung tissue from 13 patients with IPF and deduced that EMT was present in some hyperplastic ATII cells overlying the fibroblastic foci due to co-expression of thyroid transcription factor-1 (TTF-1) and vimentin. This study did not find cytoplasmic expression of α-SMA within the ATII cells overlying the fibroblastic foci, a key indicator of EMT. In this study, I also question the use of TTF-1 and surfactant protein B (SP-B) to identify ATII cells as it is known that TTF-1 is present in all lung epithelial cells and SP-B is also produced by clara cells within the lung as opposed to surfactant protein C (SP-C) which is solely secreted by ATII cells (Klaina *et al*, 1992). Both these studies relied on just a few selected markers to determine the presence of EMT in IPF lung tissue samples. One of the key features of ATII cells undergoing EMT is the loss of E-cadherin with upregulation of N-cadherin, Twist and cytoplasmic expression of α-SMA and collagen I. My study addresses the information lacking from these previous studies by examining a wider spectrum of EMT markers including E-cadherin, N-cadherin, Twist, collagen I and α-SMA, and specifically identifying ATII cells via the use of SP-C.

The induction of EMT has also been linked to viral infections such as EBV, Cytomegalovirus (CMV) and herpes virus, all linked to IPF pathogenesis (Tang *et al*, 2003, Pozharskaya *et al*, 2009, Sides *et al*, 2010), and discussed in more detail in section 1.1.3.

Selman and Pardo (2006) pose the question of whether EMT is an initiating event in IPF, or a secondary response to growth factors, cytokines or mechanical stress. No previous studies have examined the expression of markers of EMT in conserved healthy-looking areas

in IPF lungs or in the hyperplastic ATII cells away from the fibroblastic foci to detect the potential early development of myofibroblasts. By examining growth factors and EMT marker expression within these spared areas of alveolar epithelium within the recognised temporal heterogenic pattern of UIP in IPF lungs, I will provide further insight into the question posed by Selman and Pardo. In addition it may be possible to determine, when compared to control non-IPF lung, if these conserved areas are composed of functional epithelial cells or, although appearing morphologically normal, are in fact functionally different and are expressing protein and growth factors similar to the diseased areas. It also remains to be determined, if EMT is occurring, whether myofibroblasts produced are functioning normally to repair the epithelium, or are they impaired in some way, such as increased proliferation or inhibited clearance, resulting in a non-reparative environment contributing to the excessive matrix deposition observed in IPF. My study hopes to address these gaps in the knowledge gained from previous work by examining SP-C expression, alongside cell adhesion, mesenchymal markers and TGF-β in diseased and conserved areas, to determine the presence and extent of EMT in IPF lung tissue samples using dual-immunohistochemistry.

1.2.3 Cell cycle regulation and signalling.

During normal lung wound repair a balance between proliferation and apoptosis regulates the number of fibroblasts at a site of injury; if this balance tips towards increased proliferation and/or reduced apoptosis, fibrosis results (Crosby and Waters, 2010). In normal wound healing the contractile activity of myofibroblasts stops when the tissue is repaired and the myofibroblasts undergo apoptosis (Powell *et al*, 1999). The process of cell proliferation and apoptosis is under the tight control of the cell cycle which is divided into 5

phases, as seen in Figure 1.10. Progression through the cell cycle is regulated at three major checkpoints and is dependent on variations in the activities of cyclin-dependent kinases (Cdks). Cdks are activated by binding to regulatory proteins called cyclins. At various points in the cell cycle, different cyclins are produced, forming complexes with Cdks which trigger each cell cycle event in turn. As cells exit from the cell cycle they may follow one of four pathways resulting in; cell senescence, apoptosis, differentiation or proliferation (Hartwell and Weinert, 1989). The first checkpoint in the cell cycle is at G_1/S which is controlled by the binding of Cyclin E to Cdk2 triggering progression through Start (Ohtsubo *et al*, 1995). Levels of Cyclin E-Cdk2 complexes lead to the activation of M-phase Cyclin B/Cdk1 complexes driving progression through the second checkpoint (G_2/M) and entry into mitosis. The third checkpoint is during the M-phase at the metaphase to anaphase transition, segregating chromatids and completing mitosis and cytokinesis. One further class of cyclins are the G_1 cyclins (Cyclin D 1, 2 and 3). Cyclin D levels steadily increase through the cell cycle in response to growth factors and signals. These then bind to Cdk4, 6 which coordinates cell growth and entry into a new cell cycle. The actions of Cyclin D1 are inhibited by members of the INK4 family, such as $p16^{INK4A}$, binding to Cdk4 preventing progression into the S-phase. Maximum expression of Cyclin D1 occurs in mid to late G1 phase. Increased amplification of Cyclin D1 is found to coincide with the high deletion of the tumour suppressor gene $p16^{INK4A}$ (Okami *et al*, 1999). $p16^{INK4A}$ has been shown to be induced by DNA damage, oncogene stress and oxidative stress. It promotes cell senescence by competing with Cyclin D and inhibiting Cdk-2 and Cdk-4, leading to inhibited Rb phosphorylation preventing the passage of cells from the G1 to the S phase of the cell cycle (Branner *et al*, 1998).

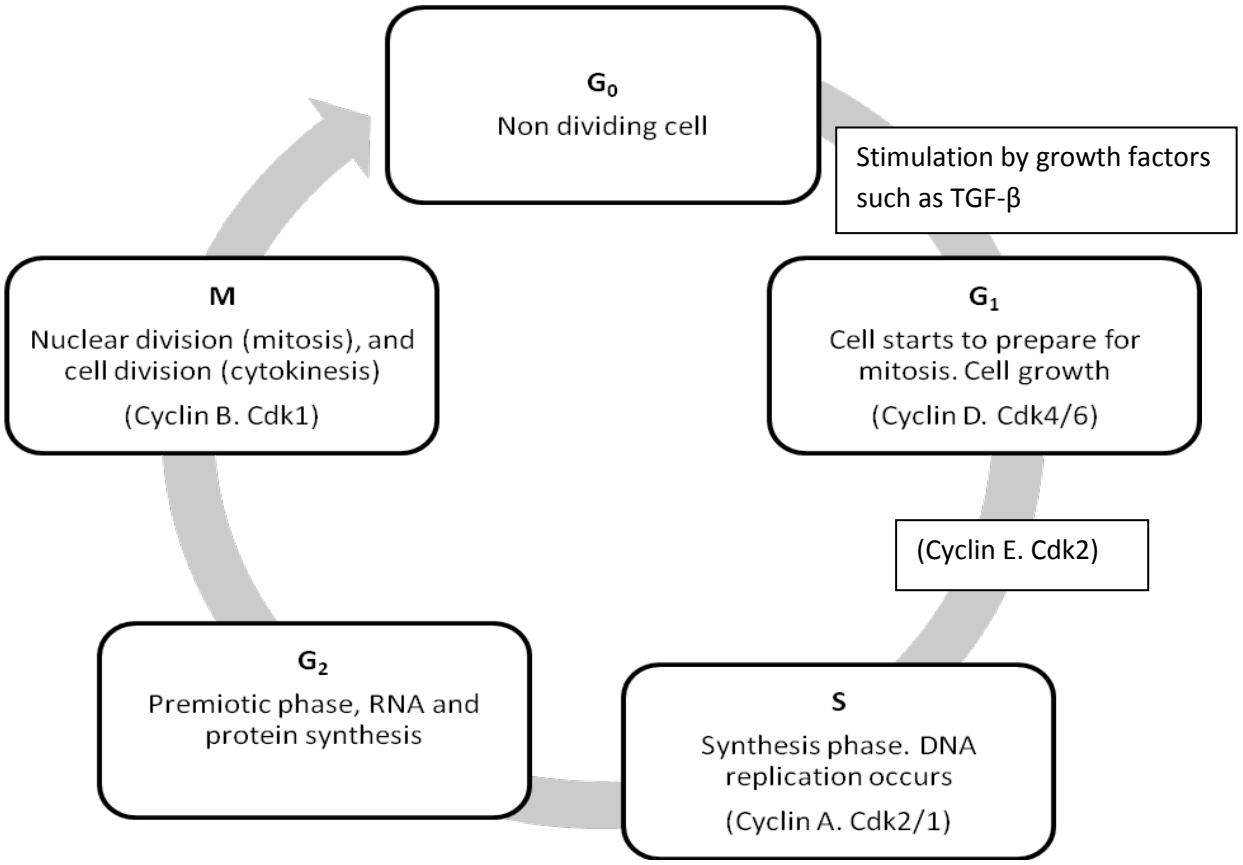

Figure 1.10 Cell cycle split into 5 stages. There are number of checkpoints within the cycle to prevent uncontrolled cell division. Dysregulation of the cell cycle may be responsible for the excessive ECM deposition and distorted wound remodelling seen in IPF lung tissue. Cell cycle control cyclin/Cdk complexes are given in brackets.

It has been shown that both DNA damage and apoptosis in bronchiolar and alveolar epithelial cells occurs in IPF (Barbas-Filho *et al*, 2001), although the precise mechanism of how epithelial cell apoptosis leads to pulmonary fibrosis is not clear. In a bleomycin induced murine model of pulmonary fibrosis the forced expression of $p21^{WAF1}$ in alveolar epithelial

cells suppressed apoptosis and pulmonary fibrosis by inducing G1 arrest and DNA repair (Inoshima *et al*, 2004).

Cytokines are secreted glycoproteins which regulate various biological processes by binding to cell receptors resulting in activation of the Janus kinase (JAK) family of tyrosine kinases and tyrosine kinase-2 (TYK2). These activated JAKs create recruitment sites for signalling proteins such as signal transducers and activators of transcription (STATs) which migrate to the nucleus to regulate gene transcription. A tight feedback loop to control this process is essential. Involved in this feedback mechanism are the suppressor of cytokine signalling (SOCS) proteins. The SOCS family consists of SOCS1-7 and cytokine-inducible SH2-containing protein (CIS). SOCS1 binds to JAKS whilst SOCS3 bind to the cytokine receptor chains (Elliot and Johnston, 2004). SOCS3 inactivates STAT3 which results in the promotion of Cyclin D1 leading to cell cycle progression. Reduction of SOCS3 in healthy fibroblasts has been shown to increase levels of messenger RNA, and protein levels of collagen. Loss of SOCS3 gene expression has also been shown to convert STAT3's function from anti-apoptotic to pro-apoptotic in rodent fibroblasts (Lu *et al*, 2006). It is therefore possible that in IPF lungs, increased SOCS3 gene expression may be present in fibroblasts conferring resistance to apoptosis, leading to an *in situ* accumulation of these cells.

Proliferation of ATII cells to maintain tissue integrity may be measured by the cell proliferation marker Ki-67. Ki-67, a nuclear protein associated with and possibly necessary for cellular proliferation, is expressed during all active phases of the cell cycle but is absent in resting cells (G_0 phase). There is no expression of Ki-67 during DNA repair processes (Key *et al*, 1994). In an immunohistochemical study on lung tissue samples from 16 patients with IPF, it was demonstrated that low levels of Ki-67, and therefore low proliferative activity, in

fibroblasts is present in this tissue (El-Zammar *et al*, 2009). This was compared with two other ILDs; bronchiolitis obliterans-organizing pneumonia (BOOP) and diffuse alveolar damage (DAD) which conversely displayed increases in proliferation of fibroblasts compared to IPF samples. This difference in proliferative activity may account for the irreversible nature of IPF compared to BOOP and DAD (El-Zammar *et al*, 2009).

An important process in the normal maintenance of tissue size and integrity is the balance between cell proliferation and apoptosis. The purpose of apoptosis is to remove cells that have the potential to harm the surrounding tissue, such as those with DNA damage or mutations. Without apoptosis cells have the potential to grow and proliferate uncontrollably. Once activated, by intracellular proteases, apoptosis is irreversible. Tumour necrosis factor–related apoptosis-inducing ligand (TRAIL) induces apoptosis in tumour cells but not normal cells when bound to receptors DR4 and/or DR5 (Song *et al*, 2000). However, if a cell expresses more decoy receptors, such as DcR1, the cell is likely to survive upon binding to TRAIL. Cells expressing more decoy receptors are usually found on normal cells, whereas cells expressing DR4/DR5 are mainly expressed by transformed cells (Wang and El-Deiry, 2003). In IPF lung tissue samples it has been demonstrated that reduced pulmonary expression of TRAIL correlated with worse pulmonary function and clinical outcome (McGrath *et al*, 2011), although the mechanisms of why this is the case remain to be elucidated.

DNA damage in G1 leads to inhibition of progression through Start by activating the protein kinase ATM which leads to targeting of the cell for ubiquitination and destruction (Pickart, 2001). This phase is known as the rapid response, occurring within minutes of the initial damage. The second phase is termed the delayed response and involves the

activation of p53. p53 oversees the response to cell stress by initiating cell cycle arrest until DNA damage can be repaired. In normal cells the wild type p53 behaves as a tumour suppressor inhibiting DNA replication and acting as a cell cycle checkpoint control molecule (Baker *et al* 1989). However, if DNA damage is too severe p53 induces apoptosis or prolonged cell senescence. p53 can be damaged by chemicals, radiation and viruses (Wahl and Carr, 2001). Studies on liver fibrosis have concluded that cellular senescence limits the fibrogenic response. In chronic liver damage, such as viral hepatitis, continual cell death and hepatic stellate cell proliferation causes the senescent cells to outpace their clearance resulting in persistent inflammation and fibrosis (Krizhanovsky *et al*, 2008). Truncated isoforms of the p63 gene (ΔN-p63) counteract the apoptotic and cell cycle inhibitory functions of p53 after DNA damage (Yang and McKeon, 2000). The expression of ΔN-p63 has been explored in a study of 16 lung tissue samples obtained from IPF patients (Chilosi *et al*, 2002). Epithelial cells expressing_ΔN-p63 and abnormal p53 were observed at sites of abnormal proliferation at the bronchiolo-alveolar junctions. Chilosi *et al*, propose that the destruction of the alveolar epithelium and lung remodelling seen in IPF lung tissue after injury could result from pneumocyte loss and alveolar collapse in one area, with progressive bronchiolar proliferation and architectural distortion in an adjacent area of the lung. This concept will be further explored in my thesis through analysis of an interactive panel of cell cycle, proliferation, apoptotic and structural markers to determine their precise localisation and relationship to key IPF histological hallmarks in diseased and conserved areas of IPF lug tissue; this may give clues for the observed pattern of temporal heterogeneity in IPF lungs.

1.3 Immunohistochemistry

My thesis will make use of immunohistochemical techniques to examine in detail components of the tissue remodelling in IPF lung samples. Immunohistochemistry (IHC) is a valuable tool for detecting in tissue samples particular cells, proteins, growth factors and viruses, as well as in the investigation of cellular events such as proliferation and apoptosis. Compared with molecular techniques, IHC makes it possible to visualise the distribution and precise localisation of specific components within a cell or tissue. Sensitivity and specificity of the antibodies, used as markers for expression of growth factors and proteins in my study, as well as technical procedure are crucial to avoid false-positive and false-negative results. Improved validity of immunohistochemical methods has been made by the introduction of polymeric methods, which have been used in my study. This system is based on dextran polymer technology providing binding of a large number of enzyme molecules (horseradish peroxidase or alkaline phosphatase) to a secondary antibody via the dextran backbone. The benefits include increased sensitivity and minimized non-specific background compared to conventional IHC techniques (Sabattini *et al*, 1998).

Although IHC is a widely accepted technique, and is used routinely in determining the diagnosis, prognosis and treatment strategies for patients with wide ranging conditions such as cancer and viral infection, it is not without its pitfalls. Several factors can cause false-negative or false-positive results mainly centred on the primary antibody. Primary antibodies can fail to detect their target antigen, even if the antigen is present in the tissue, for many reasons including: conformation changes induced by fixation/embedding, steric hindrance by interacting proteins/post-translational modifications, low affinity of the antibody for the target, or failure of the antibody to penetrate into the tissue. The use of

known positive control tissue alongside the test tissue ensures the technique is performed correctly and the marker is specific to the target being investigated. Conversely, antibodies can bind non-specifically to other targets or tissue components giving false positive results (Fritschy, 2008). These false positive results with enzymatic staining can be distinguished by their granular appearance and inappropriate localisation within the cell. An example of this is seen in figure 1.11.

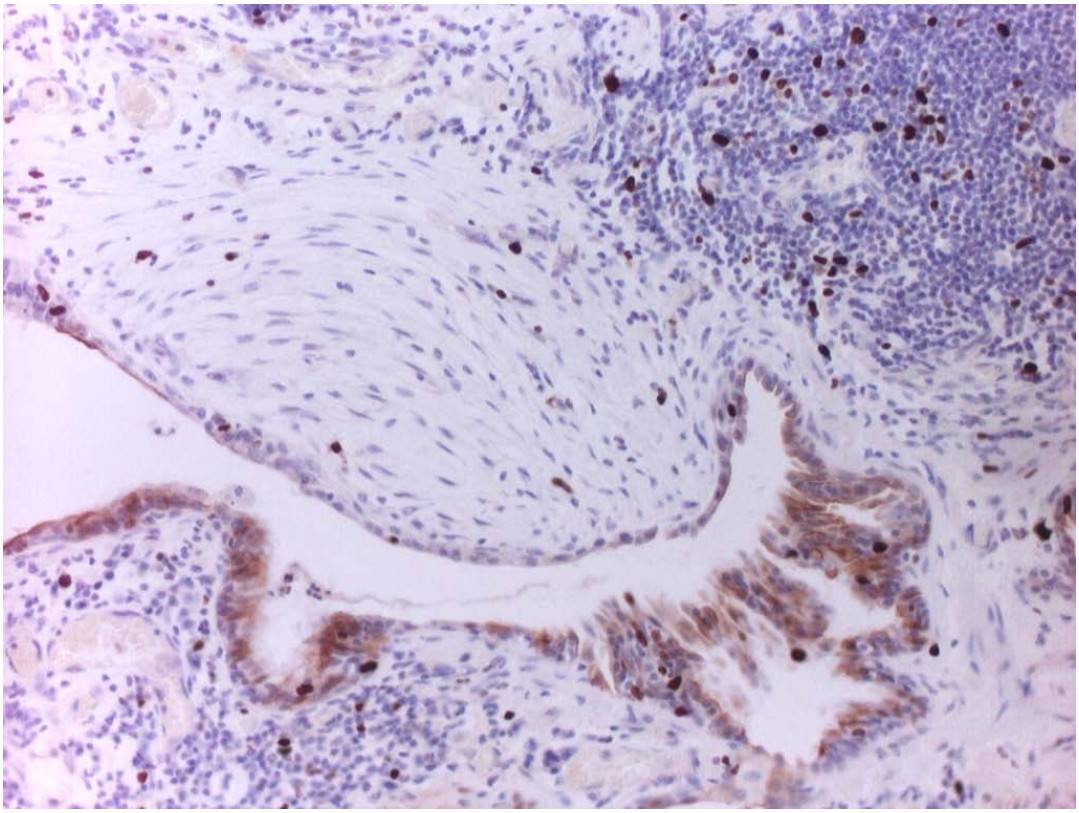

Figure 1.11 IPF lung tissue stained with the proliferation marker Ki-67. Ki-67 is a nuclear marker and should not be identified in the cytoplasm. Here granular cytoplasmic staining can be seen but is easily distinguishable from the true crisp nuclear staining. Magnification x200.

To minimise the risk of false positive expression of markers, a separate negative control section is cut from the test tissue and treated in the exact same way as the test tissue apart from the omission of the primary antibody. If, on completion of the procedure,

chromogen colouration is seen in the negative control the test material cannot be relied upon to provide accurate localisation of the target marker, and further antibody optimization is required.

Although immunohistochemistry is a useful tool in detecting marker expression *in vivo*, many argue that the technique depends on production of a protein with a longer half-life to be identified and, in the absence of this, would provide a negative result (Yemelyanova *et al*, 2011). Investigations comparing IHC with RT-PCR in detecting micro-metastasis in breast cancer reported that the RT-PCR molecular technique increased sensitivity from 84% to 93%, and specificity from 95% to 98%, compared to H&E and IHC (Mitas *et al*, 2001). Molecular techniques, such as RT-PCR, are able to identify smaller quantities of the genes producing the protein; however, detecting gene transcripts does not always imply that translation has occurred and the resultant protein products have been expressed. Therefore the detection of the protein products requires subsequent confirmation via immunohistochemistry. For example, in the investigation of the presence of viral targets, the detection of a virus by molecular methods reveals that a viral particle is present but does not necessarily imply that the virus is active, potentially leading to over reporting of viral involvement.

Another benefit of immunohistochemistry over molecular probes is the ability to visualise markers within their intracellular location such as the cytoplasm, nucleus or membrane. This is particularly important when investigating biological processes such as EMT where cellular localisation of collagen I and α-SMA can infer the presence or absence of the pathogenic process. Localisation of these markers to the cytoplasm of the ATII cells provides evidence of EMT, whilst expression only in the interstitium and fibroblastic foci would oppose this process.

1.4 Thesis objectives

From my review of the current literature into the pathogenesis of IPF a number of hypothetical concepts arise. Firstly, with regards to the conflicting findings of evidence of EMT in human IPF lung tissue; I hypothesise that if EMT is occurring in IPF lungs, there will be evidence of mesenchymal markers in the cytoplasm of ATII cells, with concomitant loss of the cell adhesion marker E-cadherin and upregulation of N-cadherin in the area immediately close to active fibrogenesis (the fibroblastic foci). Away from these sites, in those areas of conserved alveolar epithelium, the presence or absence of cytoplasmic mesenchymal markers, growth factors and cell-cell adhesion may provide the first evidence in determining whether EMT is an initiating factor or a secondary response to stimulation from growth factors such as TGF-β.

Viral instigation of EMT has been widely reported; however its involvement in the pathogenesis in IPF is still disputed. I hypothesise that, if evidence of EMT is discovered, expression of viral markers will be localised within or close to ATII cells undergoing EMT. Attempting dual immunohistochemistry for EBV and CMV with N-cadherin may provide evidence for this mechanism in IPF lungs.

As discussed in section 1.2.3, a balance should exist between proliferation and apoptosis in the lung to regulate the number of fibroblasts and alveolar epithelial cells at sites of injury; if this balance tips towards increased proliferation and/or reduced apoptosis, fibrosis and impaired lung tissue remodelling results (Crosby and Waters, 2010). I will semi-quantify the expression of markers of cell cycle control and apoptosis within fibroblastic foci and ATII cells, and correlate these results with number of fibroblastic foci per tissue section, to assess if reduced clearance via apoptosis (measured by expression of TRAIL) or

proliferation (measured by expression of Ki-67) of the myofibroblasts and/or ATII cells results in increased fibroblastic foci and potentially correlates with increased disease activity.

Areas of honeycomb lung formation, resulting in destruction of the alveolar wall, alongside progressive expansion of the interstitium via hyperplastic ATII cell proliferation and conserved alveolar epithelium in an adjacent area of the lung, may lead to increased architectural distortion and mechanical stress within the IPF lung. This concept requires further exploration. Using a specific panel of cell cycle, proliferation, apoptotic and structural markers will determine their precise localisation in IPF lung tissue, thereby providing clues to the histological pattern of temporal heterogeneity observed in IPF lung tissue.

Accordingly the objectives in my thesis are:

1. To explore EMT in lung tissue remodelling.
2. To explore cell cycle and signalling markers in lung tissue remodelling.
3. To correlate the target makers used to identify EMT, cell cycle regulation, proliferation and apoptosis with disease activity.

My findings will further previous observations from cell culture and animal studies into the pathogenesis of lung tissue remodelling in human IPF. The novel approach of exploring differences between conserved and diseased areas within the heterogenic UIP pattern in IPF lung tissue samples may provide valuable targets for future therapeutic bioengineering/novel drugs. In addition, correlation of the above target immunohistochemical markers with histological disease activity may provide novel prognostic information to enable clinical prediction of disease progression.

Chapter 2

General Methodology

2.1 Selection of lung tissue material

As noted throughout chapter 1 many previous studies into pulmonary fibrosis have been based on bleomycin-induced murine models of the disease. Whilst these have provided valuable information on potential mechanisms of fibrosis, the models do not accurately represent or replicate the pathology of the human IPF lung. Unlike human IPF bleomycin-induced fibrosis is reversible and shows responses to treatment with steroids. In addition, there are no acute exacerbations of the disease in murine models. This raises questions over the validity of extrapolating and comparing these findings with human IPF lung tissue samples. However human lung tissue samples also have their limitations. Only patients with indeterminate IPF on HRCT undergo open lung biopsy. This may afford a selection bias towards cases that display untypical features and therefore possibly a variation in the underlying mechanisms of the disease process. This, combined with the relative low numbers of people suffering from this disease in the general population, reduces the number of patient samples available for histological study. Notwithstanding these limitations, excised human lung tissue samples continue to represent the best method of investigating the disease processes *in situ*. Such samples will serve as the basis for my thesis.

Human lung tissue samples were obtained from VATS or open lung biopsy procedures undertaken for routine diagnostic evaluation. As part of this process, the excess samples were stored in the histology department at the University Hospital of North Staffordshire as required by the Human Tissue Act (HTA), 2004. There was no new intervention or any excess tissue removal affecting the patient from whom the material had been obtained. As these tissues had been removed for clinical reasons, and not specifically

for research, this eliminated the need for specific participant consent for this research (HTA; point 23, page7; point 28, page 8).

The target group was selected by performing a search using an in-house database for lung biopsies, combined with a Systematized Nomenclature of Medicine (SNOMED) code for fibrotic lung disease. SNOMED is a systematically organised computerised collection of medical terms providing codes, synonyms and definitions covering such findings as diseases, procedures, treatments and devices (http://www.snomed.org). It is an established and proven method to index, store, retrieve, and collate clinical data consistently across specialties and sites of care. From this search, histology reports were examined to select cases that had a definitive diagnosis of IPF as opposed to any other ILDs. This search was performed by consultant histopathologist Dr Daniel Gey Van Pittius to ensure anonymity of the patient details from myself in order to avoid any experimental bias. The anonymity of patient material is also covered under the Caldicott guidelines which states that "only those individuals who need access to personally identifiable information should have access to it" (http://www.dh.gov.uk). No request was made as part of the ethical approval application for patient details apart from the histological diagnosis.

The control tissue material was also surplus material from patients who had undergone lung surgery necessary for their diagnosis/treatment.

Ethical approval to conduct the studies in my thesis was granted by the South Staffordshire Local Research Ethics Committee, ref. 08/H1203/6.

For the IPF group, glass slides containing haematoxylin and eosin (H&E) stained tissue sections were retrieved and examined independently by myself and Dr Daniel Gey Van Pittius to ensure a correct diagnosis of IPF was made in line with criteria described by the American Thoracic Society and European Respiratory Society (2010) as detailed in section 1.1.7. Any cases that showed evidence of a co-existing pathology, such as cancer or emphysema, were excluded from this study. Each case has a unique laboratory number assigned to it which is the identifier used during this study.

The control group samples consisted of lobectomy specimens removed during surgery for lung cancer. During routine histological investigation, lung tissue samples were retrieved away from the tumour; these paraffin-embedded sections were assessed independently by myself and Dr Gey Van Pittius to determine suitability for use as controls. Only lung tissue samples that were histologicaly representative of disease-free, histologicaly healthy-looking morphology were selected for control material.

In total, lung tissue samples from 21 confirmed IPF patients and 19 individual controls were chosen for my studies.

Control material used for development of antibodies was selected according to manufacturer's guidelines and obtained from the histology department control tissue bank.

2.2 Lung tissue sample preparation

2.2.1 Sample fixation and processing

Following surgical removal of the lung tissue, samples were fixed in 4% phosphate buffered formalin (Genta Medical, UK) and sent to the histology department for analysis. Specimens were fixed in formalin for a minimum of 24 hours before a macroscopic description of the tissue was made and the specimen dissected by a consultant pathologist. Samples were placed in a ThermoElectron Excelsior tissue processor (Thermo Scientific, UK) and processed according to the schedule in Table 2.1.

Step	Reagent	Temperature ^{o}C	Time, hr:mins
1	4% formal saline	45	0:05
2	Industrial methylated spirit 70%	45	0:20
3	Industrial methylated spirit 90%	45	0:30
4	Industrial methylated spirit 100%	45	0:45
5	Industrial methylated spirit 100%	45	1:00
6	Industrial methylated spirit 100%	45	1:30
7	Industrial methylated spirit 100%	45	2:00
8	Xylene	45	1:30
9	Xylene	45	2:00
10	Xylene	45	2:30
11	Paraffin wax	59	1:00
12	Paraffin wax	59	1:30
13	Paraffin wax	59	2:00

Table 2.1. Processing schedule for all lung tissue samples including use of 4% formal saline, Industrial methylated spirit and Xylene (all from Genta Medical, UK) and parrafin wax (CellPath Ltd UK). Vaccum and rotation were selected for processing to ensure adequte, uniform processing of all tissue samples.

2.2.2 Tissue sample embedding and section cutting

Following processing samples were removed from the tissue processor, embedded in molten paraffin wax (CellPath, UK) and allowed to cool.

Tissue sections 3µ thick were cut using a Leica RM2255 semi-automated microtome (Leica Microsystems Inc, USA), mounted onto electrocharged glass slides (CellPath, UK) and dried at 60^{o}C for 30 minutes to ensure adhesion.

2.2.3 Haematoxylin and Eosin staining

One section from each sample was initially stained with haematoxylin and eosin to allow for initial histological reporting and subsequent assessment of disease severity. All staining was automated using a Tissue-Tek Prisma automated slide stainer (Sakura, USA).

Sections were immersed in Xylene (Genta Medical, UK) for 3 minutes to deparaffinise the tissue section followed by dehydration through a series of four 30 second immersions in industrial methylated spirits (IMS) (Genta Medical, UK) to water. Sections were then placed in haematoxylin Z (CellPath, UK) for 9 minutes, differentiated in 2% acid alcohol (Appendix 1) for 6 seconds, blued in an alkaline tap water solution (Appendix 2) and washed in tap water. The slides were then stained by immersion in Eosin solution (Appendix 3) for 3 minutes, washed in water, dehydrated through IMS (Genta Medical, UK), cleared in Xylene (Genta Medical, UK) and mounted using Xylene-activated adhesive-backed Tissue-Tek film (Sakura, USA).

2.3 Immunohistochemistry

2.3.1 Target marker selection

Selection of a panel of immunohistochemical markers for investigation was determined by a thorough literature review of previous studies that had utilised similar immunohistochemical approaches to investigate processes of EMT and cell cycle regulation. Furthermore, my thesis also explores for presence of expression of the viral markers EBV and CMV, specifically chosen as they had been implicated in IPF (Sides *et al*, 2011, Tang *et al*, 2003). Further details of marker selection are included in sections 3.2.2 and 4.2.2.

Where possible, monoclonal antibodies to selected markers were sourced to ensure more accurate localization and reduce the possibility of false positive expression and non-specific background staining which may occur using polyclonal antibodies. All marker antibodies were developed and tested using positive control material according to manufacturer guidelines. Antigen retrieval and dilution factors of primary antibodies were developed in parallel using a combination of manufacturer guidelines and previous reports. The markers E-cadherin, α-SMA, Ki-67, EBV, CMV and Cyclin D1 were previously developed and are used routinely in the histopathology department at the University Hospital of North Staffordshire. Final protocols for these markers are detailed in Appendix 4. All other markers were developed and optimised by myself and are detailed in section 2.3.2.

2.3.2 Target marker antibody development and optimisation

Antibody development is an essential process to ensure accurate localisation of markers in tissue samples undergoing immunohistochemical analysis. Formalin fixed paraffin embedded tissues provide an excellent source of tissue for scientific investigation, however formalin fixation can mask the target antigens via the cross linkage of un-

associated proteins rendering the antigen unavailable for attachment to the required target marker antibody. The first step in antibody development is to unmask these antigens via a process termed antigen retrieval.

Antigen retrieval methods vary depending on the antigen being investigated. Some antigens are only weakly cross-linked with un-associated protein complexes within the tissue and require gentle enzymatic digestion to disassociate the antigen from the surrounding proteins without destroying the epitope. Other antigens require a more harsh method of unmasking, such as heat-mediated retrieval in varying pH buffer solutions using a microwave or pressure cooker. A basic guide to appropriate antigen retrieval for each antibody is provided by the antibody supplier in most cases, however as fixation and processing schedules differ from laboratory to laboratory the exact duration and degree of antigen retrieval required also varies. An attempt was made to standardise the antigen retrieval step to accommodate dual-immunohistochemistry. Most markers purchased for this study recommended heat-mediated antigen retrieval at pH6 (standard antigen retrieval); where antigen retrieval methods were not provided by the manufacturer (such as for surfactant protein C), both enzyme and heat-mediated antigen retrieval methods were tested and compared. Standard heat mediated antigen retrieval consisted of immersion of the slides in citrate buffer pH6 (Appendix 5), which was then microwaved (Panasonic, 800W, Japan) at 100% power for 10 minutes followed by a further 10 minutes at 70% power. For enzymatic digestion deparaffinised slides were placed in a 5% trypsin solution at 37 degrees for 10 minutes.

For antigen $p21^{WAF1}$ high pH9 antigen retrieval was recommended by the manufacturer in order to unmask the antigen for antibody binding, with microwave heating

for 20 minutes at 100% power. Sections were allowed to cool in the buffer solution for 30 minutes before washing in tap water. Initial primary antibody dilution for $p21^{WAF1}$ was 1:50 for 30 minutes at room temperature. This resulted in some slight non-specific cytoplasmic staining. With high pH antigen retrieval methods non-specific background staining will always be an issue therefore no attempt to increase the primary antibody dilution or incubation time was made. When the protocol was tested on IPF lung tissue clear nuclear expression was identified within ATII cells and scattered cells within the bronchiolar epithelium.

The SOCS3 antibody was initially trialled using standard heat mediated antigen retrieval. Initial antibody dilution was 1:50 with a 30 minute incubation time at room temperature resulting in intense staining within the cytoplasm of a range of cell types with non-specific background staining present. As a result the primary dilution was increased to 1:75 and a higher pH buffer was tested. Increasing the dilution to 1:75 should reduce the amount of non-specific background staining. Changing the buffer solution from pH6 to pH8 can help to determine if insufficient antigen retrieval is resulting in non-specific binding. Antigen retrieval was therefore changed to EDTA buffer pH8 (Appendix 6), microwaved at 100% for 10 minutes, followed by 10 minutes at 70%. The slides and buffer were allowed to cool for 20 minutes before being washed for 10 minutes in tap water. This protocol resulted in very strong cytoplasmic expression within a range of cells but also increased the amount of background staining. SOCS3 is a *polyclonal* antibody and can therefore sometimes cross react with other non specific epitopes and antigens leading to the non-specific background staining seen. To reduce this background staining, which can mask specific binding, a reduction in primary antibody incubation temperature to 4 degrees overnight was trialled.

However, even with a reduction in temperature non-specific background was still present within the tissue and so the antibody dilution was increased to 1:100. This then provided clear cytoplasmic expression within the ATII cells with no non-specific staining.

The manufacturer recommended using a pH8 EDTA antigen retrieval solution for p53 antigen retrieval. Control tissue slides were placed in EDTA buffer pH8 and microwaved at 100% power for 10 minutes followed by 10 minutes at 70% power. Slides were allowed to cool within the buffer solution for 30 minutes prior to washing in tap water. Initial dilution was 1:800 with the incubation time 30 minutes at room temperature resulting in little expression in the control lung and only few cells expressing the marker in the ovary control tissue. In normal tissue p53 behaves as a tumour suppressor initiating cell senescence in cells with DNA damage to allow time for repair. According to the manufacturer the p53 protein has a very short half-life and is therefore only present in minute amounts, not normally detectable by immunohistochemistry in un-diseased tissue. Continued stimulation or mutations of the p53 gene however results in accumulation of the protein, which is then detectable via immunohistochemistry. The absence of p53 in control lung is not a reliable indicator of antibody optimization. I therefore continued antibody development on IPF tissue samples keeping the antibody dilution at 1:800 for 30 minutes incubation at room temperature. This resulted in clear nuclear expression in hyperplastic ATII cells of IPF cases and scattered bronchiolar epithelial cells.

After antigen retrieval slides were washed in running tap water for 10 minutes to ensure removal of the antigen retrieval solutions.

Antibody dilution was based on initial recommendations by the manufacturer and subsequent adjustment made by myself during the development process. For the collagen I

antibody the manufacturer did not provide a starting dilution therefore I selected three starting dilutions; 1:500, 1:300, 1:200. All dilutions tested resulted in positive expression of collagen I fibres; however a dilution of 1:500 demonstrated the least amount of non-specific background staining.

Incubation time of the antibody was initially set at 30 minutes at room temperature and only increased to 1 hour at room temperature if adjustments to the antibody dilution failed to achieve crisp clear marker visualisation with no non-specific background staining; this was necessary for SP-C, Twist, TGF-β and TGF-β receptor.

IPF lung tissue contains increased numbers of macrophages, which also have the potential to cross-react with the marker antibodies in a non-specific manor, possibly due to the engulfment of cellular debris and associated antigens, resulting in a brown colouration within the cytoplasm of these cells that can be mistaken for positive staining when using Diaminobenzidine (DAB) as a chromogen. Therefore following optimisation in control tissues and to avoid the loss of valuable IPF lung tissue I only attempt the protocol on a few test cases in the first instance.

TGF-β antibody was developed using placenta as a positive control tissue where cytoplasmic expression is seen in trophoblastic cells. As several proteins are synthesised in the placenta a protein block is included before addition of the primary antibody to prevent non–specific hydrophobic or ionic interactions with the primary antibody. Protein blocks are also required for $p16^{INK4A}$, TRAIL, DR4 and DR5 to reduce non-specific background staining masking the antibody expression. On occasion, although antibodies are developed to an optimal standard in control tissues, when the same protocol is performed on test tissues the technique may require further refinement. This is especially true for tissues that contain

high degrees of avidin and/or biotin, such as liver, kidney or tissues with large quantities of red blood cells. The avidin naturally present in these tissues and cells can cross-react with the peroxidase-conjugated streptavidin detection system used by the DAKO REAL detection kit. The Dako REAL detection kit uses *Streptomyces avidinii* refined by a two-step glutaraldehyde method to reduce the isoelectric point to close to neutral in an attempt to prevent non-specific ionic interaction (Dako UK, 2006). The placental control tissue for TGF-β contained a high number of red blood cells, however as there are fewer red blood cells within lung tissue compared with placental tissue non-specific background was not an issue when the protocol was applied to the test sections.

Control slides for TGF-β receptor were subjected to standard heat mediated antigen retrieval. Initial dilution tested was 1:30 for 60 minutes at room temperature. This resulted in clear but weak membrane expression of the marker; however there was some non-specific background staining present. To reduce the background staining I increased the dilution of the primary antibody to 1:40 and extended the DAB incubation time by three minutes to compensate for the increased dilution. When tested on IPF and control lung samples the expression of the target marker was too pale and so I placed the slides into a copper sulphate solution (Appendix 7) to enhance the DAB intensity without increasing non-specific background staining. Inflammatory cells within the lung tissue samples demonstrated clear positive membrane expression of the antibody.

Development of the TRAIL antibody began by subjecting the control tissue sections to standard heat mediated antigen retrieval. Initial antibody dilutions were tested at 1:50 and 1:00 and tissue sections incubated for 30 minutes at room temperature. Weak staining intensity was identified and therefore a reduction in antibody dilution to 1:20 with

incubation time set at 30 minutes and a 1:50 dilution with 1 hour primary antibody dilution were trialled on three random IPF tissue sections alongside the control tissue. In IPF tissue samples all cells demonstrated very strong DAB staining and non-specific background, therefore an increase in dilution to 1:00 for 30 minutes with the addition of incubation with a protein blocking solution (Dako, Denmark) was performed prior to incubation with the primary antibody. Again this resulted in non-specific staining in the lung tissue sections. Despite multiple attempts and variations in protocol target marker expression was still unsatisfactory. Consultation with the manufacturer resulted in the recommendation of an alternate positive control tissue, skin containing basal cell carcinoma. The company also provided a replacement antibody. Following microwave antigen retrieval as before lung tissue sections were incubated for 30 minutes with an antibody dilution of 1:75 following pre-treatment with a protein blocking solution. This gave similar results so the dilution was further increased to 1:80, resulting in clear expression of TRAIL in BCC skin, control and IPF lung tissue samples with no non-specific background staining.

A summary of each antibody antigen retrieval method, dilution, and incubation time and control material are listed in Tables 3.1 and 4.1.

Negative control slides from each IPF and control lung tissue samples were run alongside each test section, replacing the primary antibody with Tris-buffered saline (Appendix 8) to rule out the presence of endogenous pigment or cross reaction providing a false positive result.

Following antigen retrieval as detailed above slides were placed on a DakoCytomation flat bed linear automated immunostainer (Dako, Denmark) and were stained following the protocol outlined in Table 2.2.

Step	Reagent and incubation time	Source of reagent and product code
1	Dako REAL™ peroxidase-blocking solution 5 minutes	DakoCytomation (Demnark) S2023
2	Wash in Tris-buffered saline	Made in house (Appendix 8)
3	Incubation with primary antibody 30 or 60 minutes	See sections 2.3.2
4	Wash in Tris buffered saline	
5	Dako REAL™ link, biotinilated secondary antibody 15 minutes	DakoCytomation (Denmark) K5001
6	Wash in Tris buffered saline	
7	Dako REAL™ Detection system streptavidin peroxidase 15 minutes	DakoCytomation (Denmark) K5001
8	Wash in Tris buffered saline	
9	Dako REAL™ detection system (DAB+) 2 x3minutes	DakoCytomation (Denmark) K5001
10	Wash in water	

Table 2.2 Standardised step-wise approach to immunohistochemical procedure following antigen retrieval detailed in section 2.3.2.

Sections are removed from the automated stainer, washed in tap water and counterstained with Haematoxylin Z (CellPath, UK) for 3 minutes, differentiated in 2% acid alcohol solution (Appendix 1), blued in an alkaline water solution (Appendix 2), dehydrated through a series of alcohols (Genta Medical, UK), cleared in Xylene (Genta medical, UK) and coverslipped.

2.3.3 Dual staining immunohistochemistry

Dual staining immunohistochemistry is a useful tool in the research setting to detect potential interactions between target molecules. The technique allows for the detection of two antigens on the same tissue section as long as the antigens are located in different cell types or different cellular compartments. Previously dual antibody staining was only performed using fluorescent markers, which required specialist viewing equipment. The development of dual immunohistochemistry provides a permanent preparation viewed using a standard light microscope that can be performed on formalin-fixed paraffin embedded tissue.

Dual immunohistochemistry can only be performed on antigens located in different cellular compartments or cell types to clearly visualise each antigen separately, for antigens located in the same cellular compartment immunofluorescent techniques must still be performed. Specific antigen retrieval methods and antibody dilution times are detailed in sections 3.2, Table 3.1 and 4.2, Table 4.1. The protocol for dual immunohistochemical staining is detailed in Table 2.3.

The order of the antibodies is dependent on cellular localisation. Best results are obtained by performing dual immunohistochemistry in the following order; 1st nuclear, 2nd membrane, 3rd cytoplasmic. Visualisation of the antibody used either DAB (brown, Dako Cytomation, Denmark) or very intense purple (VIP, purple, LabVision, UK, product code SK-4600).

Step	Reagent and incubation time	Source of reagent and product code
1	Dako REAL™ peroxidase-blocking solution 5 minutes	DakoCytomation (Demnark) S2023
2	Wash in Tris buffered saline	Made in house (Appendix 8)
3	Protein block 20 minutes	DakoCytomation (Denmark) X0909
4	1st Primary antibody	See section 2.3.2 and tables 3.1, 4.1 for individual markers.
4	Wash in Tris buffered saline	
5	Dako REAL™ link, biotinilated secondary antibody 15 minutes	DakoCytomation (Denmark) K5001
6	Wash in Tris buffered saline	
7	Dako REAL™ Detection system streptavidin peroxidase 15 minutes	DakoCytomation (Denmark) K5001
8	Wash in Tris buffered saline	
9	Dako REAL™ detection system (DAB+) 2 x3minutes	DakoCytomation (Denmark) K5001
10	Wash in water	
11	Avidin block 15 minutes	Vectorlabs (UK) SP-2001
12	Wash in Tris buffered saline	
13	Biotin block 15 minutes	Vectorlabs (UK) SP-2001
14	Wash in water	
15	Protein block 20 minutes	DakoCytomation (Denmark) X0909
16	Blot sections	
17	2nd Primary antibody incubation	See tables 3.1 and 4.1 for individual dilutions and times
18	VECTASTAIN® ABC 30 minutes	VectorLabs (UK) PK-6200
19	Wash in Tris buffered saline	
20	Incubation with second chromogen Very Intense Purple (VIP) 5 minutes	VectorLabs (UK) SK-4600
21	Wash in water	

Table 2.3. Standardised step-wise approach followed in dual staining immunohistochemistry following antigen retrieval detailed in sections 2.3.2 and 2.3.3.

Sections are counterstained in haematoxylin Z (CellPath, UK) for 3 minutes, differentiated in 2% acid alcohol, blued in an alkaline water solution, dehydrated through a series of alcohols (Genta Medical, UK), cleared in Xylene (Genta Medical, UK) and coverslipped.

2.3.3.1 Dual immunohistochemistry of Twist and N-cadherin

Dual IHC of Twist and N-cadherin was performed to attempt to identify cells undergoing EMT. If EMT is occurring one or both markers would be expected to be present in an individual epithelial cell. Antigen retrieval methods and antibody dilutions are as detailed in section 2.3.2.

The first nuclear marker Twist is identified by DAB, the second membrane expressing marker, N-cadherin, is identified by VIP. This gave clear membrane expression of the N-cadherin with defined nuclear expression of Twist. No further development was needed.

2.3.3.2 Dual immunohistochemistry of Epstein Barr Virus and α-smooth muscle actin

EBV has been shown to induce EMT in cell culture studies (Tang *et al*, 2003, Pozharskaya *et al*, 2009, Sides *et al*, 2010), while cytoplasmic expression of α-SMA in epithelial cells is an indicator of EMT. Co-localisation of EBV and α-SMA in ATII cells would therefore suggest a potential causal link between viral infection and the pathogenesis of IPF via EMT. Antigen retrieval methods and antibody dilutions are as detailed in section 2.3.2 and tables 3.1 and 4.1 unless otherwise stated.

The first marker EBV is indentified by DAB, the second marker α-SMA is identified by VIP. EBV requires gentle trypsin antigen retrieval whilst α-SMA requires a more aggressive

heat mediated microwave antigen retrieval when stained individually. Microwave antigen retrieval would destroy the EBV epitope; therefore I reduced the dilution of α-SMA from 1:800 to 1:500 to see if this would enable visualisation of the marker using enzymatic digestion by trypsin. EBV was identified in the control tissue; however α-SMA expression was weak and patchy with some blood vessels that would be expected to be expressing the marker being negative. Further reduction in dilution of the α-SMA antibody down to 1:400 with the inclusion of a protein block after the addition of the avidin/biotin blocking treatment reduced any non-specific staining by α-SMA.

2.3.3.3 Dual immunohistochemistry of cytomegalovirus and α-smooth muscle actin.

CMV has been shown to induce EMT (Tang *et al*, 2003, Pozharskaya *et al*, 2009, Sides *et al*, 2010), whilst cytoplasmic expression of α-SMA identifies cells undergoing EMT. Co-localisation of CMV and α-SMA would therefore suggest a potential causal link between viral infection and EMT in the pathogenesis of IPF. Antigen retrieval methods and antibody dilutions are as detailed in section 2.3.2 and tables 3.1 and 4.1 unless otherwise stated.

The first antibody marker CMV is identified by DAB, the second marker α-SMA is identified by VIP. Initial testing using the α-SMA primary antibody dilution for standard immunohistochemical analysis, 1:500, resulted in non-specific background staining. The dilution was increased to 1:600, however CMV staining intensity is weak compared to α-SMA resulting in masking of the CMV marker. It was therefore not possible to perform a dual-immunohistochemical technique for CMV and α-SMA.

2.3.3.4 Dual immunohistochemistry of Cyclin D1 and Suppressor of cytokine signalling 3

Cyclin D1 and SOCS3 were selected for dual IHC as SOCS3 has been shown to inactivate STAT3 resulting in the promotion of Cyclin D1 leading to cell cycle progression (Lu *et al*, 2006). Therefore I predict that a portion of cells would express both markers. Antigen retrieval methods and antibody dilutions are as detailed in section 2.3.2 unless otherwise stated.

The first nuclear marker to be applied, Cyclin D1, is identified by DAB resulting in a brown colouration of the target antibody. The second cytoplasmic marker SOCS3 is identified by Very Intense Purple (VIP) (Vector Labs, UK). No counter stain was used as recommended by Vector Labs (UK).

Initial testing revealed non-specific background staining which was prevented in subsequent testing by the inclusion of a protein block after the avidin/biotin blocking stage and prior to the addition of the SOCS3 antibody. Manufacturer guidelines on dual-immunohistochemistry did not advocate the use of a nuclear counterstain as this would detract from the dyes used in the detection of the marker antibodies. However identification of fibroblastic foci and ATII cells proved extremely difficult and so a haematoxylin counterstain was added in my studies.

2.3.3.5 Dual immunohistochemistry of p53 and surfactant protein C

p53 and SP-C were selected for dual immunohistochemistry to determine differences between control and IPF ATII cells with regards to cell senescence, as detected by the expression of p53 and absence of SP-C. Pattern of expression of these markers in IPF lung will be examined in temporally conserved and fibrotic areas within same specimens and compared to control samples to determine whether the alveolar epithelium in IPF

conserved areas are equivalent to control alveolar epithelium and functioning normally. For the development of individual antibodies p53 required a harsh antigen retrieval method; EDTA pH8, compared to SP-C; standard microwave pre-treatment in citrate buffer pH6. To standardise the initial antigen retrieval method sections were microwaved in EDTA pH8 for 10 minutes at 100% power and 10 minutes at 70% power. Dilutions for p53 and SP-C remained as previously developed; 1:800 and 1:1500 respectively. No further development was necessary.

2.3.2.6 Dual immunohistochemistry of $p21^{WAF1}$ and surfactant protein C

$p21^{WAF1}$ and SP-C dual immunohistochemistry is performed to identify ATII cells within the IPF lung tissue samples that are non-proliferative and are not progressing through the cell cycle. The pattern of expression will be compared to p53 to determine if $p21^{WAF1}$ is operating in a p53-independent manor. Particular attention with focus on the ATII cells overlying the fibroblastic foci to determine any potential interaction (such as contact inhibition between the myofibroblasts and ATII cells). The $p21^{WAF1}$ marker was initially developed using an intense high pH9 heat mediated antigen retrieval method compared to the gentler citrate buffer pH6 for SP-C (section 2.3.2). As $p21^{WAF1}$ could not be detected when using citrate buffer pH6, a compromise was made resulting in weaker expression of the SP-C marker using pH9 antigen retrieval solution and microwaving at 100% power for 20 minutes.

2.4. Imaging and observational analysis

Sections were viewed using a Nikon Eclipse E600 microscope (Nikon, Japan) with Nikon Digital NET camera Dn100 (Nikon, Japan) digital camera attachment. I performed an overall scan of each immunohistochemicaly stained section for each target marker, starting at the top of the section (marked with pen) then systematically examining marker expression localisation in a clockwise approach to the mark, ensuring review of the whole section. Both IPF and control tissue sections that showed typical and unusual features were selected for microphotography. In IPF tissue samples, areas of fibroblastic foci, ATII cell hyperplasia and conserved areas were specifically photographed. In the control lung tissue images were captured of normal alveolar epithelium and in the case of α-SMA and collagen, blood vessels were imaged to show typical expression of these markers. Images were taken at magnifications of x10, x40, x100, x200 and x400. Images were captured and stored as JPEG (Joint Photographic Experts Group) images on a SanDisk CompactFlash™ (USA) memory card for macroscopic presentation of results. JPEG images can be compressed to varying degrees with little perceptible loss in image quality (http://www.jpeg.org, retrieved 13-5-2012).

The distribution of markers expressed by ATII cells in conserved and disease-affected areas were described for IPF lung tissue sections and compared to expression in ATII cells of the control group. Marker expression was also described for fibroblastic foci in IPF lung samples. An overall assessment was made to identify any marker expression in all other cell types including ATI cells, macrophages and inflammatory cells if present and noteworthy. Within the IPF tissue sections particular focus was placed on examining differences between conserved and diseased areas.

2.5. Semi-quantitative analysis

Sections were reviewed by myself and then separately by an independent pathologist to ensure accurate localisation of markers. I then scored each tissue section by examining expression of markers at sites of fibroblastic foci and ATII cells in IPF and control samples. For the ATII cells in IPF samples, 3 random fields of 100 hyperplastic cells were counted at x100 magnification and the proportion of cells expressing each marker was recorded with the mean of the three fields giving the final value used in this study. Within control lung sections the distribution of the ATII cells is scattered and 100 cells cannot be counted in just one field, therefore, a systematic scan of the section starting at the 12 o'clock position of the section and scanning in a clockwise direction was performed to count 100 cells.

For fibroblastic foci within IPF lung biopsies, the scanning method was as used for the ATII cells in the control group. 100 cells were counted within the fibroblastic foci; if there were enough fibroblastic foci this was repeated three times and the mean expression used for analysis.

A semi-quantitative analysis was used to compare groups using a modified Allred scoring system, also referred to as the Quick score method (Harvey *et al*, 1999) (Table 2.4). My modification to this scoring system is the omission of the staining intensity. In support of this, intensity of staining was equally not assessed in two key studies into EMT and IPF, Yamada *et al* (2008), and Harada *et al* (2010). The study by Harada semi-quantified their results by determining percentage of cells expressing the target marker. According to Walker (2006) an arbitrary weak, moderate or strong is not appropriate and, if intensity is being assessed there has to be a positive control demonstrating different levels of staining

included with each staining batch. As many of the markers used in my thesis are, according to the manufacturers, purely for research purposes only and are not verified for clinical use, no control tissue demonstrating weak, moderate or strong expression is available. When examining protein expression it is recommended that several different antibodies are used against the same protein because different antibodies detect different epitopes (Walker, 2006). This is supported by an investigation into the p53 antibody marker where it was reported that the extent of p53 expression varied depending on the antibody used, making it difficult to compare between publications (McCluggage *et al*, 2005).

In addition variability in intensity of staining can be a result of the plane of the tissue section; a cell may be entirely within the plane of a tissue section, or only part of the cell may be present affecting staining intensity (Taylor and Levenson, 2006). Computerized image analysis software has been developed to aid in quantification of immunohistochemistry by measuring absorption. Using DAB as a chromogen there is only a linear relationship between the amount of antigen and staining intensity at lower levels of staining intensity (Fritz *et al*, 1995). At high levels of antibody expression the non linear relationship can lead to inaccurate readings. It is for these reasons and in order to compare my results with those published by Harada that a staining intensity is not calculated in my studies.

Previous investigations into the validity of the Allred and alternate 'H score' scoring technique revealed no discernible statistical difference and concluded that there was no advantage to using the more labour intensive H score approach (Detre *et al*, 1995).

Staining score	Positive staining cells (%)	Descriptive expression
0	0	No expression
1	<1	Negligible expression
2	1 to 10	Scanty expression
3	10 to 33	Low-moderate expression
4	33 to 66	Moderate expression
5	>66	Extensive expression

Table 2.4 Modified Allred scoring system for semi-quantitative immunohistochemical analysis of ATII cells and cells contained within fibroblastic foci.

For assessment of disease activity in IPF cases, I performed a semi-quantitative assessment of H&E stained sections for each individual biopsy using a scale of 0–6 for the extent of fibroblastic foci as previously described by Nicholson *et al* (2002) and illustrated in Figure 2.1. The investigation by Nicholson *et al* published representative images of the number of fibroblastic foci per field of view, but did not give exact number of foci per measurable area. In my thesis, I therefore scored the tissue sections based on comparison to the images presented by Nicholson *et al*. Sections were examined at a magnification of x40 using a systematic scanning of the slides starting at the 12 o'clock position and scanning the section in a clockwise approach to the marked start point. A score of 0 was assigned to those samples containing no fibroblastic foci, a score of 6 was given to those samples with the most profuse number of foci. These scores were then correlated against the mean expression scores for each target immunohistochemical marker described in section 2.3.6.

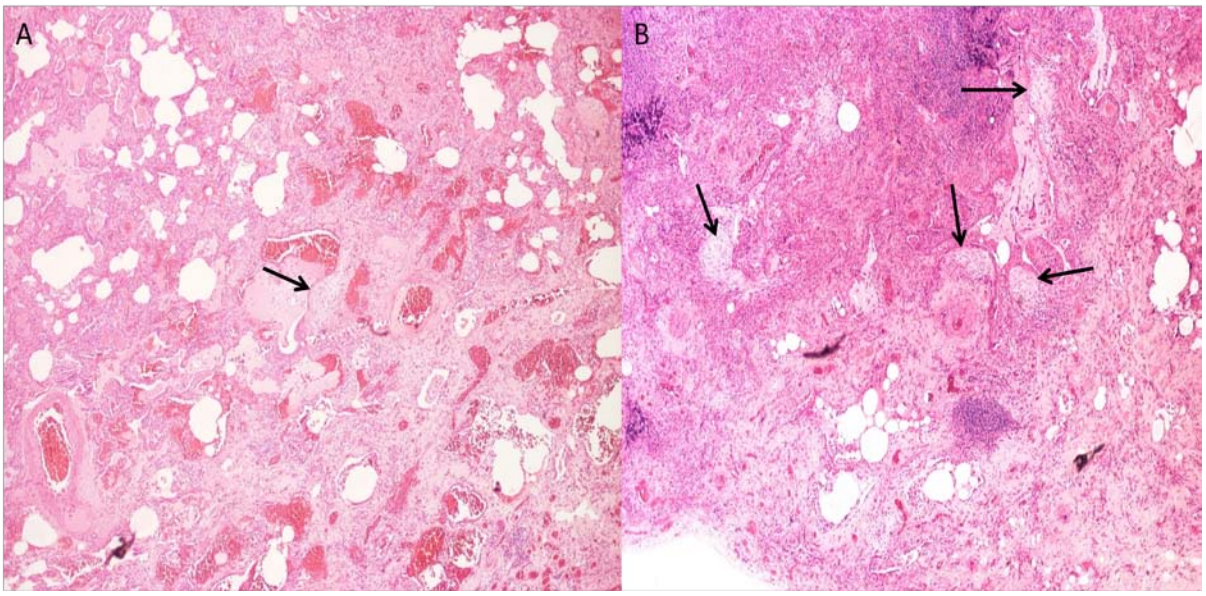

Figure 2.1 Representative histological images of IPF lung tissue stained with H&E used for assessing disease activity. A. IPF lung tissue with only one fibroblastic foci in the field of view (score 1). B. IPF lung tissue showing a high number of fibroblastic foci in the one field of view (score 6).

2.6. Statistical analysis

A Mann Whitney U test was used for comparisons between IPF and control ATII cells. This method was selected as the data is ordinal/non-parametric with variation in population size between the two groups. Results are presented as a mean ±SD score for each marker. Differences were considered significant if $p \leq 0.05$. Statistical analyses we re performed using WinSTAT, (R. Fitch Software, Bad Krozingen, Germany).

To determine correlations of target marker expression levels in hyperplastic ATII cells and cells within fibroblastic foci with disease activity, a Pearson correlation co-efficient was calculated. The results were interpreted and categorised as no correlation, weak, moderate and strong correlation according to Cohen (1998), Table 2.5. Statistical analysis was performed using Minitab® 15 Statistical Software (USA).

Correlation	Negative	Positive
None	-0.09 to 0.0	0.0 to 0.09
Weak	-0.3 to -0.1	0.1 to 0.3
Moderate	-0.5 to -0.3	0.3 to 0.5
Strong	-1.0 to -0.5	0.5 to 1.0

Table 2.5 Categorisation of Pearson correlation scores as devised by Cohen (1998)

Chapter 3

Exploration of epithelial mesenchymal transition in lung tissue remodelling: correlation to disease activity

3.1 Introduction

One of the key features of IPF is the histological identification of fibroblastic foci within areas of ATII hyperplasia as described in chapter 1.1.7. These foci are composed of differentiated fibroblasts called myofibroblasts (Maher *et al,* 2007) responsible for the excessive collagen deposition and tissue remodelling seen in IPF. There are four proposed sources of the myofibroblast, 1) Resident fibroblast proliferation and activation (Phan 2002), 2) Circulating fibrocytes attracted to regions of lung injury (Lama and Phan 2006), 3) endothelial-mesenchymal transition (EndEMT) (Hashimoto *et al* 2010) and 4) Epithelial-mesenchymal transition (EMT) (Willis *et al* 2005, Kim *et al* 2006). Accordingly, this chapter focuses on the extent to which the process of EMT provides a source of myofibroblasts in fibrogenesis and what role it plays, if any, in the tissue remodelling characteristic of IPF.

As described in chapter 1.2.2, EMT has been characterised by the *loss* of epithelial cell-cell adhesion proteins (e.g. E-cadherin) and the transformation to a mesenchymal phenotype with *gain* of markers such as α-SMA and N-cadherin (mediator of calcium-ion-dependent adhesion (De Wever *et al* 2004)). It is hypothesised that hyperplastic ATII cells and/or lung endothelial cells in IPF transform to produce the fibroblastic foci observed in IPF (Harada *et al* 2010).

A number of transcription and growth factors have been implicated in the pathogenesis of IPF and as drivers of EMT. The transcription factor Twist, not normally expressed in healthy human adult lung, induces proliferation and differentiation of epithelial cells and is proposed to drive both EMT (Pozhaeskaya *et al* 2009) and EndMT (Potenta *et al* 2008, Zeisberg *et al* [a] 2007, Zeisberg *et al*[b] 2007). Conversely, in hepatocellular carcinoma

cell lines, Twist expression did not increase cell proliferation; however indicators of cell migration increased (Matsuo *et al*, 2009). Twist 1 has been shown to directly or indirectly repress E-cadherin expression via Enhancer boxes (E-boxes) which are target sequences for transcription factors that are involved in the control of tissue differentiation (Pozharskaya *et al*, 2009). The mediator of calcium-ion-dependent adhesion and proposed indicator of EMT, N-cadherin, is a transcriptional target of Twist. Upregulation of Twist 1 has been reported in cell culture and animal models resulting in induction of N-cadherin (Ng *et al*, 2012). Hypoxia or mechanical stresses are known to turn on Twist expression (Sun *et al* 2009) with a disproportional erythyropoietic response being a notable feature of IPF (Tsantes *et al*, 2003) and the notion of alveolar collapse/mechanical stress leading to formation of fibroblastic foci being proposed in IPF disease pathogenesis (Leslie, 2011). In IPF lung tissue, expression of Twist was identified in the nuclei of ATII cells, with co-localisation of SP-C and N-cadherin (Pozharskaya *et al*, 2009). The same study found that E-cadherin repression alone is not sufficient to induce EMT and that epithelial cells still require the acquisition of mesenchymal markers, such as α-SMA (Pozharskaya *et al*, 2009) to complete the differentiation.

Transforming Growth Factor-β (TGF-β) is involved in mediating fibrotic tissue remodelling and the inhibition of ATII cell proliferation (Bartram *et al* 2004). TGF-β has also been reported to be an inducer of EMT (Willis *et al* 2005) in cultured alveolar epithelial cells through Snail1, Snail2 and Smad-mediated signalling. In addition collagen I, which accumulates in the lungs of IPF patients, has been shown to promote EMT in lung cancer cells via associated TGF-β signalling (Shintani *et al* 2008).

To support the hypothesis of an EMT mechanism in the development of interstitial fibrosis and the formation of fibroblastic foci in IPF, I would expect to find down-regulation of E-cadherin in the ATII cells overlying areas of established fibrosis combined with upregulation of N-cadherin and Twist. TGF-β protein would be expected to be present within the ATII cells overlying the fibroblastic foci, with concomitant upregulation of the TGF-β receptor. Antibody markers for α-SMA and N-cadherin will be used in my study to confirm a mesenchymal phenotype within fibroblastic foci; a marker for SP-C will distinguish ATII cells from other epithelial cells present. Correlation of multiple EMT markers with number of fibroblastic foci will aid in identifying the magnitude of involvement of EMT in the formation of fibroblastic foci and disease activity. The cell proliferation marker Ki-67 will be used to assess wound remodelling via proliferation of ATII cells, rather than the process of differentiation.

Chapters 1.1.3 and 1.2.2 described the role of viruses as both causative agents and instigators of EMT with links to IPF pathogenesis (Egan *et al*, 1995, Kelly *et al*, 2002, Arase *et al*, 2008, Sides *et al*, 2011, Pozharaskaya *et al*, 2009). The latter study demonstrated an association between the epithelial injury caused by chronic herpes virus infection and lung fibrosis in rodents. This study also provided evidence of EBV involvement in the inducement of EMT in IPF lung tissue using RT-PCR. A study by Tang *et al* (2003) examined viral expression and load, reporting that herpes virus-8 (HHV-8) was detected significantly more in sporadic IPF cases than the control group. However, when examining both groups for any variant of herpes virus both had levels of viral positivity of almost 100%. A more recent study by Wootton *et al* (2011) examined the sputum from 43 IPF patients; using multiplex

PCR, microarrays and cDNA sequencing they found EBV in only 2 cases and HPV in only one case of IPF.

However despite the above quoted studies the precise involvement of viruses in IPF remains unclear. It is plausible that the observed discrepancies in findings across the studies may be due to the use of various molecular probes to locate the gene fragments of the viruses rather than determining actual protein expression, leading to over-reporting of viral incidence in IPF pathogenesis.

To date, much of the evidence presented on the potential source of fibroblasts and myofibroblasts has been based on cell culture and animal models of pulmonary fibrosis which do not accurately reflect the disease. The aim of this chapter is to determine whether EMT is taking place and to further the understanding of lung tissue remodelling observed in patients with IPF using detailed immunohistochemical analysis. If there is evidence of EMT occurring in IPF it is reasonable to assume that there would be a correlation between the extent of EMT markers and the numbers of fibroblastic foci within the tissue. If proven these findings could then be used to create a marker panel of immunohistochemical antibodies to enable histopathologist's and clinicians to highlight individuals with increased disease activity. Furthermore, I will determine the extent of viral involvement, if any, in IPF pathogenesis and the potential inducement of EMT using immunohistochemistry to identify and quantify protein expression of EBV and CMV in *ex vivo* IPF lung tissue.

3.2 Materials and methods

3.2.1 Lung tissue samples

Lung tissue samples were selected and prepared as detailed in chapter 2.2. Samples were analysed from 21 randomised patients with histologicaly confirmed IPF and 19 histologicaly normal lung tissue samples for the control group.

3.2.2 Selection of markers

The selection of markers for exploring the role of EMT in IPF was based on markers used in previous investigations of EMT discussed in detail in section 1.2.2 and summarised in Table 3.1. Multiple markers were analysed to provide a comprehensive analysis of the role and potential mechanism of EMT in IPF lung tissue samples. To exploit previous findings in the literature, my study included exploration of the co-localisation of Twist and N-cadherin using dual-immunohistochemistry; this evaluated direct interaction of Twist inducement of N-cadherin within those ATII cells present in areas of fibroblastic foci. In addition expression of the proliferation marker Ki-67 was used to determine if ATII cells were undergoing proliferation, rather than differentiating or transforming via EMT. EBV and CMV viral protein markers were chosen to determine potential viral inducement in IPF/EMT as proposed by previous investigators (Sides *et al*, 2009, Tang *et al*, 2003). Markers are summarised in Table 3.1.

3.2.3 Immunohistochemistry

Preparations of lung tissue samples for analysis are detailed in chapters 2.2.1 and 2.2.2. Briefly, lung tissue sections, 3µ thick, were cut from paraffin embedded lung tissue samples and placed onto electro-statically charged slides (CellPath Ltd, UK). Sections were

deparaffinised in Xylene for 3 minutes and rehydrated through alcohol to water prior to antigen retrieval.

An attempt was made to standardise antigen retrieval methods for all markers to allow for dual-immunohistochemistry; however this was not possible for viral markers as microwave antigen retrieval methods resulted in destruction of the viral epitope. Initial dilution factors and selection of positive control material for the development of target marker antibodies were based on manufacturer guidelines and previous published reports. The development of final antibody dilutions and antigen retrieval methods is described in section 2.3.2. Development of markers for dual immunohistochemistry are detailed in section 2.3.3.

All lung tissue samples were placed on an automated linier immunostainer, (Dako Autostainer Plus, DakoCytomation, Denmark) with positive and negative control samples run alongside. Visualisation was via the DakoEnvision detection system (Dako, Denmark), using chromogens DAB (DakoCytomation, Denmark) and/or Very Intense Purple (Vector Labs, UK).

Final dilutions, incubations times and control material are detailed in Table 3.1.

Antibody	Source	Antigen retrieval	Dilution/ incubation time	Positive control	Localisation/role
Surfactant protein C	Abcam (UK)	Citrate buffer pH6 MW 20mins 100% power Cool 20mins	1:1500, ON, 4ºC	Normal lung tissue	Cytoplasmic. Identifies ATII cells (Zhou *et al*, 1994)
E-cadherin	Vector Labs (UK)	Citrate buffer pH6 MW 20mins 100% power Cool 20mins	1:50, 60 mins, RT	Breast ductal cells	Membrane. Cell adhesion marker, loss associated with EMT (Hay *et al*, 1995)
N-cadherin	Dako Cytomation (Denmark)	Citrate buffer pH6 MW 20mins 100% power Cool 20mins	1:50, 30mins, RT	Kidney, renal tubular epithelium	Membrane and cytoplasmic. Mediates calcium dependent cell adhesion. Mesenchymal marker leads to decreased E-cadherin (De Wever *et al*, 2004)
Twist	Abcam (UK)	Citrate buffer pH6 MW 20mins 100% power Cool 20mins	1:50, 60mins, RT	Breast	Nuclear. Promotes proliferation, migration, differentiation and is associated with EMT (Pozharskaya *et al*, 2009)
α-smooth muscle actin (α-SMA)	Dako Cytomation (Denmark)	Citrate buffer pH6 MW 20mins 100% power Cool 20mins	1:800, 30mins, RT	Bowel	Muscle, myofibroblasts and mesenchymal marker (Zhang *et al*, 1994)
Collagen I	Abcam (UK)	Citrate buffer pH6 MW 20mins 100% power Cool 20mins	1:500. 30mins, RT	Kidney	Type I collagen fibres. Has been shown to promote EMT in lung cancer cells (Shintani *et al*, 2008)
TGF-β protein	Novocastra (UK)	Citrate buffer pH6 MW 20mins 100% power Cool 20mins	1:20, 60mins, RT	Placenta	Granular cytoplasmic. Growth factor affecting cell growth, differentiation and extracellular matrix production (Godin *et al*, 1991,Willis *et al*, 2005)
TGF-β receptor	Novocastra (UK)	Citrate buffer pH6 MW 20mins 100% power Cool 20mins	1:40, 60mins, RT	Bowel	Membrane. Receptor for TGF-β protein
Ki-67	Dako Cytomation (Denmark)	Citrate buffer pH6 MW 10mins 100%, 10mins 70% power. Cool 10mins	1:50, 30mins, RT	Breast cancer	Nuclear. Marker of cell proliferation (Bullwinkel *et al*, 2006)
EBV	Vector labs (UK)	Trypsin 10mins 37ºC	1:40, 60mins, RT	Hodgkins disease EBV positive lymph node	Cytoplasmic. (Sides *et a*l, 2009)
CMV	Dako Cytomation (Denmark)	Trypsin 40mins 37ºC	1:25, 30mins, RT	Kidney with CMV confirmed infection	Nuclear/cytoplasmic. (Tang *et al*, 2003)

Table 3.1 Details of the antibodies, dilution, incubation times and cellular localisation of markers used in chapter 3. ON=overnight, RT= room temperature, MW=microwave. Further details of markers are in section 2.3.2.

3.2.4 Semi-quantitative analysis

Semi-quantitative analysis is described in detail in section 2.5. In summary, sections were scored by myself and reviewed by an independent pathologist (Dr D Gey van Pittius) by examining expression of markers at sites of fibroblastic foci and ATII cells in IPF and control samples.

For assessment of disease activity, discussed in section 1.1.8 and described in section 2.5, I scored sections and made a semi-quantitative assessment for each individual biopsy using a scale of 0-6 for the extent of fibroblastic foci, previously described and illustrated by Nicolson *et al* (2002). Representative images used for scoring are seen in Figure 2.1. A score of 0 was assigned to those samples containing no fibroblastic foci; a score of 6 was given to those samples with the most profuse number of foci. Further details are provided in section 2.5. These scores were then correlated against the mean expression scores for each immunohistochemical marker in each IPF tissue sample in ATII cells and cells within fibroblastic foci as described in section 2.6.

3.2.5 Statistical analysis

A Mann Whitney U test was used for comparisons between IPF and control type II pneumocytes as detailed in chapter 2.6. Results are presented as mean expression score ±SD, as demarcated in the modified Allred scoring system (Table 2.4). Graphical results are presented as mean expression score ±SD for each marker. Marker expression differences were considered significant between IPF and control lung tissue samples if $p \leq 0.05$. Statistical analyses were performed using WinSTAT, (R. Fitch Software, Bad Krozingen, Germany).

As described in more detail in section 2.6, a Pearson correlation co-efficient was calculated to determine correlations between mean target marker expression levels in hyperplastic ATII cells and cells within fibroblastic foci with disease activity. The results were interpreted and categorised as no correlation, weak, moderate and strong correlation according to Cohen (1998), Table 2.5. Statistical analysis was performed using Minitab® 15 Statistical Software (USA). The Pearson correlation co-efficient is a measure of variability, therefore if all the mean expression scores for a particular marker are identical, there is no variability, and the calculation cannot be performed.

3.3 Results

Mean marker expression scores for ATII cells and fibroblastic foci, demonstrating the degrees of variation between individual cases, for each tissue sample are shown in Table 3.2. and 3.3. Mean marker expression scores were identical for all IPF tissue samples for E-cadherin, Twist and TGF-β expression within ATII cells, and E-cadherin, N-cadherin and α-SMA expression within fibroblastic foci. Consequently a Pearson correlation cannot be calculated. Only one case (number 3) revealed EBV protein expression within a lymphoid cell. It is therefore not included in Tables 3.2 and 3.3 for ATII and fibroblastic foci mean expression score. No Pearson correlation could be performed for CMV as no IPF lung tissue samples expressed the viral protein. Table 3.4 lists the Pearson correlation scores for markers of EMT and proliferation against number of fibroblastic foci.

Case Number	SP-C	E-cad	N-cad	Twist	α-SMA	Collagen I	TGF-β protein	TGF-βR	Ki-67
1	2	5	0	0	0	0	5	0	1
2	5	5	0	0	0	0	5	0	2
3	4	5	1	0	0	4	5	0	2
4	1	5	1	0	0	0	5	2	2
5	2	5	1	0	0	4	5	1	2
6	3	5	1	0	1	0	5	0	3
7	4	5	3	0	1	0	5	0	2
8	4	5	1	0	1	0	5	0	2
9	4	5	5	0	0	1	5	0	1
10	4	5	4	0	1	0	5	2	1
11	4	5	2	0	0	0	5	0	1
12	5	5	2	0	1	0	5	1	1
13	4	5	2	0	1	0	5	0	2
14	3	5	1	0	0	0	5	0	3
15	3	5	1	0	0	0	5	0	2
16	4	5	2	0	0	0	5	0	2
17	3	5	1	0	0	0	5	0	1
18	3	5	2	0	0	0	5	0	2
19	3	5	1	0	0	0	5	2	1
20	3	5	3	0	0	4	5	0	2
21	4	5	2	0	0	0	5	2	2
Mean	3.4286	5.0000	1.7143	0.0000	0.2857	0.6190	5.0000	0.4762	1.7619

Table 3.2 Mean marker expression scores in ATII cells for individual cases. Highlighted scores represent greatest variation between individual cases (>30%).

Case Number	E-cad	N-cad	Twist	α-SMA	Collagen I	TGF-β protein	TGF-βR	Ki-67
1	0	0	5	5	5	0	0	2
2	0	0	5	5	2	2	0	0
3	0	0	4	5	4	2	0	0
4	0	0	5	5	4	0	1	0
5	0	0	2	5	5	2	2	0
6	0	0	1	5	4	2	0	0
7	0	0	5	5	5	3	1	0
8	0	0	3	5	4	3	0	0
9	0	0	4	5	5	2	0	1
10	0	0	4	5	5	4	1	1
11	0	0	1	5	5	4	0	0
12	0	0	4	5	5	1	0	0
13	0	0	5	5	5	3	1	0
14	0	0	3	5	5	4	0	1
15	0	0	4	5	5	5	0	0
16	0	0	2	5	5	4	0	0
17	0	0	5	5	5	1	0	0
18	0	0	4	5	5	2	1	0
19	0	0	5	5	5	3	3	0
20	0	0	5	5	5	5	0	0
21	0	0	2	5	4	2	2	0
Mean	0	0	3.7143	5	4.6190	2.5714	0.5714	0.2381

Table 3.3 Mean marker expression scores in fibroblastic foci for individual cases. Highlighted scores represent greatest variation between individual cases (>30%).

Target Marker	Pearson correlation for marker expression within ATII cells	Pearson correlation for marker expression within fibroblastic foci
Surfactant protein C	-0.023	n/a
E-cadherin	n/a	n/a
N-cadherin	0.557	n/a
α-SMA	0.08	n/a
Collagen I	0.242	0.468
TGF-β protein	n/a	0.195
TGF-β receptor	0.181	0.292
Twist	n/a	0.402
Ki-67	-0.366	0.232

Table 3.4 Pearson correlation of mean expression score of immunohistochemical markers within ATII cells and fibroblastic foci correlated against fibroblastic foci score. For cases where all expression scores were the same a Pearson correlation coefficient could not be calculated and is recorded as not applicable (n/a). Weak correlation pink, moderate correlation yellow, strong correlation green.

3.3.1 Surfactant protein C (SP-C) expression (Marker of ATII cells)

Cytoplasmic SP-C expression in the hyperplastic ATII cells in IPF lungs had a patchy pattern of distribution in all biopsy samples (Figure 3.1B, C, D). However, cytoplasmic SP-C expression was uniformly present in the ATII cells of control lungs (Figure 3.1A). The degree of SP-C expression in IPF lung tissue samples varied with the size of ATII cell, with

hypertrophic cells exhibiting greater SP-C immunoreactivity (Figure 3.1, 2, D). Conserved areas of IPF lung tissue contained ATII cells with morphology and SP-C expression comparable to control lung ATII cells.

There was a decrease of cytoplasmic SP-C expressing ATII cells present in IPF tissue samples (mean expression score 3.42, SD± 0.978), compared to the control tissues (mean expression score 4.36, SD± 0.760) although this did not reach statistical significance (Figure 3.10).

SP-C expression within ATII cells showed no correlation with fibroblastic foci score (Pearson correlation co-efficient -0.023). As expected SP-C expression was absent within the fibroblastic foci where mesenchymal phenotypes are dominant.

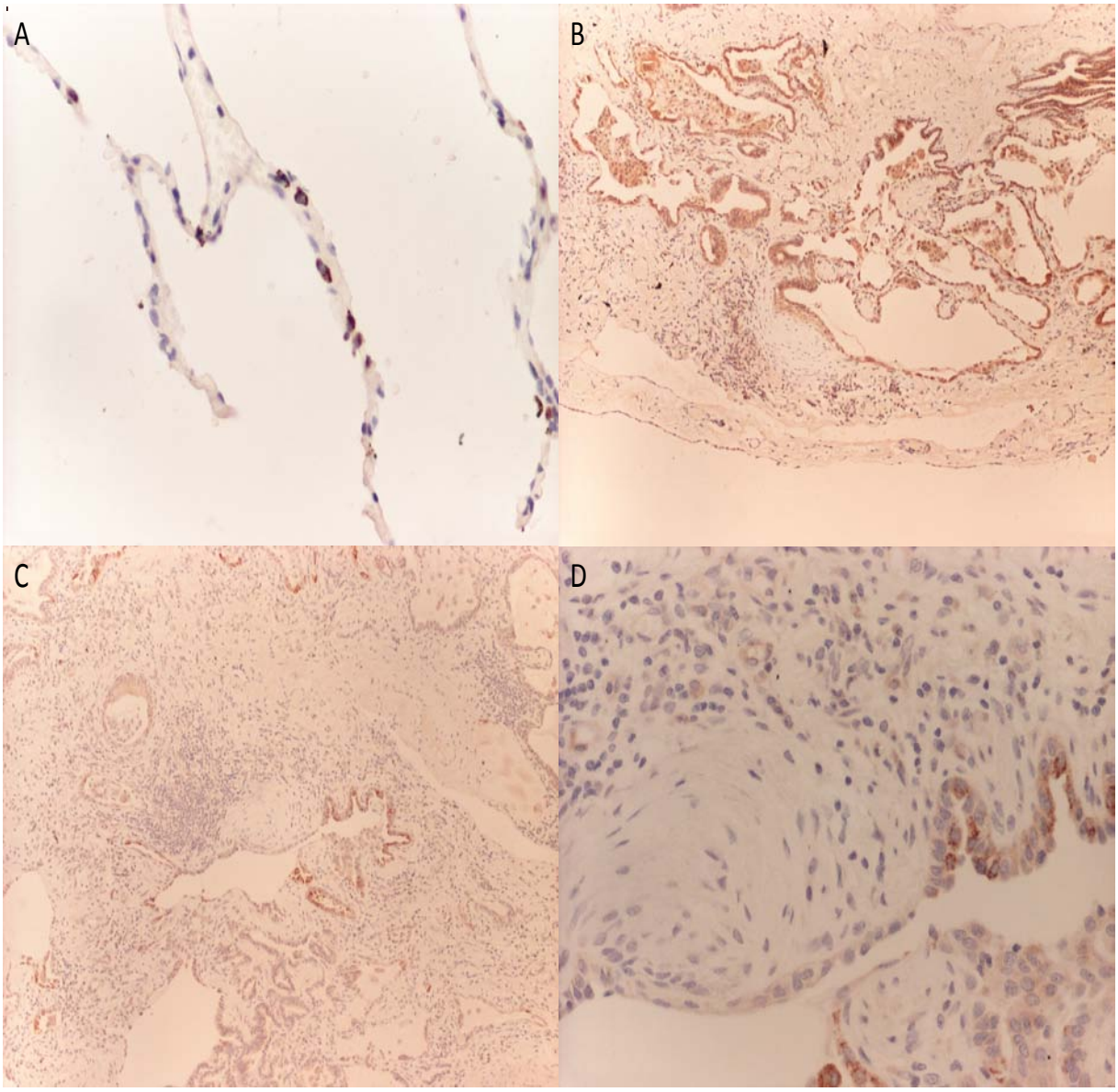

Figure 3.1. Immunohistochemical analysis of IPF and control lungs for SP-C expression. A. SP-C expression in the cytoplasm of ATII cells (arrow), magnification x400. B. Low power image of SP-C expression in hyperplastic ATII cells in a case of IPF, magnification x40. C. Medium power image of SP-C expression in the ATII cells (black arrow) adjacent to a fibroblastic foci (red arrow), magnification x100. D. High power image of SP-C expression (black arrow) adjacent to a fibroblastic foci, magnification x400.

3.3.2 E-cadherin marker expression (Marker of cell adhesion)

In all control lung samples, E-cadherin expression was evident in the cell membrane of ATII cells and bronchiolar epithelium (mean expression score 4.21, SD± 0.854) (Figure 3.2 A). In the IPF group E-cadherin expression was observed in the cell membrane of hyperplastic ATII cells present in areas of interstitial fibrosis and also overlying the fibroblastic foci (mean expression score 5, SD± 0) (Figure 3.2 B, C, D). E-cadherin expression was absent within fibroblastic foci (Figure 3.2 B, C, D). Overall there was no difference between ATII cell E-cadherin expression in control and IPF lung tissue samples (Figure 3.11).

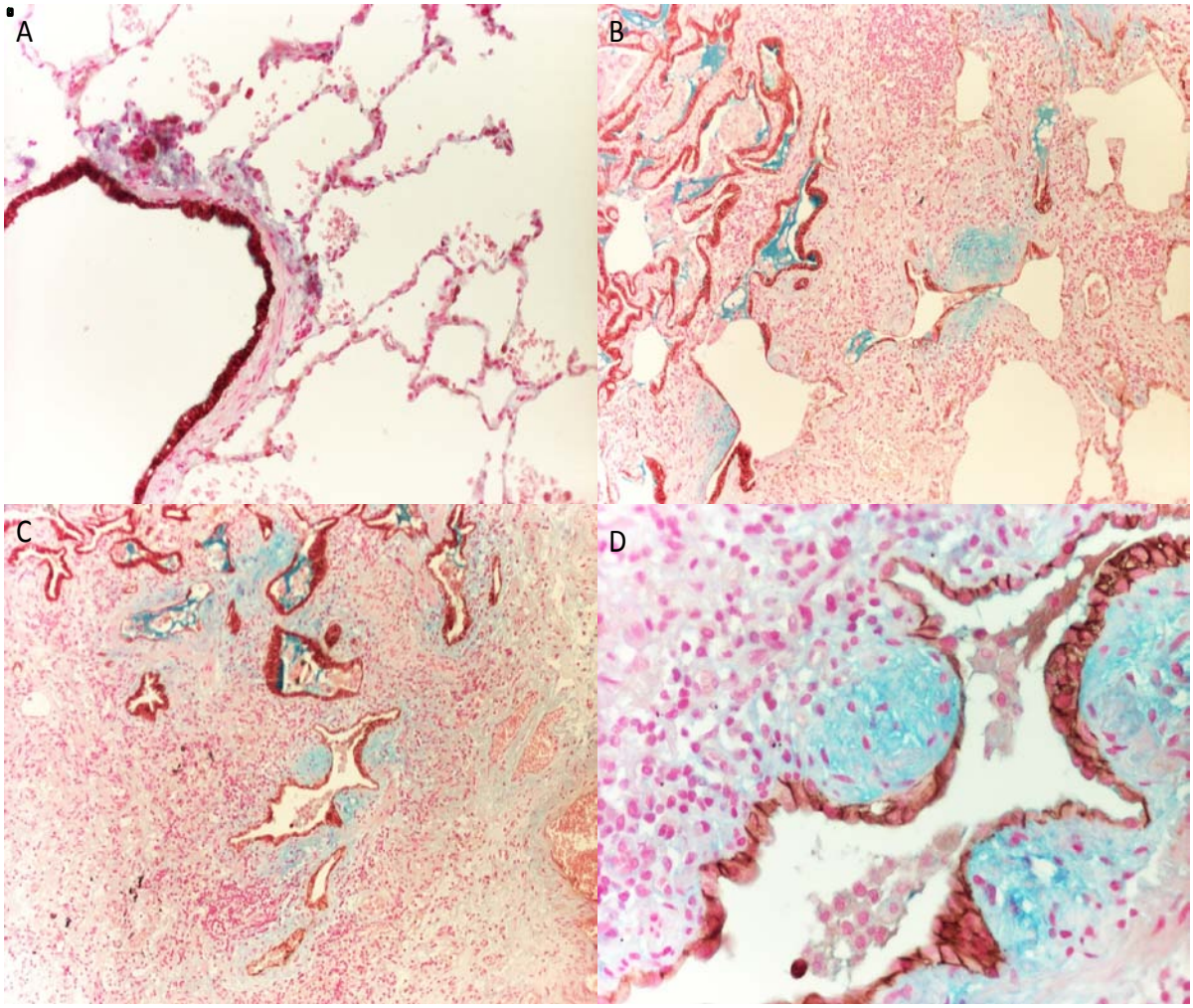

Figure 3.2 Representative images of E-cadherin expression in IPF and control lungs. A. Histological image of E-cadherin expressed around bronchiolar epithelial cells in control lung tissue, magnification x200. B. Membrane expression of E-cadherin overlying fibroblastic foci (arrow) and in hyperplastic ATII cells to the left of the image, magnification x200. C. Separate case of IPF lung demonstrating E-cadherin expression overlying a fibroblastic foci and magnified in D, magnification C x200, D x 400.

3.3.3 N-cadherin marker expression (mediator of calcium-dependent cell adhesion)

Scanty N-cadherin expression (mean expression score 1.71, SD± 1.230) was observed in the hyperplastic ATII cells of IPF lung tissue samples and no expression in ATII cells of control cases ($p<0.05$) (Figure 3.10). Within the IPF group, four tissue samples demonstrated ATII cell expression scores of 3 or above. The distribution of these cells was patchy, with

small clusters of hyperplastic ATII cells expressing N-cadherin within areas of hyperplasic ATIIs not expressing the N-cadherin marker (Figure 3.3 B, C). N-cadherin expression was not expressed in conserved areas of IPF lung tissue. No N-cadherin expression was detected within the fibroblastic foci (Figure 3.3 D).

N-cadherin expression within ATII cells had a strong positive correlation with disease activity (Pearson correlation co-efficient 0.557). No expression of N-cadherin was identified in the fibroblastic foci; hence a correlation cannot be performed.

3.3.4 Twist marker expression (transcription factor proposed to drive EMT and EndMT)

Nuclear expression of Twist was absent in ATII cells in both the control and IPF group (Figure 3.3 A, D, 3.10). In contrast, moderate nuclear expression of Twist was detected within myofibroblasts in the fibroblastic foci, with a mean expression score of 3.71 (SD± 1.383) (Figure 3.3 D, 3.11).

As there was no expression of Twist within ATII cells in all lung tissue samples a Pearson correlation cannot be performed. For Twist expression in fibroblastic foci a moderate positive correlation was identified (Pearson correlation co-efficient 0.402).

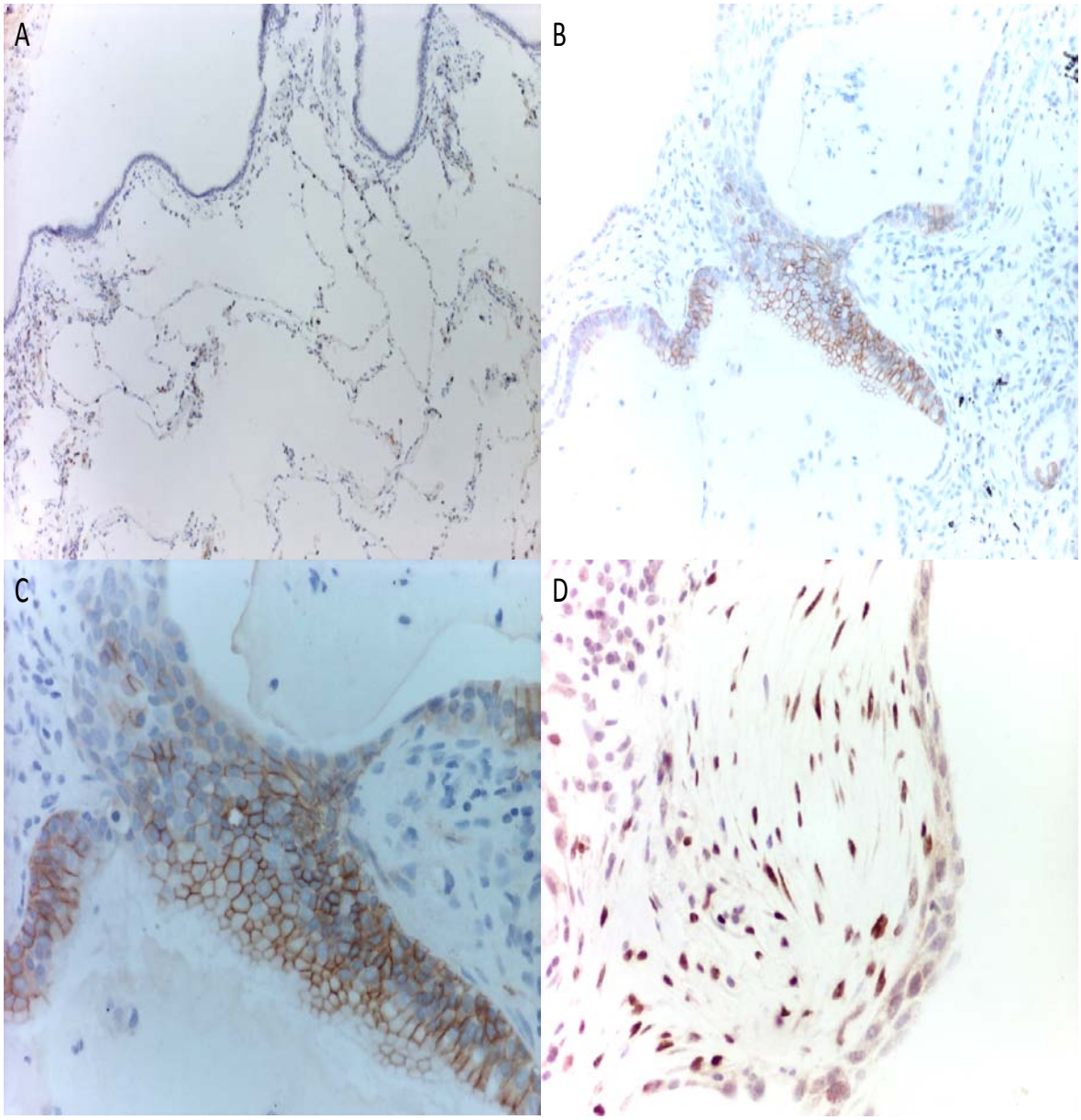

Figure 3.3 Representative Immunohistochemical images of N-cadherin and Twist expression in IPF and control lung tissues. A. Dual labelled immunohistochemistry reveals no expression of N-cadherin or Twist in control lung tissue, magnification x100. B and C. N-cadherin expression is seen in a cluster of ATII cells (arrow), magnification B x100, C x400. D. IPF lung tissue demonstrates Twist reactivity within the fibroblastic foci, but no N-cadherin expression, magnification x400

3.3.5 α-smooth muscle actin (α-SMA) marker expression (mesenchymal marker, implicated in fibroblast differentiation)

Negligible α-SMA was expressed in hyperplastic ATII cells of the IPF samples (mean expression score 0.28, SD± 0.462) with no expression observed in ATII cells in the control group, $p<0.05$. (Figure 3.4, 3.10). Extensive expression of α-SMA was detected within the fibroblastic foci (mean expression score 5, SD± 0) consistent with the presence of a predominant myofibroblast phenotype (Figure 3.4B, C, D, 3.11).

Expression of α-SMA within ATII cells in the IPF lung tissue samples did not correlate with number of fibroblastic foci (Pearson correlation co-efficient 0.08). Mean expression scores for α-SMA expression within the fibroblastic foci in each tissue sample were all graded as 5 (percentage expression score >66%). As all values were identical a Pearson correlation co-efficient cannot be calculated.

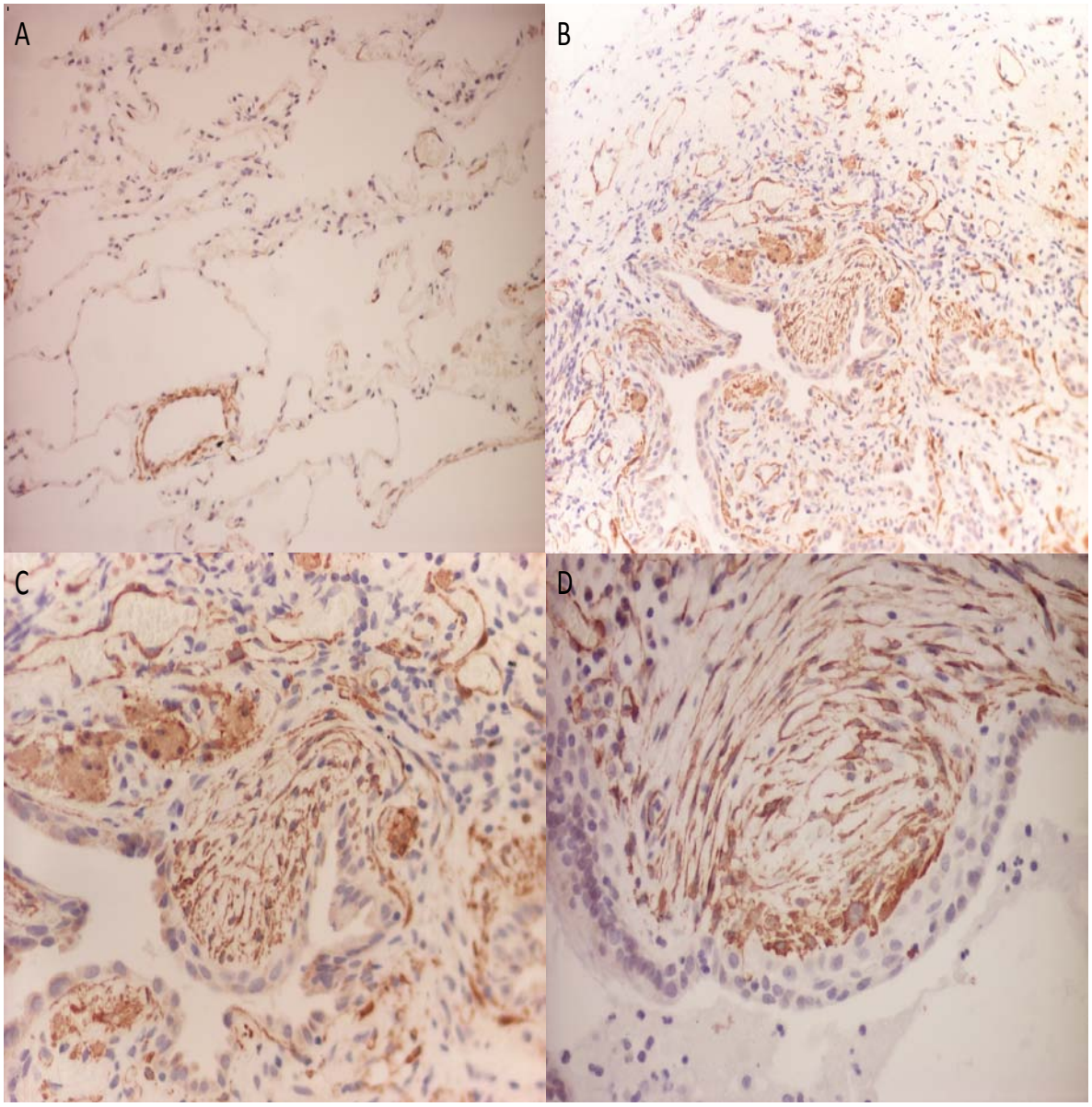

Figure 3.4. Immunohistochemical analysis of IPF and control lung tissue for the mesenchymal marker α-SMA. A. Representative image of α-SMA expression around a blood vessel in control lung. B. and C. α-SMA expression within the interstitial fibrotic areas and identifying a fibroblastic foci (arrow), magnification B x100. C x200. D. Separate IPF lung tissue demonstrates α-SMA expression within a fibroblastic foci, magnification x400.

3.3.6 Collagen I marker expression (extracellular matrix protein)

Within the IPF group, three samples contained ATII cells which expressed cytoplasmic collagen I with a score of 4 (percentage expression range score 33-75%), one

case showed negligible expression (mean expression score 1, percentage expression range score 1%), all other samples had no collagen I expression within the ATII cells with a mean ATII expression score of 0.61 (SD± 1.430), compared with no expression in the control ATII cells ($p<0.05$) (Figure 3.10). Collagen I expression was present in the fibroblastic foci consistent with these active areas of fibrosis (mean expression score 5, SD± 0.740) (Figure 3.5 B, C, D). Collagen I expression was observed to a lesser extent within interstitial areas of the IPF tissue and in the control samples collagen I was restricted to vessel walls.

Mean expression score of ATII cells in IPF lung tissue samples revealed a weak positive correlation with number of fibroblastic foci (Pearson correlation co-efficient 0.242). A moderate positive correlation was identified between collagen I expression within the fibroblastic foci and number of fibroblastic foci (Pearson correlation co-efficient 0.468).

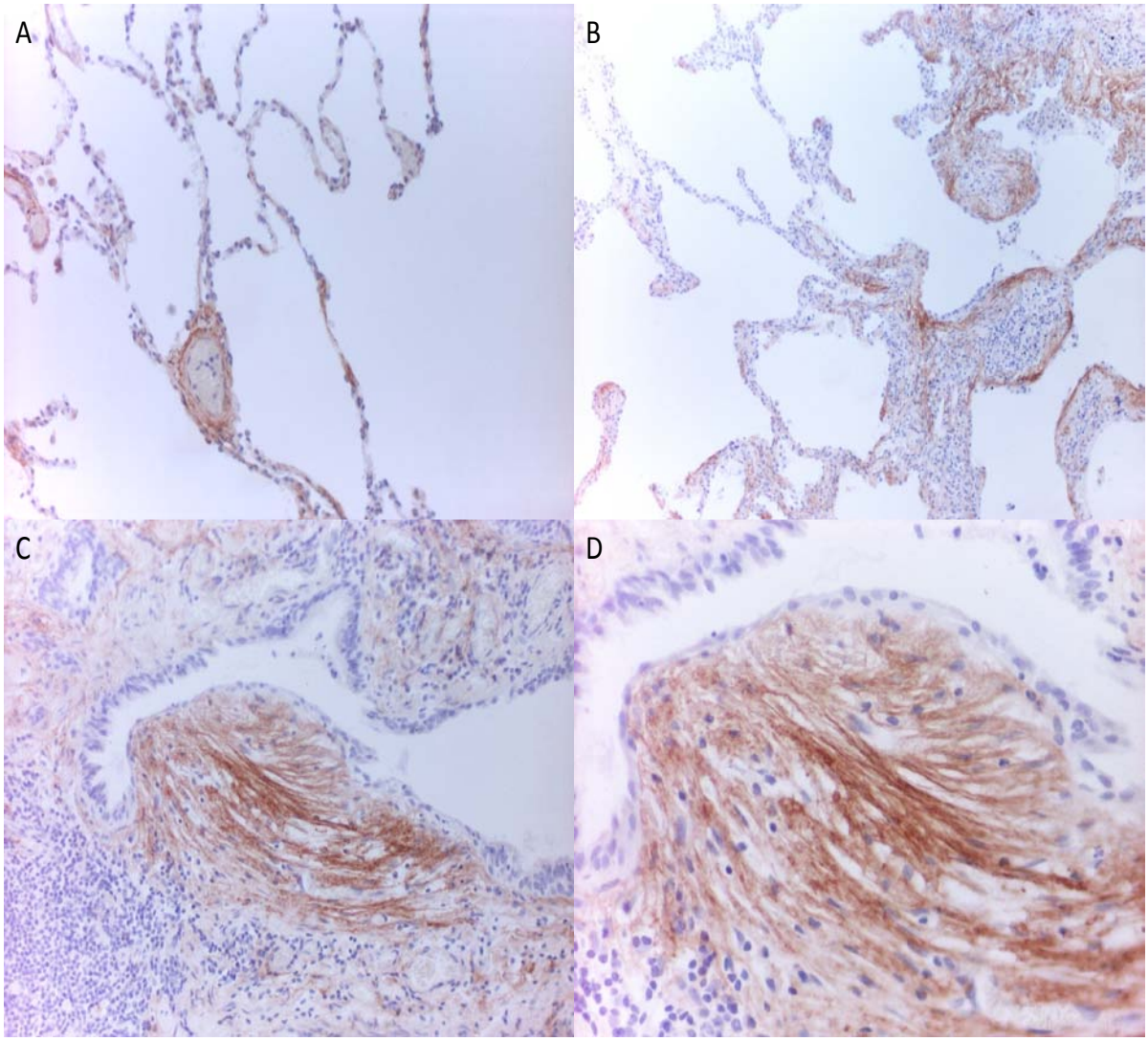

Figure 3.5. Immunohistochemical analysis of IPF and control lungs for collagen I expression. A. Representative histological image of collagen I surrounding a vessel in control lung tissue, magnification x100. B, C, D. Collagen I expression in IPF lung tissue predominantly localised within the fibroblastic foci, magnification B x40, C x200, D x400.

3.3.7 TGF-β protein and TGF-βR marker expression (pro-fibrogenic growth factor and receptor)

A significant increase in cytoplasmic TGF-β protein expression (mean expression score 5.0, SD± 0) was observed in IPF hyperplastic ATII cells compared with control cells

(mean expression score 0.52, SD± 0.772) $p<0.05$ (Figure 3.6, 3.10). TGF-β receptor was only present in a small number (<1%) of epithelial cells in both the IPF (mean expression score 0.47, SD± 0.813) and control group (mean expression score 0.57, SD± 0.768) (Figure 3.7, 3.10). TGF-β protein expression within the fibroblastic foci demonstrated variability, with mean expression scores ranging from 0 to 5 (0% - >66%) giving a mean proportion of positive expressing fibroblasts/myofibroblasts of 2.57 (SD± 1.434) (Figure 3.11). However, although TGF-β protein was expressed in the foci, its receptor was negligible (mean expression score 1, SD± 0.870) (Figure 3.11).

A Pearson correlation cannot be performed using the data from TGF-β protein within ATII cells as mean expression values for all IPF samples was 5 (SD± 0). A weak positive correlation was identified for TGF-β protein expression within the fibroblastic foci and number of fibroblastic foci (Pearson correlation co-efficient 0.195).

A weak positive correlation was identified for TGF-β receptor expression within ATII cells and cells within the fibroblastic foci when assessed against number of fibroblastic foci (Pearson correlations co-efficient 0.181 and 0.292 respectively).

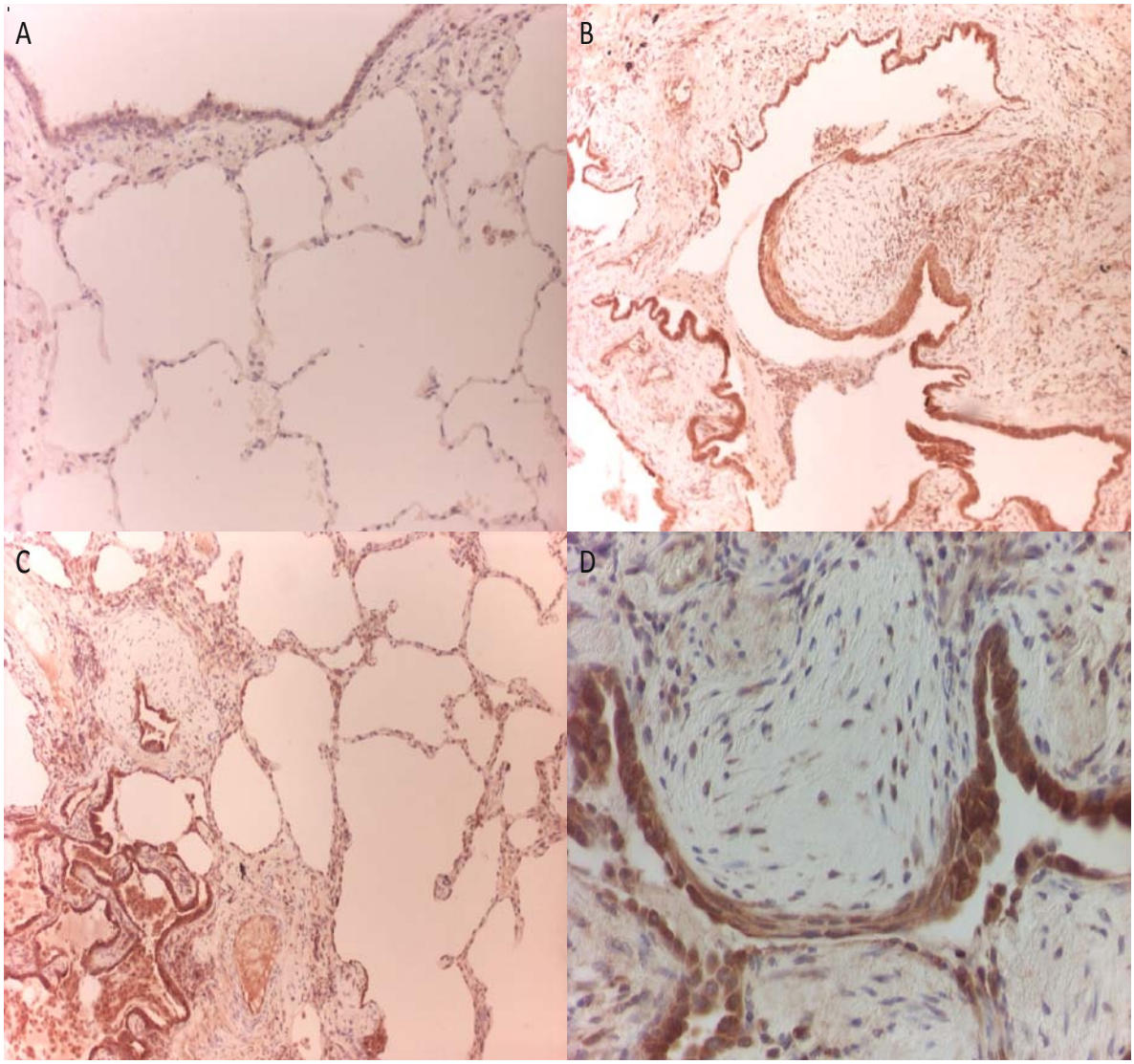

Figure3.6. Immunohistochemical analysis of IPF and control lung samples labelled for TGF-β protein. A. Representative image of cytoplasmic TGF-β protein within bronchiolar epithelium but not in ATI or ATII cells, magnification x100. B. TGF-β protein expression is seen in ATII cells overlying a fibroblastic foci (arrow) and within the foci, magnification x200. C. Junctional areas of ATII cell hyperplasia and conserved lung in IPF lung tissue with marked TGF-β expression in the hyperplastic area, magnification x100. D. High power representative image of TGF-β protein expression in the ATII cells overlying a weakly expressing fibroblastic foci, magnification x400.

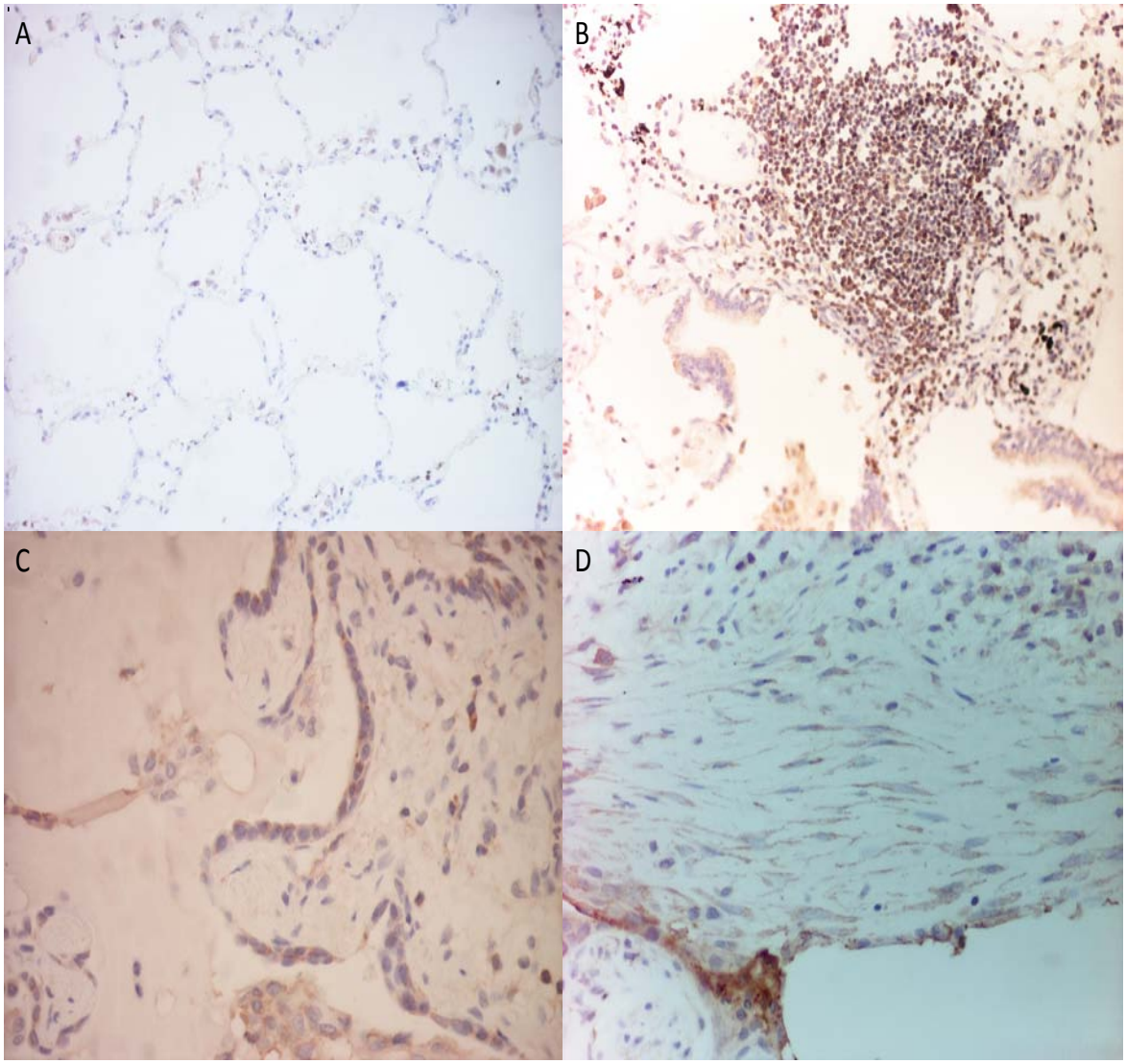

Figure 3.7. Immunohistochemical analysis of IPF and control lungs for TGF-β receptor antigen. A. Representative image of control lung with no TGF-β receptor expression, magnification x100. B. TGF-β receptor is upregulated in a cluster of inflammatory cells in a representative IPF lung tissue sample, magnification x200. C. Representative image of TGF-β receptor in inflammatory cells with interstitial fibrotic areas of IPF lung tissue, magnification x400. D. TGF-β receptor is identified in the membrane of the myofibroblasts within a fibroblastic foci in a representative section of IPF lung tissue magnification x400.

3.3.8 Antigen Ki-67 marker expression (marker of cell proliferation)

Antigen Ki-67 expression was negligible in the nuclei of control lung ATII cells (mean expression score 0.21, SD± 0.713) compared to the IPF group (mean expression score 1.76, SD± 0.624) $p<0.05$ (Figure 3.8, 3.10). In IPF lung tissue there was nuclear expression of antigen Ki-67 in ATII cells localised within the areas of interstitial fibrosis away from the fibroblastic foci. However, there was no evidence of antigen Ki-67 expression in ATII cells directly overlying fibroblastic foci. Myofibroblasts within the fibroblastic foci showed negligible antigen Ki-67 expression (mean expression score 0.23, SD± 0.538) (Figure 3.11).

Expression of Ki-67 within ATII cells of IPF lung tissue samples demonstrated a moderate negative correlation with fibroblastic foci score (Pearson correlation co-efficient -0.366). A weak positive correlation was identified for Ki-67 expression within the fibroblastic foci and number of fibroblastic foci (Pearson correlation co-efficient 0.231).

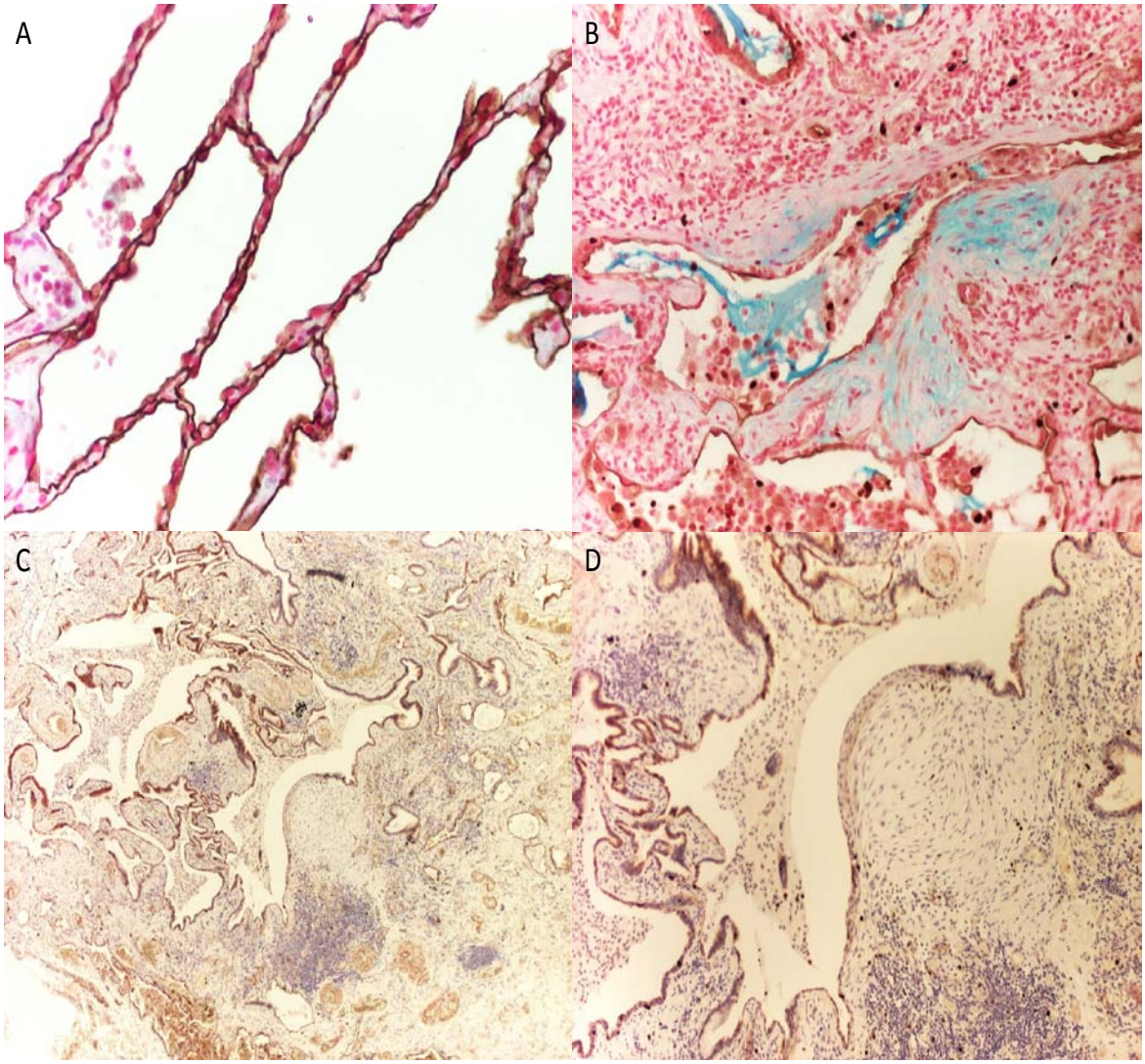

Figure 3.8. Immunohistochemical analysis of IPF and control lungs for the cell proliferation marker Ki-67. A. Representative image shows antigen Ki-67 is not observed in control lung tissue, magnification x400. B. Fibroblastic foci, highlighted by Alcian blue staining are not expressing Ki-67, with inflammatory cells in the interstitial fibrotic areas expressing the marker, magnification x200. C and D. Representative images of IPF lung tissue demonstrating expression of Ki-67 at the edges and away from the fibroblastic foci, magnification C. x40, D. x200.

3.3.9 Epstein Barr virus (EBV) marker expression

EBV latent membrane protein was expressed in only one patient's IPF lung tissue out of 21 cases. The viral protein marker was also absent in all control lung tissue samples. The

positive control tissue, run alongside the test tissues, demonstrated expression of EBV in the Reed Sternberg cells of a case of Hodgkin's lymphoma (Figure 3.9.A). Furthermore, within the above positive IPF sample, only one lymphocytic cell was identified as expressing the viral protein (Figure 3.9 B).

The lung tissue sample with EBV expression, case number 3, was not one of the 4 high N-cadherin expressing cases.

3.3.10 Cytomegalovirus (CMV) marker expression

Expression of CMV was seen in infected cells of the positive kidney control tissue, run alongside the test tissues (Figure 3.9.C). There was no expression of CMV detected in any control or IPF lung tissue samples (Figure 3.9 C, D).

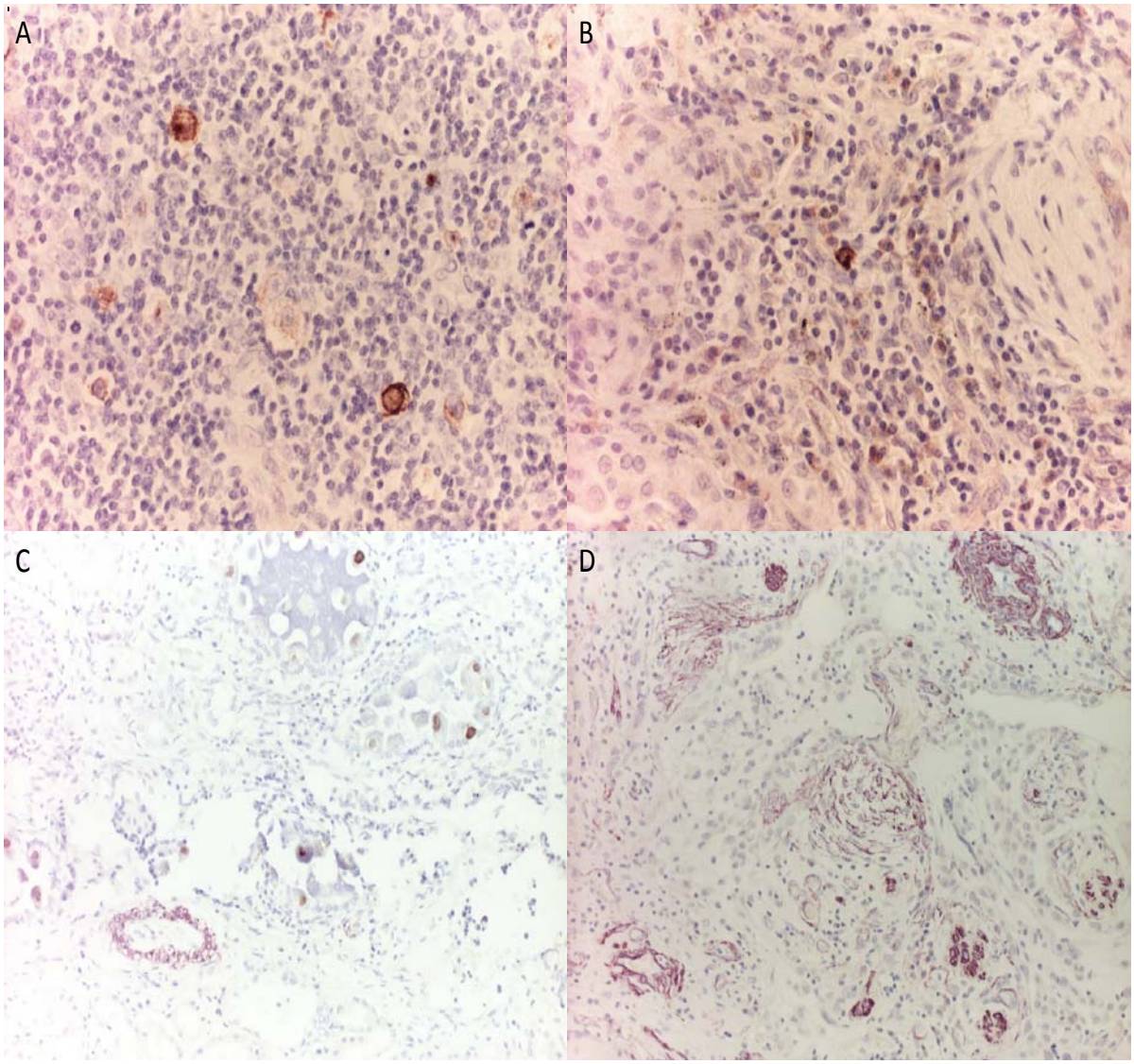

Figure 3.9. Representative images of EBV and CMV expression in positive control material and IPF lug tissue. A. Membrane expression of EBV latent membrane protein in a lymph node tissue of Hodgkins disease, magnification x400. B. EBV expressed in a lymphocyte in IPF lung tissue, magnification x400. C. Kidney tissue with membrane CMV expression used as positive control material, magnification x200. D. Dual-immunohistochemistry demonstrates no expression of CMV, with a fibroblastic foci identified by α-SMA expression, magnification x200.

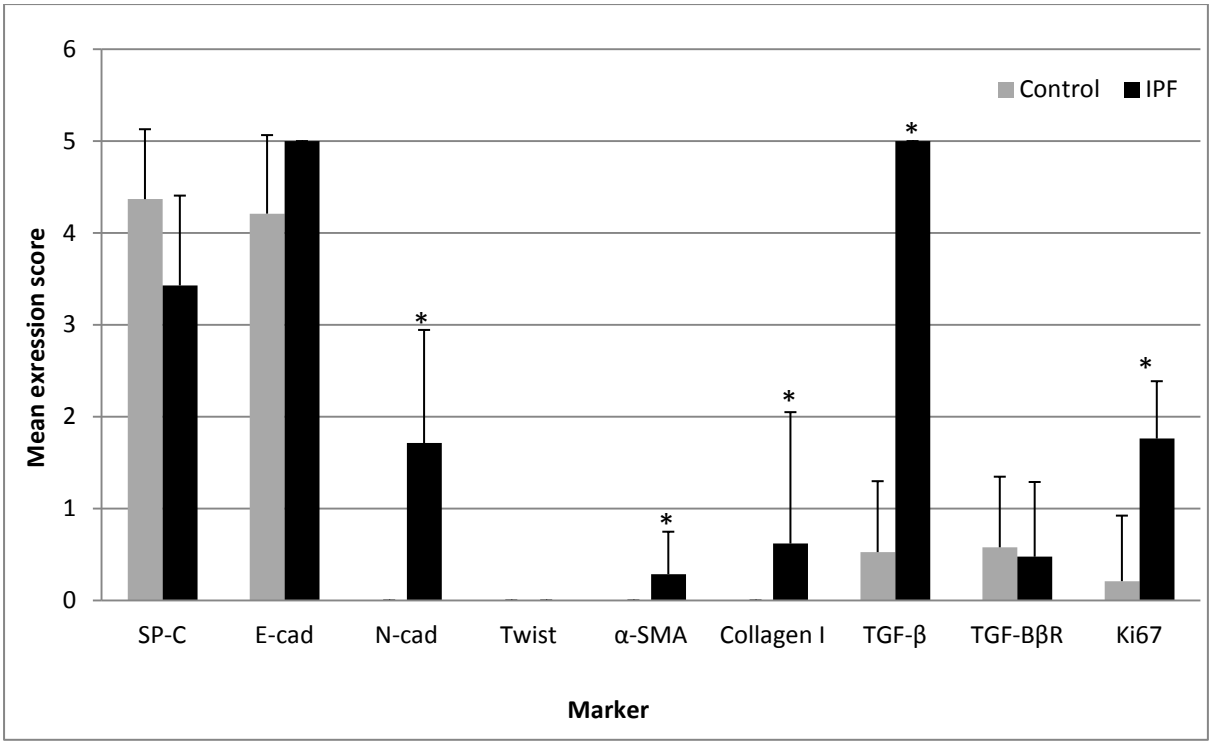

Figure 3.10. Semi-quantitative analysis of target molecule expression within ATII cells of IPF and control lung samples. Data are presented as mean expression ±SD. * = significant difference in expression between the control and IPF group p≤0.05.

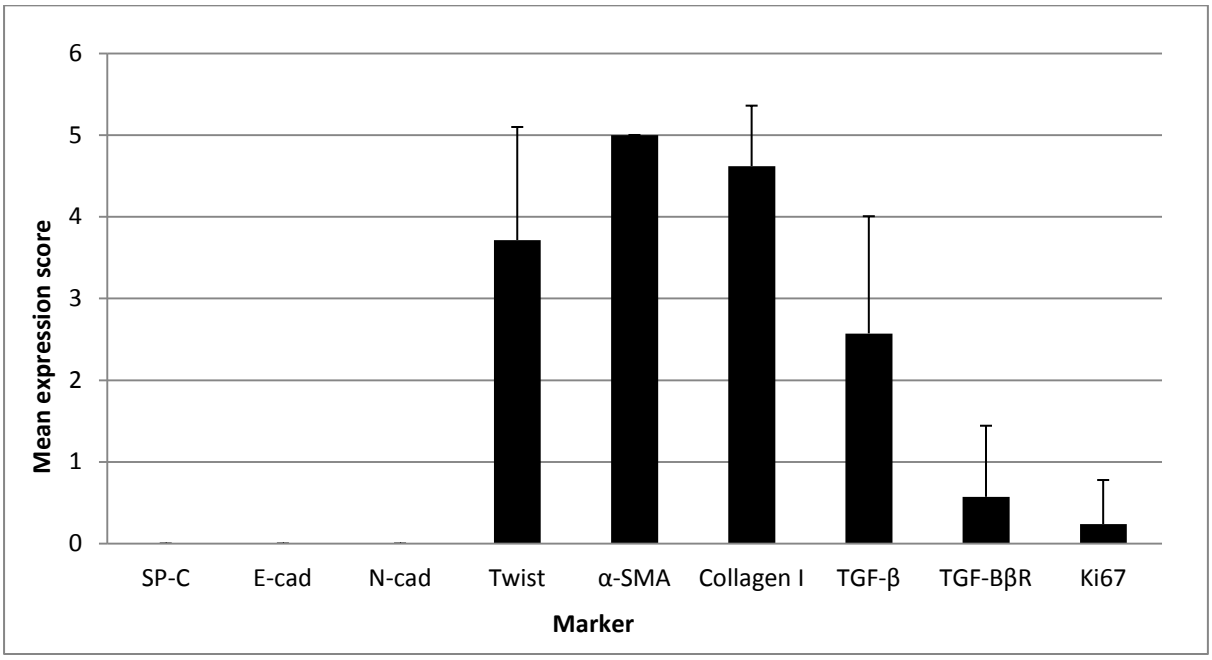

Figure 3.11. Semi-quantitative analysis of target molecule expression within the fibroblastic foci of IPF lung tissue samples. Data are presented as mean expression score ±SD.

3.4 Discussion

SP-C is a protein produced by functional ATII cells. Previous reports have found genetic mutations in SP-C are found infrequently in IPF patients and rarely in cases of sporadic IPF (Lawson *et al* 2004). I am the first to observe reduced and varied SP-C expression throughout human IPF lung tissue samples (mean expression scores from 1-5). The wide variation of mean expression scores for SP-C in ATII cells did not correlate to number of fibroblastic foci in IPF lung tissue samples and is therefore not associated with disease activity levels. This variation may be linked to the maturity of the cell, as it appears the larger ATII cells secrete SP-C. The atrophic ATII cells, (non-SP-C producing cells observed in the IPF group), may be transforming into type I pneumocytes following injury, potentially loosing the ability to produce SP-C. However, as EMT is characterised by the loss of epithelial markers and acquisition of fibroblast markers, I cannot rule out the possibility that these cells are undergoing EMT and are in a transition from ATII to a fibroblast phenotype. These results further the observation by Lawson *et al* (2005), that mice deficient in SP-C are predisposed to the development of pulmonary fibrosis with increased lung collagen accumulation and greater numbers of fibroblasts.

N-cadherin is significantly increased, although scanty in IPF. On closer inspection of the data only four of the IPF cases had mean expression scores of 3 or more. If concomitant loss of E-cadherin was observed it would suggest loss of cellular adhesion and the possibility of EMT occurring. My results revealed that high levels of E-Cadherin were detected in the hyperplastic ATII cells of all IPF cases suggesting no significant loss of cell-cell adhesion in the IPF tissue at the time of biopsy, a finding also reported by Kelly *et al* (2006) and Yamada *et al* (2008), but in dispute with the majority of experiments into the role of EMT in IPF

pathogenesis (Willis *et al*, 2005, Pozharskaya *et al*, 2009, Kim *et al*, 2009). I believe this discrepancy is due to differences in sample study material and immunohistochemical marker panels used by those promoting EMT mechanisms in IPF. The studies by Willis *et al* and Kim *et al*, primarily utilised cell culture models of EMT in lung fibroblast production, with the experiment by Willis *et al* furthering their investigation by the use of only three cases of confirmed IPF lung. The study by Wilis *et al* in IPF lung tissue samples did not investigate cell-cell adhesion markers as part of their panel of EMT markers, which I feel are necessary to validate the presence of EMT. The study by Pozharskaya's group examined 13 IPF lung tissues but did not explore expression of a key indicator of EMT; α-SMA.

A novel finding of my study was the strong correlation between increased ATII cell N-cadherin expression and increased number of fibroblastic foci. This would indicate that EMT is linked to the formation of fibroblastic foci supported by previous research by Willis *et al* (2005) and Kim *et al* (2006). However, the remaining data in this chapter demonstrated little support for the role of EMT within IPF lung tissue samples. This discrepancy in the literature may be due to differences between A549 cell culture studies, used by Kim *et al*, and the bleomycin induced pulmonary fibrosis model used by Kasai *et al*, neither of which accurately reflect IPF. The study by Willis et al in IPF lung tissues did not investigate cell-cell adhesion markers as part of their panel of EMT markers, which I feel are necessary to validate the presence of EMT. An alternative concept is based on the finding that N-cadherin is associated with increased cell migration and invasion (Derycke *et al*, 2006). It may be that increased ATII cell mobility and migration are caused by products, such as growth factors, released by the increased numbers of fibroblastic foci. Alternatively the process of increased ATII cell invasion through the extracellular matrix and alveolar epithelium allowing the

spread and invasion of fibroblasts/fibrocytes through the lung architecture could result in the seeding of new fibroblastic foci.

N-cadherin has been shown to have an inhibitory effect on cell proliferation in embryonic kidney cell culture studies (Derycke and Bracke, 2004). Overexpression of N-cadherin within these cells was shown to suppress cell proliferation by prolonging the G2/M phase and inducing β-catenin dependent expression of $p21^{WAF1}$ (Kamei *et al*, 2003). I suggest that, in IPF lung tissue, a similar mechanism is occurring in ATII cells. This finding correlates with my data that demonstrated a moderate negative correlation of ATII cell Ki-67 expression and increased number of fibroblastic foci, thus substantiating my supposition that cell senescence could play an important role in the pathogenesis of IPF.

Interestingly, a heterogeneous pattern of N-cadherin expression as found within our IPF cohort, has also been described by Pozharskaya *et al* (2009), who reported similar expression of N-cadherin expression in IPF lung tissue samples. This pattern of expression could not be linked to a subset of patients with EBV or CMV infection; however this does not rule out the possibility that an alternate viral infection may lead to N-cadherin expression and potentially the occurrence of EMT. Only one of the IPF lung tissue samples in this study demonstrated EBV expression. This result differs from previous reports of significant EBV and CMV viral presence in IPF (Tang *et al*, 2003). The differences may be a result of the PCR methodology used by other workers, which detects *bystander sequences of viral DNA*. The PCR methodology has superior sensitivity and may result in over reporting of viral presence. In addition the detection of DNA in this context may not result in the production of a functional viral protein. My study utilised immunohistochemistry to detect the *protein product* of the virus which is a more meaningful measure of viral presence. In addition, the

study by Tang *et al*, examined 25 IPF patients of whom only 5 were not on immunosuppressive therapy, which predisposes the individual to viral infection. It may be that the viral DNA detected in the study by Tang *et al*, is a result of this therapy predisposing the individual to infection rather than the infection being an instigator of IPF. Further investigations into the presence of viral DNA via PCR analysis in my IPF lung tissue samples would allow for more accurate comparisons to be made to other studies.

Dual-immunohistochemistry did not reveal co-localisation of N-cadherin and Twist in ATII cells of IPF cases. When combined with the upregulation of E-cadherin and lack of cytoplasmic α-SMA expression, these data raise questions regarding the role of EMT as a mechanism in fibroblast development in IPF lung. I propose that Twist may be involved in differentiation of residential fibroblast/circulating fibrocytes into mesenchymal cells rather than EMT differentiation of ATII cells to myofibroblasts. As yet there are no studies in the literature to substantiate or indeed contradict my hypothesis in IPF lung. However, experiments on the tracking of fibrocytes in animal models of allergen-induced asthma suggest that circulating fibrocytes can be recruited to the lung and are involved in airway remodelling (Schmidt *et al*, 2003). Further investigation using immunohistochemical analysis for markers such as CD34, CD13, CD45RO and Major Histocompatibility Complex class II, specific for fibrocytes, may provide evidence to support my idea.

Besides EMT, Twist *activation* has been implicated in the suppression of cell senescence and promotion of proliferation with DNA damage accumulation in prostate epithelial cells (Kwok *et al*, 2007) and bone marrow-derived mesenchymal stem cells (Tsai *et al*, 2011). Twist *inactivation* therefore leads to the promotion of cell senescence and growth arrest (Kwok *et al*, 2007). My results of moderate expression of Twist within the fibroblastic

foci suggest suppressed cell senescence, which could allow replication and accumulation of cells with DNA damage.

Fibroblast cell culture studies have demonstrated that reduction or inactivation of N-cadherin could result from TGF-β signalling, leading to the loss of directional movement and disorganised wound repair (Hinz *et al*, 2004), with fibroblasts switching from a migratory to a contractile phenotype. This loss may enable myofibroblast motility and invasion through the collagen rich ECM and alveolar basement membrane. My findings may lead to the supposition that disorganised repair processes and wound contraction are occurring in IPF.

Key markers of the myofibroblast phenotype (α-SMA and collagen I) were highly expressed in the fibroblastic foci (where a myofibroblast phenotype dominates); however negligible expression was detected in the cytoplasm of the overlying hyperplastic ATII cells in IPF cases. These findings, combined with E-cadherin expression, suggest that EMT was not a key pathogenetic process in IPF at the time of biopsy in our patient cohort but does not exclude its potential involvement either prior or subsequent to biopsy. It is equally plausible to surmise that EMT is not a major player in IPF pathogenesis. This would be in agreement with previous work by Kelly *et al* (2006) and Yamada *et al* (2008) who also failed to find supporting evidence of EMT in both bleomycin-induced animal models and within human IPF tissue samples.

Twist and collagen I expression within the fibroblastic foci demonstrated a moderate positive correlation with number of fibroblastic foci; Twist promotes the proliferation of myofibroblasts within these foci (Kida *et al*, 2007). It follows that an increase in myofibroblasts would result in increased deposition of collagen I and therefore increased disease activity. Collagen I has been shown to promote EMT in non-small cell lung cancer

lines via TGF-β signalling (Shintani *et al*, 2008), which is prevented by blocking the TGF-β receptor. I observed significantly increased expression of TGF-β protein in the ATII cells of IPF cases with varied expression of TGF-β protein in the fibroblastic foci. In addition negligible and equivocal expression of the TGF-β receptor was observed in the ATII cells of both IPF and control groups. The increased TGF-β protein may have multiple roles in the pathogenic development of IPF by promoting fibroblast to myofibroblast differentiation (Chambers *et al*, 2003), driving EMT via Smad proteins (Willis *et al*, 2005, Kim *et al*, 2007), or suppressing epithelial cell proliferation (Chambers *et al*, 2003). Combined with my findings of absent Ki-67 expression in ATII cells overlying fibroblastic foci, I propose that these cells are inhibited by the production of TGF-β protein.

My results showed that only inflammatory cells present in the lung interstitium consistently expressed the TGF-β receptor. As TGF-β protein has been shown to inhibit proliferation (Bullwinkel *et al*, 2006), this may indicate that these interstitial inflammatory cells are subject to inhibition via TGF-β. This concept is supported by observations of limited inflammation in the classical histological picture of IPF (Gauldie, 2002).

The absence of proliferation in ATII cells that are in direct contact with areas of fibroblastic foci, combined with the varied SP-C expression, within the same cells, suggests that the ATII cell could be in cell-cycle arrest or senescence, a theory supported by previous work by Chilosi *et al* (2002) who examined p53 expression in IPF lung tissue samples. In addition the proliferation of hyperplastic ATII cells away from areas of fibroblastic foci may suggest an attempt at wound repair. A moderate negative correlation of ATII cell Ki-67 expression and increased number of fibroblastic foci suggests cell senescence may play an important role in the pathogenesis of IPF. From the observed pattern of Ki-67 expression, I

propose the possibility that α-SMA expressing myofibroblasts may provide a scaffold for ATII cells, (dividing at the edge of the insult) to migrate over the foci surface, rather than transforming, via EMT, into the myofibroblasts below. This variable pattern of ATII cell proliferation and inhibition, surrounding micro-niche areas of fibroblastic foci, could contribute to the heterogenic distortion of lung tissue remodelling in IPF.

Interestingly there was negligible expression of Ki-67 antigen identified within the fibroblastic foci. When combined with moderate expression of Twist within these areas, these results support the findings of Matsuo *et al* (2009) who reported that Twist expression did not increase proliferation, but disagrees with the majority of published work including Kwok *et al* (2007) and Lee *et al* (2011). This discrepancy may be explained by Matsuo's group detecting the Twist marker in epithelial cells from human liver tissue samples as opposed to the isolated cell culture models used by Kwok and Lee, emphasising the importance of *ex vivo* experiments when confirming the involvement/role of molecular pathways in human disease processes. Interestingly, Matsuo *et al* found that cell migration activities increased within Twist expressing cells in *in vitro* wound healing assays. My data revealed concomitant expression of Twist and α-SMA suggest fibroblastic foci are sites of active wound remodelling, with myofibroblasts contracting in order to close the injured alveolar epithelium. Twist has also been shown to inhibit p53 mediated cell death and is therefore considered as an anti-apoptotic factor (Maestro *et al*, 1999). This role of cell senescence and proliferation in IPF tissue remodelling will be investigated in chapter 4.

My observations would suggest that EMT may not be a key driver in fibroblast/myofibroblast production in IPF; I propose an alternate hypothesis that resident fibroblasts/myofibroblasts, attracted to a site of initial injury, produce gelatinases A and B,

destroying the alveolar basement membrane. This action allows fibroblasts/myofibroblasts, present in the circulation, and attracted to sites of wound injury, to accumulate forming the fibroblastic foci. TGF-β and Twist may provide protection for these myofibroblasts from apoptosis, possibly in part due to the activation of phosphoinositide 3-kinase (PI3K) and the (PTEN)-AKT pathway (Horowitz *et al*, 2004) and, in the case of Twist, via the inhibition of p53 (Maestro *et al*, 1999). The ATII cell expression of TGF-β protein may inhibit the production of matrix metalloproteinases (MMPs), stimulating production of tissue inhibitors of metalloproteinases (TIMPs), and leading to the continued accumulation of collagen I observed within fibroblastic foci (Ma and Chegini, 1999).

Whilst EMT mechanisms may vary, depending on the processes involved in organ development, fibrogenesis, wound remodelling or cancer development, the common features of loss of cell adhesion and cytoplasmic epithelial expression of mesenchymal markers remain universally accepted. I therefore conclude that EMT *does not* constitute a major factor in the pathogenesis of IPF and the development of fibroblastic foci. Tissue remodelling in IPF is a complex process involving multiple driving factors which vary depending on cell type and location. Myofibroblasts, present within the fibroblastic foci, may migrate and contract whilst also providing a scaffold for ATII cells, dividing at the edges of the foci, to be drawn over the surface to bridge the damaged alveolar basement membrane. Contact inhibition of ATII cells overlying these foci may be responsible for limited differentiation of ATII cells available to replace the damaged ATI cells. This would lead to impaired and dysregulated alveolar repair in localised micro niche areas, which could in turn partly explain the pathognomonic feature of temporal heterogeneity observed in IPF lungs. The identification of effector pathways that are activated during contact inhibition

between the fibroblastic foci and overlying ATII cells holds the promise of revealing novel targets for the much needed treatment of IPF.

Chapter 4

Exploration of cell cycle marker activity and localisation in IPF lung tissue.

4.1 Introduction

Key histological markers of IPF include ATI cell destruction, ATII cell hyperplasia and the formation of fibroblastic foci leading to irreversible architectural distortion of lung tissue. The mechanisms driving these aberrant wound repair processes remain poorly understood. It is thought that alveolar cells are only able to undergo a limited number of cell cycles before entering senescence (Tsuji *et al*, 2006). Once alveolar cells reach this senescence stage the proliferation that compensates for apoptosis of the damaged cells stops. This process may occur in areas of active tissue remodelling located in the vicinity of established fibroblastic foci, as described in chapter 1.2.1. (Katzenstein and Myers, 1998).

A sign of active disease remodelling in the lung, as opposed to end stage honeycomb formation, is the proliferation of ATII cells. In Chapter 3, I demonstrated a previously unreported pattern of ATII cell proliferation at the edges of, and away from established fibroblastic foci, with diminished proliferation markers in the cells directly overlying the foci and a negative correlation of Ki-67 with increasing numbers of fibroblastic foci. This leads me to question whether direct contact or cross-talk via soluble factors/signals such as TGF-β and TRAIL, within focal areas of active pro-fibrogenic activity induces these ATII cells to enter cell senescence; whilst ATII cells away from the foci are uninhibited by these suppressive mechanisms and are attempting to repair the damaged alveolar epithelia. Figures 1.7 and 1.10 show that once cell division is complete epithelial and mesenchymal cells involved in lung repair may be under the control of external growth factors such as TGF-β. TGF-β has been shown in epithelial tracheal cell culture studies to prevent cells from proliferating and possibly cause ATII cell and fibroblast differentiation (Boland *et al*, 1996). In support of TGF-β mediated differentiation, chapter 3 findings revealed enhanced

expression of TGF-β in both ATII cells and fibroblastic foci; however, there was no concomitant loss of E-cadherin. When combined with areas of N-cadherin expression in ATII cell clusters away from the foci, these findings raise doubts as to the process of ATII cell differentiation forming the fibroblastic foci, but does not preclude ATII cells differentiating into ATI cells. These results therefore question whether TGF-β, as a recognised major player in IPF pathogenesis, could play a dominant role in the inhibition of ATII cell proliferation rather than their differentiation, via EMT, into myofibroblasts.

Cell culture studies have shown that one difference in determining whether a cell enters a state of cell senescence or reversible cell cycle arrest is by the presence and amount of growth factors (Leontieva and Blagonsklonny, 2010, Blagosklonny, 2011). It is hypothesised that over-activation of a growth-promoting pathway, such as mitogen-activated protein kinase (MAPK) or Target of Rapamycin (mTOR) (Demidenko and Blagosklonny, 2009), when the cell cycle is blocked downstream, leads to cellular hypertrophy and senescence rather than the growth factor-independent and reversible cell cycle arrest (termed quiescence) (Blagosklonny, 2006). In chapter 3 I report significant expression of TGF-β protein in fibroblastic foci and within the overlying ATII cells which, when combined with the absence of Ki-67 expression overlying the foci would support that the ATII cells are senescent. To prove this theory I would expect to find a positive correlation of cell senescence markers, p53, $p21^{WAF1}$ and $p16^{INK4A}$ within ATII cells and increasing number of fibroblastic foci.

To maintain effective and homeostatic lung wound repair in response to constant insult/injury exposure, the ATII cells are under tight cell cycle control by cyclins and cyclin dependent kinases (cdks) at specific checkpoints. This is covered in more detail in section

1.2.3. and summarised in Figure 1.10. Briefly, SOCS3 inhibits STAT3 resulting in the promotion of Cyclin D1, which then complexes with cdk4 driving the cell through the S-phase of the cell cycle. Cdk4 may be inhibited by the tumour suppressor $p16^{INK4A}$ preventing the Cyclin/cdk complex forming and leading to cell cycle arrest. To explore this mechanism in IPF, I will determine the localisation of Cyclin D1, SOCS3 and $p16^{INK4A}$ in ATII cells within IPF lungs, examining both the affected and conserved areas of the tissue samples and make comparisons to control lung sections.

Results from chapter 3 revealed varied SP-C expression amongst hyperplastic ATII cells which may indicate variation in maturity or functionality; however, it may be possible that deregulation of the cell cycle, or cross-talk between fibroblastic foci and overlying ATII cells may account for the variation in SP-C protein expression levels and proliferation/apoptosis observed in IPF. To examine this hypothesis the cell cycle mediator p53 will be studied. As described in chapter 1.2.3, p53 may induce the CDK inhibitor $p21^{WAF1}$, suppressing cell proliferation by inhibiting Cyclin D1 and promote cellular differentiation in response to DNA damage (Gartel and Tyner, 2002). Previous studies, using immunohistochemistry in 16 IPF lung tissue samples, have shown over-expression of p53 triggering cell cycle arrest and induction of apoptosis (Chilosi *et al*, 2002). This study focused on broncho-alveolar junctions proposing that deregulated interactions between epithelial and mesenchymal cells, as well as abnormal proliferation of epithelial cells after injury, leads to abnormal lung tissue remodelling in IPF. If my hypothesis of cross-talk between fibroblastic foci and ATII cells, and consequent deregulated cell cycle processes is correct, then I would expect to see expression of p53 and $p21^{WAF1}$ in areas of non-SP-C producing ATII cells, especially surrounding the fibroblastic foci. Such findings would add support to

the concept that fibroblastic foci represent areas of active ongoing injury (Fukuda *et al*, 1995, Paakko *et al*, 2000).

In addition to abnormal ATII cell proliferation, an important component of wound remodelling and clearing of damaged cells in the IPF lung is the presence of apoptosis, described in more detail in chapter 1.2.3. Apoptotic cells are known to lose cell-cell adhesion properties, eventually breaking down into fragments that are engulfed by neighbouring cells (Santini *et al*, 2000). In chapter 3, I reported continued expression of the cell-cell adhesion marker E-cadherin in the ATII cells; this leads me to question whether the pathogenic mechanisms driving IPF may in part involve dysfunctional apoptotic signalling pathways, such as the Fas signalling pathway (Maeyama *et al*, 2001). It is known that in IPF alveolar epithelial damage leads to destruction of the underlying basement membrane with subsequent recruitment of residential fibroblasts and possibly circulating fibrocytes (Phan, 2002, Moore *et al*, 2005, Kim *et al*, 2006). These fibroblasts have been reported to be resistant to apoptosis, resulting in excessive collagen deposition in cell culture studies (Moodley *et al*, 2004).

I propose that this apparent resistance to apoptosis may be linked to failure of the TRAIL signalling mechanism. As discussed in more detail in section 1.2.3, TRAIL binds to the death receptors DR4/DR5 in transformed or cancer cells but not normal cells (Wand and El-Deiry, 2003). If the cells within the fibroblastic foci are transformed from either residential or circulating fibroblasts/fibrocytes, or indeed EMT, I would anticipate TRAIL/DR4/DR5 expression within the fibroblastic foci, and a negative correlation between these markers and increased numbers of fibroblastic foci.

It is therefore possible that, in the lung tissue remodelling associated with IPF, cells undergoing proliferation, senescence and apoptosis also follow a temporal distribution in separate and distinct areas, leading to patchy and diffuse distortion of the lung architecture, rather than a coordinated repair response. To assess this hypothesis, the panel of target markers discussed in this chapter and in section 1.2.3, involved in proliferation, cell cycle regulation and apoptosis will be examined in diseased areas compared to microscopically apparent conserved areas of IPF lung tissue samples. The conserved areas will then be compared to control lung tissue samples to determine if the cells are functioning "normally", or whether subtle differences in ATII cell functionality can be identified though detailed immunohistochemical analysis. This may provide fresh insights into the characteristic temporal heterogeneity associated with a diagnosis of IPF, a key distinguishing feature of this disease not present in other ILDs. Performing dual-immunohistochemistry will allow for histological correlation of markers within the same cell and reduces the risk of losing features of interest during multiple tissue sectioning. These studies may also provide clues as to the variability in maturity or functionality of SP-C production in ATII cells, reported in chapter 3. By performing a Pearson correlation between cell cycle expression levels in ATII cells and fibroblastic foci numbers I aim to explore the extent to which cross talk between the foci and overlying ATII cells results in ATII cell senescence, proliferation or apoptosis and how this relates to disease activity. Correlations between cell cycle marker expression levels within the fibroblastic foci and number of foci may identify which cell regulatory pathways are involved in maintaining the presence of myofibroblasts leading to increased disease activity.

4.2 Materials and methods

4.2.1 Lung tissue samples

Lung tissue samples were selected and prepared as detailed in chapters 2.1 and 2.1. Samples were analysed from 21 randomised patients with histologicaly confirmed IPF and 19 histologicaly normal lung tissue samples for the control group.

4.2.2 Selection of markers

The selection of target markers for exploring cell cycle marker activity and localisation in IPF was based on markers used in previous investigations of cell cycle regulation, senescence and apoptosis discussed in detail in section 1.2.3 and summarised in Table 4.1. Multiple markers were analysed to provide a comprehensive analysis of the role and distribution in diseased and apparently conserved areas of IPF lung tissue samples. The optimised final dilutions and incubation times are summarised in Table 4.1.

4.2.3 Immunohistochemistry

Preparations of lung tissue samples for analysis are detailed in chapter 2.2. Lung tissue sections, 3µ thick were cut from paraffin embedded lung tissue samples and placed onto electro-statically charged slides (CellPath Ltd, UK). Sections were deparaffinised in Xylene for 3 minutes and rehydrated through alcohol to water prior to antigen retrieval.

An attempt was made to standardise all antigen retrieval methods for all markers to allow for dual-immunohistochemistry to be performed; however dual-immunohistochemistry is not possible for markers expressed in the same cellular compartment. Initial dilution factors and selection of positive control material for the development of target marker antibodies were based on manufacturer guidelines and

previous published reports. The development of final antibody dilutions and antigen retrieval methods is described in section 2.3.2. Development of markers for dual immunohistochemistry is detailed in section 2.3.3.

All lung tissue samples were placed on an automated linier immunostainer, (Dako Autostainer Plus, DakoCytomation, Denmark) with positive and negative control samples run alongside. Visualisation was via the DakoEnvision detection system (Dako, Denmark), using chromogens DAB (DakoCytomation, Denmark) and/or Very Intense Purple (Vector Labs, UK).

Final dilutions, incubations times and control material are detailed in Table 4.1.

Antibody	Source	Antigen retrieval	Dilution/ incubation time	Positive control	Localisation/role
Cyclin D1 SP4.	Lab Vision Corporation (USA)	Citrate buffer pH6 MW 10mins 100%, 10mins 70% power. Cool 20 mins	1:10 RT 30mins	Mantel cell lymphoma	Nuclear. Co-ordinates cell growth and stimulates entry into a new cell cycle at the Start checkpoint (Bova *et al* 1999)
SOCS3	Abcam (UK)	Citrate buffer pH6 MW 10mins 100%, 10mins 70% power. Cool 20 mins	1:100 RT 30mins with PB	Lung	Cytoplasmic SOCS3 inactivates STAT3 which results in the promotion of Cyclin D1 leading to cell cycle progression. (Lu *et al*, 2006)
$p16^{INK4A}$	BD Bioscience (UK)	Citrate buffer pH6 MW 10mins 100%, 10mins 70% power. Cool 20 mins	1:20 RT 30 mins with PB	Breast	Nuclear/cytoplasmic Tumour suppressor gene induced by DNA damage, oncogene stress and oxidative stress (Belinsky *et al*, 1998)
p53	Dako Cytomation (Denmark)	EDTA pH8 MW 10mins 100%, 10mins 70% power. Cool 30 mins	1:800 RT 30mins	Hodgkins disease affected lymph node	Nuclear/cytoplasmic Wild type p53 behaves as a tumours suppressor. In normal cells has a short half life, generally below the detection level of immunohistochemistry. (Eccles *et al*, 1992)
$p21^{WAF1/Cip1}$	Dako Cytomation (Denmark)	High pH9. MW 20mins 100%power. Cool 30 mins	1:50 RT 30mins	Colon mucosa	Nuclear Cyclin dependent kinase inhibitor. (Inoshima *et al,* 2003)
TRAIL	Abcam (UK)	MW citrate buffer pH6 10mins 100%, 10mins 70%. Cool 30mins	1:75 30mins RT with PB	Skin	Membrane Induces apoptosis in tumour cells but not normal cells when bound to DR4 and/or DR5. (Wang and El-Deiry, 2003)
DR4	Abcam (UK)	MW citrate buffer pH6 10mins 100%, 10mins 70%. Cool 30mins	1:200 30mins RT with PB	Skin demonstrating basal cell carcinoma	Membrane Death receptor for TRAIL. (Wang and El-Deiry, 2003)
DR5	Abcam (UK)	MW citrate buffer pH6 10mins 100%, 10mins 70%. Cool 30mins	1:800 30mins RT with PB	Skin demonstrating basal cell carcinoma	Membrane Death receptor for TRAIL. (Wang and El-Deiry, 2003)

Table 4.3. Final antibody dilution, incubation times and cellular localisation of markers used in chapter 4. RT=room temperature. MW=microwave. PB=protein block.

4.2.4 Semi-quantitative analysis

Semi-quantitative analysis is described in detail in section 2.5. In summary, sections were scored by myself and then reviewed independently by a pathologist (Dr D Gey van Pittius) by examining expression of markers at sites of fibroblastic foci and ATII cells in IPF and control samples. For the ATII cells in IPF samples, 3 random fields of 100 hyperplastic cells were counted at x100 magnification and the proportion of cells expressing each marker was recorded with the mean of the three fields giving the final value used in this study. Within control lung sections the distribution of the ATII cells is scattered therefore, a systematic scan of the section starting at the 12 o'clock position of the section and scanning in a clockwise direction was performed to count 100 cells. For fibroblastic foci the scanning method was as used for the ATII cells in the control group. 100 cells were counted within the fibroblastic foci, if there were enough fibroblastic foci this was repeated three times and the mean expression used for analysis. If the disagreement between myself and Dr Gey van Pittius was >15%, the cells were counted again.

For assessment of disease activity sections were scored by myself and a semi-quantitative assessment was made for each individual biopsy using a scale of 0-6 for the extent of fibroblastic foci, previously described and illustrated by Nicolson *et al* (2002). Representative images used for scoring are seen in Figure 2.1. A score of 0 was assigned to those samples containing no fibroblastic foci; a score of 6 was given to those samples with the most profuse number of foci. Further details are provided in section 2.5. These scores were then correlated against the mean expression scores for each immunohistochemical marker in each IPF tissue sample in ATII cells and cells within fibroblastic foci as described in section 2.6.

4.2.5 Statistical analysis

A semi-quantitative analysis was used to compare groups using a modified Allred scoring system (Harvey *et al* 1999) described in section 2.5 and set out in Table 2.4. Results are presented as mean expression score ± standard deviation. A Mann Whitney U test was used for comparisons between IPF and control ATII cells, as described in section 2.6. Graphical results are presented as mean expression score ±SD. Differences were considered significant if $p \leq 0.05$. Statistical analysis was performed using WinSTAT, (R. Fitch Software, Bad Krozingen, Germany).

As described in more detail in section 2.6, a Pearson correlation co-efficient was calculated to determine correlations between mean target marker expression levels in hyperplastic ATII cells and cells within fibroblastic foci with disease activity. The results were interpreted and categorised as no correlation, weak, moderate and strong correlation according to Cohen (2002), Table 2.5. Statistical analysis was performed using Minitab® 15 Statistical Software (USA). The Pearson correlation co-efficient is a measure of variability, therefore if all the mean expression scores for a particular marker are identical, there is no variability, and the calculation cannot be performed.

4.3 Results

Mean marker expression scores for ATII cells and fibroblastic foci, demonstrating the degrees of variation between individual cases, for each tissue sample are shown in Table 4.2. and 4.3. Table 4.4 lists the Pearson correlation scores for markers of EMT and proliferation against number of fibroblastic foci.

Case Number	Cyclin D1	SOCS3	$p16^{INK4A}$	p53	$p21^{WAF1}$	TRAIL	DR4	DR5
1	5	5	5	4	4	3	4	5
2	4	5	5	4	3	4	4	5
3	5	5	5	4	4	4	5	5
4	4	5	5	3	4	5	5	5
5	5	5	4	3	3	4	5	5
6	4	5	5	2	2	5	5	5
7	4	5	5	3	4	4	5	5
8	4	5	5	3	3	5	5	5
9	5	5	5	2	3	4	5	5
10	5	5	5	2	3	3	5	5
11	4	5	4	2	3	4	5	4
12	3	5	4	2	4	4	5	5
13	5	5	5	3	4	4	5	5
14	5	5	4	3	4	5	5	5
15	5	5	5	4	4	5	5	5
16	3	3	5	3	2	5	5	5
17	4	4	4	3	4	4	5	5
18	5	5	5	3	3	4	4	5
19	5	5	3	4	4	5	5	5
20	5	5	4	4	3	5	5	5
21	5	4	5	4	4	5	5	5
Mean	4.4762	4.8095	4.6190	3.0952	3.4286	4.3333	4.8571	4.9524

Table 4.2 Mean marker expression scores in ATII cells for individual cases. Highlighted scores represent greatest variation between individual cases (>30%).

Case Number	Cyclin D1	Socs3	$p16^{INK4A}$	p53	$p21^{WAF1}$	TRAIL	DR4	DR5
1	0	2	0	0	0	0	4	5
2	0	0	0	0	0	0	4	3
3	0	0	1	0	0	4	4	5
4	0	0	1	0	0	4	4	2
5	0	0	0	0	0	0	0	3
6	0	1	1	0	0	0	3	5
7	0	0	4	0	0	4	4	3
8	0	0	0	0	0	3	4	3
9	2	4	4	0	0	4	4	4
10	2	3	4	0	0	3	5	4
11	2	0	3	0	0	1	2	4
12	0	3	2	0	0	2	5	5
13	2	2	3	0	0	3	5	4
14	0	1	1	0	0	1	3	4
15	0	3	4	0	2	5	4	5
16	0	0	4	0	0	4	4	4
17	0	2	2	0	0	2	2	4
18	0	0	2	0	0	5	2	2
19	0	0	0	2	2	4	3	3
20	0	2	0	1	0	5	4	5
21	x	0	2	0	0	3	2	2
Mean	0.4	1.0952	1.8095	0.1429	0.1905	2.7143	3.4286	3.7619

Table 4.3 Mean marker expression scores in fibroblastic foci for individual cases. Highlighted scores represent greatest variation between individual cases (>30%). X = no foci in tissue section.

Target Marker	Pearson correlation for marker expression within ATII cells	Pearson correlation for marker expression within fibroblastic foci
Cyclin D1	0.407	0.196
SOCS3	0.439	0.465
$p16^{INK4A}$	-0.156	0.225
p53	-0.029	0.308
$p21^{WAF1}$	0.158	0.27
TRAIL	-0.353	0.359
DR4	-0.051	0.148
DR5	0.169	0.078

Table 4.4 Pearson correlation of mean expression score of immunohistochemical markers within ATII cells and fibroblastic foci correlated against fibroblastic foci score. Weak correlation pink, moderate correlation yellow, strong correlation green.

4.3.1 Cyclin D1 (regulates and promotes entry into S-phase of the cell cycle)

Nuclear Cyclin D1 expression was scanty in control type II pneumocytes (mean expression score 1.42, SD± 1.387) (Figure 4.1A), compared to extensive expression in hyperplastic ATII cells in the IPF group (mean expression score 4.47, SD± 0.679) ($p<0.05$) (Figure 4.1B, C, D). Negligible expression of cyclin D1 was identified within the fibroblastic foci (mean expression score 0.4, SD± 0.820).

Cyclin D1 expression within ATII cells of IPF lung tissue samples identified a moderate positive correlation with number of fibroblastic foci (Pearson correlation co-efficient 0.407). A weak positive correlation was identified for Cyclin D1 expression with fibroblastic foci and number of fibroblastic foci (Pearson correlation co-efficient 0.196).

4.3.2 SOCS3 (Suppressor of cytokine signalling)

A significant increase in cytoplasmic SOCS3 expression (mean expression score 4.80, SD± 0.511) was observed in IPF ATII cells compared with control cells (mean expression score 0.10, SD± 0.458) $\leq p$ 0.05 (Figure 4.1A, Figure 4.1B, C, D and Figure 4.6). Scanty expression of SOCS3 was identified within the fibroblastic foci (mean expression score 1.09, SD± 1.338).

A moderate positive correlation was identified for SOCS3 expression within ATII cells and fibroblastic foci against number of fibroblastic foci (Pearson correlation co-efficient 0.439 and 0.465 respectively).

4.3.3 Dual immunohistochemistry of Cyclin D1 and SOCS3 (STAT3 inhibitor; promotes Cyclin D1)

Cyclin D1 was co-expressed with cytoplasmic expression of SOCS3 in ATII cells overlying fibroblastic foci. Negligible expression of CyclinD1 and SOCS3 (mean expression score 0.4, and 1.09 respectively) were seen within fibroblastic foci (Figure 4.1C, D and Figure 4.7) with no dual expression identified within the myofibroblasts.

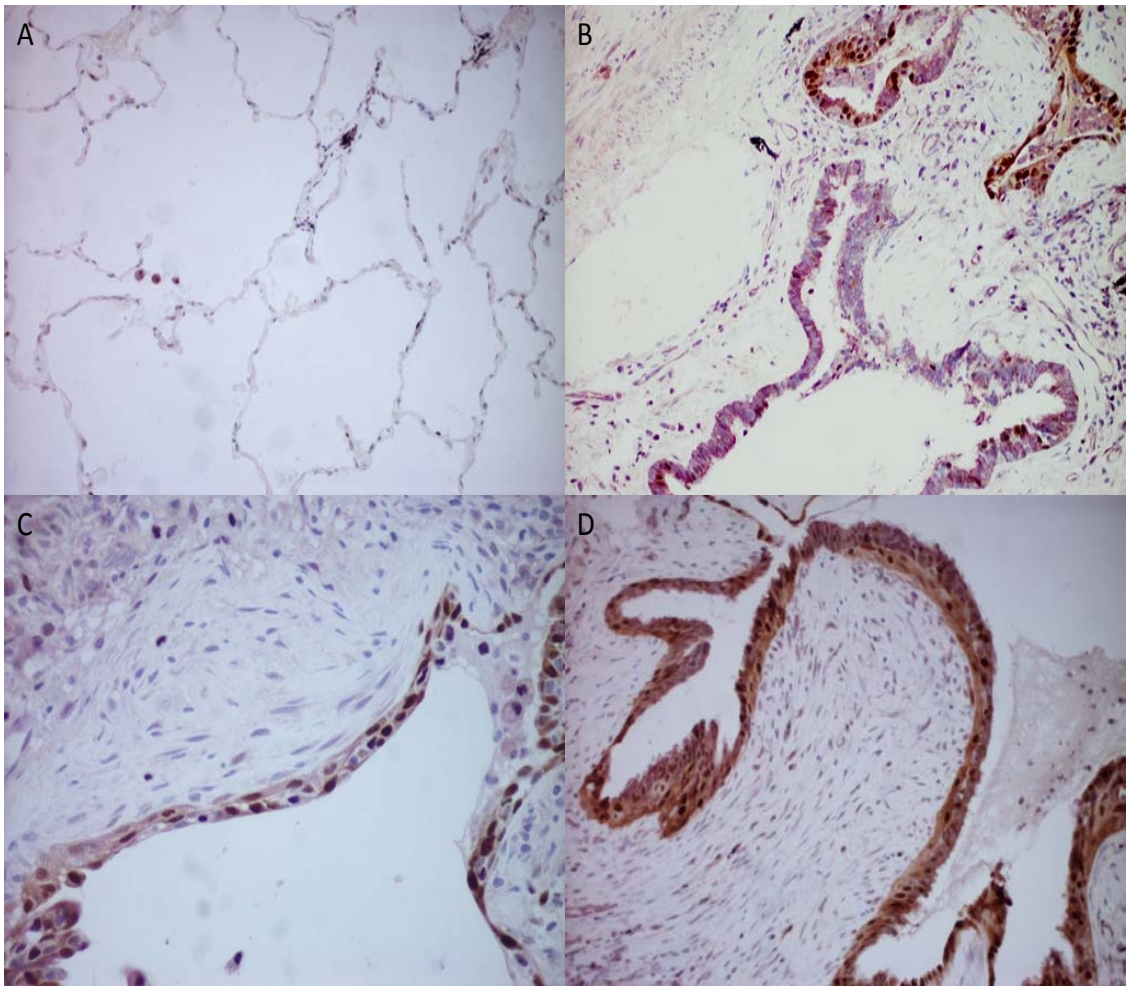

Figure 4.1 Dual-labelled immunohistochemistry of IPF and control lung samples for Cyclin D1 and SOCS3 expression. A. Representative histological image of control lung tissue shows no Cyclin D1 or SOCS expression within the alveoli. SOCS3 expression is expressed by macrophages (arrow). Magnification x200. B. IPF lung tissue demonstrates variable expression of Cyclin D1 (brown) and SOCS3 (purple) in the hyperplastic ATII cells (black arrow), with extensive expression within the ciliated epithelium (blue arrow). Magnification x200. C and D. Two separate IPF tissue samples with ATII cells overlying fibroblastic foci expressing both Cyclin D1 (brown) and SOCS3 (purple), however, cells within the foci did not express either marker. Magnification x400

4.3.4 p16^{INK4A} (Tumour suppressor gene, inhibits cdk4)

p16^{INK4A} expression was absent or negligible in ATII cells of control samples (mean expression score 0.52, SD± 0.904) (Figure 4.2A and 4.6). In IPF tissue samples cytoplasmic p16^{INK4A} expression was observed in ATII cells directly overlying fibroblastic foci (Figure 4.2B). p16^{INK4A} was expressed to a lesser extent in ATII cells away from these areas. Overall a significant increase in ATII cells expressing p16^{INK4A} was noted in IPF samples (mean expression score 4.61, SD± 0.589; $p<0.05$ (Figure 4.6). Scanty p16^{INK4A} expression was identified within fibroblastic foci (mean expression score 1.809, SD± 1.569) (Figure 4.7).

Expression of p16^{INK4A} in ATII cells of IPF lung tissue samples revealed a weak negative correlation with number of fibroblastic foci (Pearson correlation co-efficient -0.156). p16^{INK4A} expression within fibroblastic foci indicated a weak positive correlation with number of fibroblastic foci (Pearson correlation co-efficient 0.225).

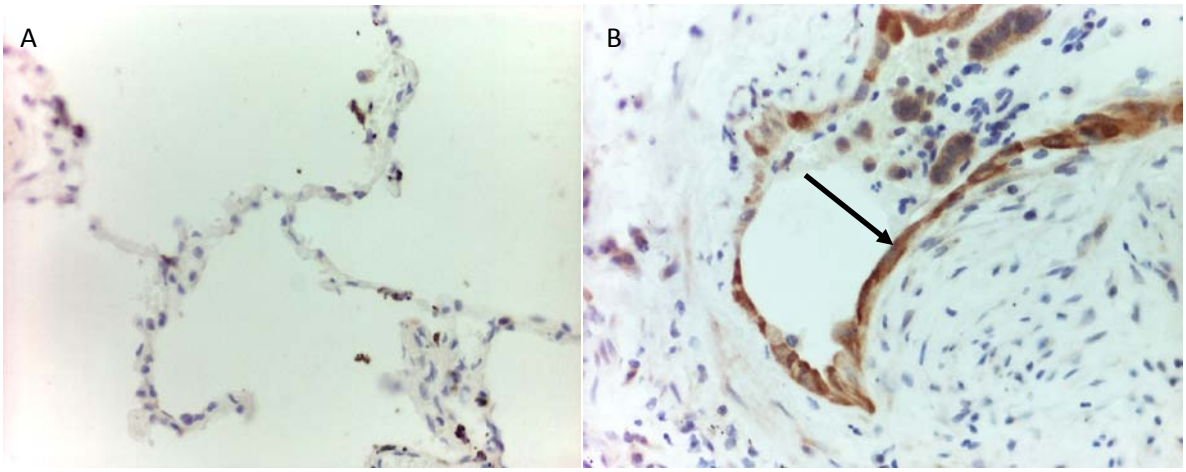

Figure 4.2. Immunohistochemical analysis of IPF and control lungs for p16^{INK4A}. A. p16^{INK4A} reactivity is not observed in control lung tissue in this representative image. B. Cytoplasmic p16^{INK4A} reactivity is seen in the ATII cells overlying fibroblastic foci (arrow) in a representative histological image of IPF lung tissue. Magnification x400.

4.3.5 p53 (transcription factor involved in apoptosis regulation)

No expression of p53 was observed in control ATII cells (Figure 4.3A) with scattered p53 expression identified in bronchiolar epithelium. p53 expression was increased in IPF cases $p \leq 0.05$; however this varied between cases with mean ATII cells expression scores ranging from 2-4 (mean expression score 3.091, SD± 0.768) (Figure 4.3B, C, D, Figure 4.6). p53 expression within fibroblastic foci revealed only two cases with scores of 2 and 3 (mean expression score 0.14, SD±1.478), all other IPF tissue samples were negative (Figure 4.7).

No correlation was identified for p53 expression within ATII cells of IPF lung tissue samples against number of fibroblastic foci (Pearson correlation co-efficient -0.029). A moderate negative correlation was present for p53 expression within fibroblastic foci and number of fibroblastic foci (Pearson correlation co-efficient -0.308).

4.3.6 p53 and SP-C dual immunohistochemistry.

Using dual-staining immunohistochemistry, the predominant pattern of expression involved areas of ATII cells expressing SP-C but not p53 in distinct patches from those areas of ATII cells expressing p53 but negligible or no SP-C (Figure 4.3B and C). Cells directly overlying the fibroblastic foci consistently expressed p53; SP-C expression was varied (Figure 4.3C); however, SP-C expression may be masked by strongly expressing p53 cells in these areas. Conserved areas of IPF lung tissue samples demonstrated SP-C expression but little or no p53 (Figure 4.3D).

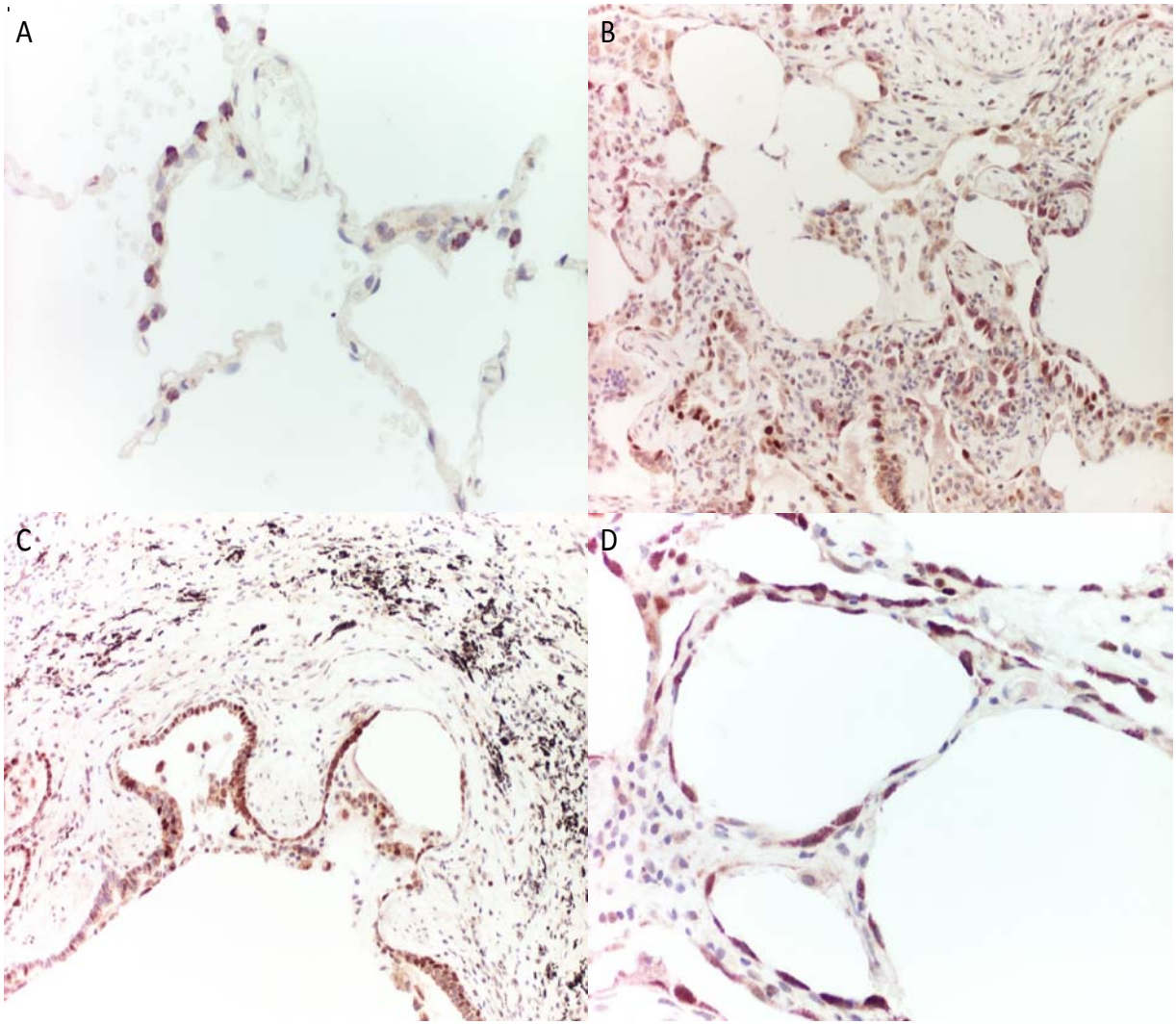

Figure 4.3 Dual immunohistochemistry analysis of p53 and SP-C expression in IPF and control lungs. A. Representative image of SP-C expression in the cytoplasm of ATII cells in control lung tissue (arrow), no expression of p53 is observed. B. Patchy expression of p53 in a representative IPF tissue sample (black arrow) with reduced expression of SP-C. C. p53 expression of ATII cells overlying a fibroblastic foci (black arrow). SP-C is expressed away from the foci and does not co-express with p53 (blue arrow). D. Representative image of a conserved area of IPF lung tissue adjoining diseased lung expressing SP-C (arrow) but not p53. Magnification A and D x400, B and C x200.

4.3.7 $p21^{WAF1}$ (cyclin dependent kinase inhibitor)

No $p21^{WAF1}$ was detected in the alveolar epithelial cells of control tissue samples, with scattered expression observed only in ciliated bronchial epithelium (Figure 4.4A and B). Conserved areas of IPF lung did not express $p21^{WAF1}$ within ATII cells (Figure 4.4D). $p21^{WAF1}$ expression within hyperplastic ATII cells in the IPF group was variable but significantly increased compared to control lung, with mean IPF expression scores ranging from 2 to 4 (mean expression score 3.42, SD± 0.676) $p \leq 0.05$ (Figure 4.6). Fibroblastic foci demonstrated negligible expression of $p21^{WAF1}$ (mean expression score 0.19, SD± 0.601), (Figure 4.4C and 4.7).

Weak positive correlations were identified for $p21^{WAF1}$ expression within ATII cells and fibroblastic foci against number of fibroblastic foci (Pearson correlation co-efficient 0.158 and 0.27 respectively).

4.3.8. $p21^{WAF1}$ and SP-C dual immunohistochemistry

Dual immunohistochemistry of SP-C protein and $p21^{WAF1}$ was difficult to interpret due to antigen retrieval methods affecting SP-C antigen integrity and the strong staining from $p21^{WAF1}$ masking SP-C expression. However it appears that the pattern of $p21^{WAF}$ is similar to that of p53 as tissue sections were sequentially cut; nuclear expression was seen in ATII cells surrounding and overlying the fibroblastic foci (Figure 4.4C). No expression of $p21^{WAF1}$ was detected in conserved areas of IPF lung (Figure 4.4D).

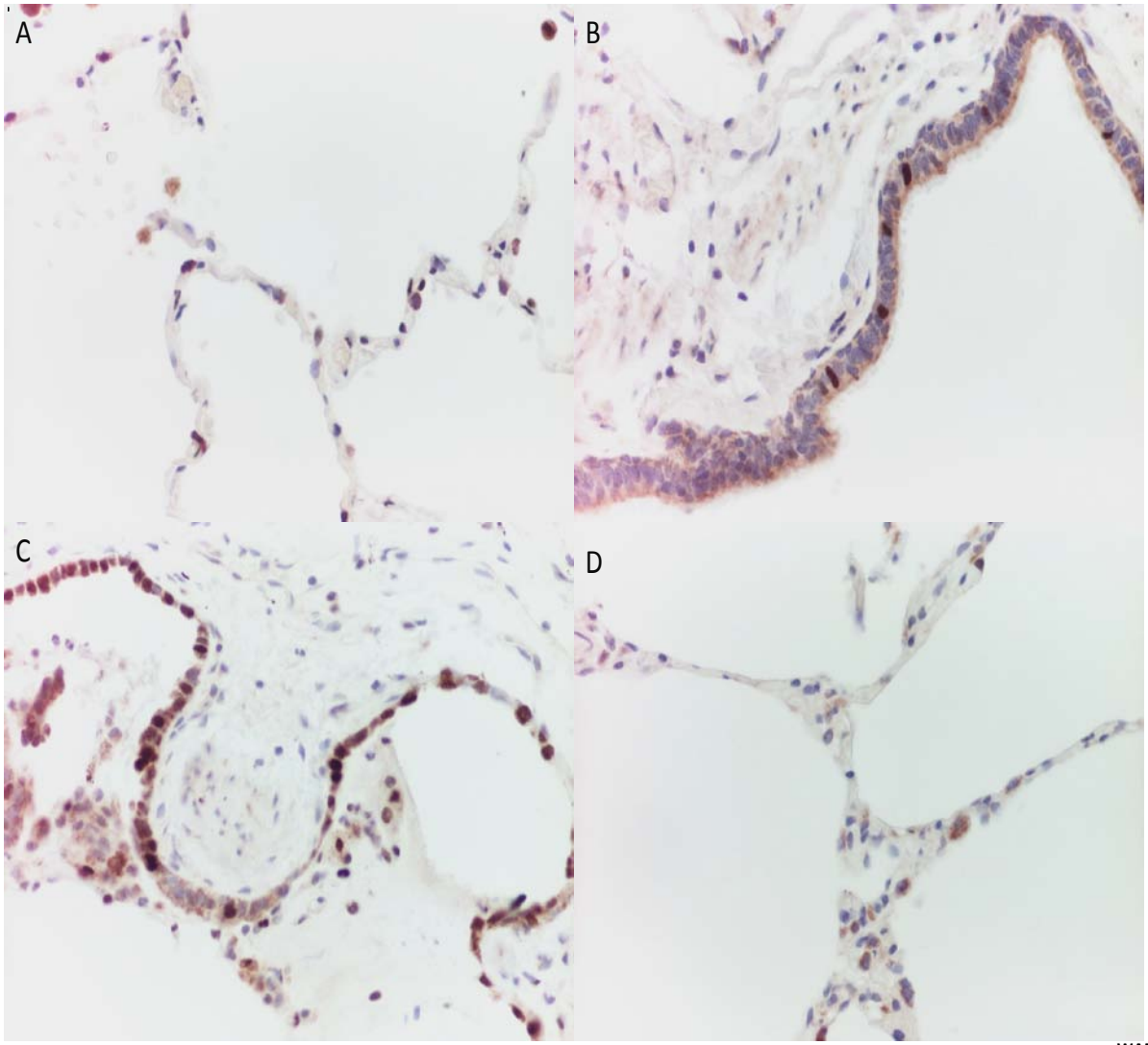

Figure 4.4. Dual-labelled immunohistochemistry of IPF and control lung samples for $p21^{WAF1}$ (brown) and SP-C expression (purple). A. Representative image of control lung tissue shows expression of SP-C within the cytoplasm of ATII cells (arrow). No expression of $p21^{WAF1}$ is expressed. B. Ciliated bronchiolar epithelium in control lung tissue demonstrating scattered $p21^{WAF}1$ expressing cells (arrow). C. IPF lung tissue samples demonstrate $p21^{WAF1}$ reactivity in the ATII cells overlying and surrounding a fibroblastic foci (arrow). D. A representative image of IPF lung demonstrating no $p21^{WAF1}$ expression. Magnification x400.

4.3.5 TRAIL and its receptors DR4/DR5

TRAIL induces apoptosis when bound to death receptors DR4/DR5 in transformed cells (Wang and El-Deiry, 2003). Cytoplasmic TRAIL and nuclear DR4/DR5 expression was scanty in the ATII cells of control tissue samples (mean expression scores 1.26, 1.68, 1.25 respectively, SD± 1.147, 1.376, 1.407 respectively) compared to significantly elevated extensive expression levels in IPF lung samples (mean expression scores; TRAIL 4.33, DR4 4.85 and DR5 4.95, SD± 0.658, 0.358, 0.218 respectively) $p \leq 0.05$ (Figures 4.5A-F and Figure 4.6). TRAIL, DR4 and DR5 markers were expressed directly overlying fibroblastic foci and in the hyperplastic ATII cells away from these areas. Within fibroblastic foci the mean expression scores for TRAIL and DR4 were 2.71 (SD± 1.764) and 3.42 (SD± 1.247) respectively; however, within the sample population expression scores varied between 0 and 5 (expression range 0 - >66%) (Figure 4.5B, D and Figure 4.6). Myofibroblasts within the fibroblastic foci showed scanty to moderate DR5 expression (mean expression score 3.76, SD± 1.044) (Figure 4.5F and Figure 4.7).

A moderate negative correlation was identified for TRAIL expression in ATII cells against number of fibroblastic foci (Pearson correlation co-efficient -0.353). For TRAIL expression in fibroblastic foci a moderate positive correlation was recorded (Pearson correlation co-efficient 0.359).

No correlation was identified for DR4 expression in ATII cells (Pearson correlation co-efficient -0.051) or for DR5 expression within fibroblastic foci against number of fibroblastic foci (Pearson correlation co-efficient 0.078). A weak positive correlation was identified for DR4 expression within the fibroblastic foci (Pearson correlation co-efficient 0.148) and DR5 expression within ATII cells (Pearson correlation co-efficient 0.169).

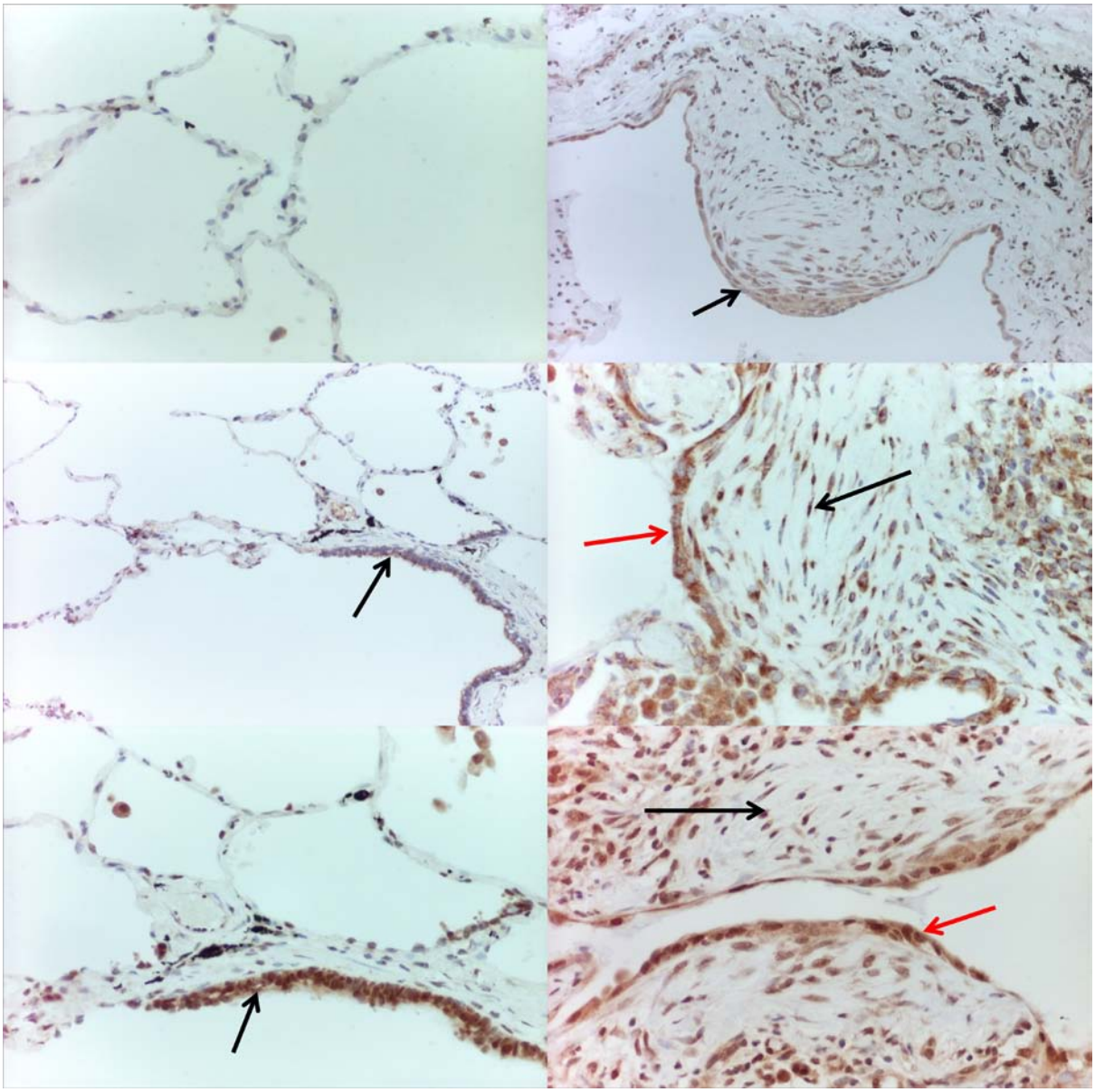

Figure 4.5. Immunohistochemical analysis of IPF and control lungs for TRAIL. A. Representative image of control lung tissue shows no TRAIL expression. B. IPF lung tissue demonstrates TRAIL both in the ATII cells overlying a fibroblastic foci (arrow) and also within the foci itself. C. Representative image of control lung tissue shows no cytoplasmic DR4 expression within ATII cells, scattered DR4 expressing ciliated cells are seen (arrow). D. IPF lung tissue demonstrates cytoplasmic DR4 expression within the fibroblastic foci (black arrow) and in the surrounding hyperplastic ATII cells (red arrow). E. Control lung demonstrates DR5 expression in the ciliated (arrow) but not alveolar epithelium. F. IPF lung tissue demonstrates extensive DR5 expression both within the fibroblastic foci (black arrow) and in the overlying hyperplastic ATII cells (red arrow). Magnification A x400, B x200.

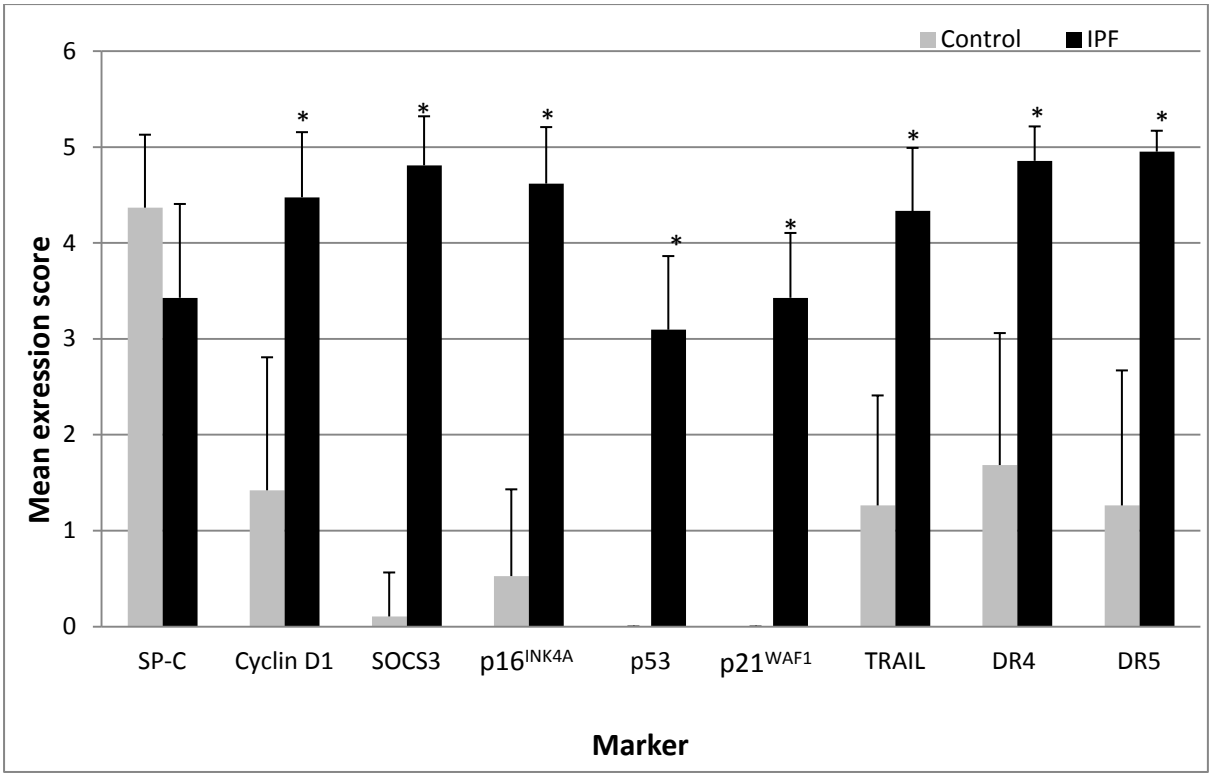

Figure 4.6 Semi-quantitative analysis of target molecule expression within ATII cells of IPF and control lungs samples. Data are presented as mean expression score ±SD. *=significant difference in expression between the control and IPF group p≤0.05.

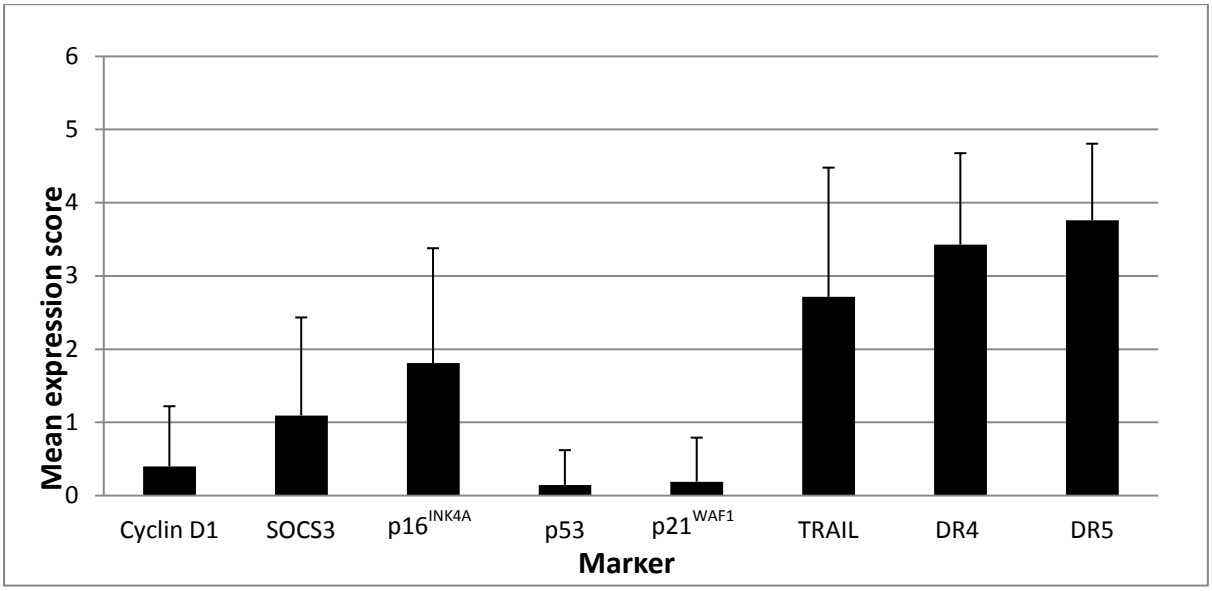

Figure 4.7 Semi-quantitative analysis of target molecule expression within the fibroblastic foci of IPF lung tissue samples. Data are presented as mean expression score ±SD.

4.4. Discussion

In this study I have demonstrated that in conserved areas of IPF lungs, ATII cells have consistent expression of SP-C but do not express $p21^{WAF1}$ or p53. This expression pattern was the same as in the control lung tissue samples. In contrast, within the same IPF lung tissue samples, hyperplastic ATII cells in the affected fibrotic regions expressed upregulation of $p21^{WAF1}$, p53, Cyclin D1, $p16^{INK4A}$ and SOCS3 markers with variable SP-C. A previous study examining lung tissue samples from 12 cases of IPF also found increased expression of p53 and $p21^{WAF1}$ within hyperplastic ATII cells compared to conserved and control alveolar epithelium (Plataki *et al*, 2005). In addition, Plataki *et al* examined the anti-apoptotic marker BCL-2, reporting down-regulation in hyperplastic ATII cells in IPF lung tissue samples. In my study these hyperplastic ATII cells also showed moderate to extensive expression of the apoptotic marker TRAIL and its receptors DR4 and DR5. This contrasts to the control lung tissue which revealed negligible expression of TRAIL and its death receptors and no expression of p53 or $p21^{WAF1}$. There are no previous published reports examining the expression of $p21^{WAF1}$, p53 or Cyclin D1 within fibroblastic foci of IPF lung tissue samples. I therefore provide the first report of negligible Cyclin D1, p53 and $p21^{WAF1}$ expression within these foci combined with moderate expression of TRAIL and its receptors DR4/DR5.

The lack of expression of $p21^{WAF1}$ and p53 with consistent expression of SP-C in ATII cells in the conserved areas of IPF lungs confirms that areas of “spared”, lung appear to be functioning as normal alveolar epithelia. These unaffected areas are intertwined with areas of *in situ* aberrant repair involving hyperplastic ATII cells that appear to have variable expression of SP-C, p53 and $p21^{WAF1}$. The variation of SP-C and p53 levels in ATII cells did not correlate with number of fibroblastic foci with $p21^{WAF1}$ demonstrating only a weak positive

correlation with increased numbers of foci (Table 4.4). Taken alone this correlation would suggest no interaction between fibroblastic foci and ATII cells. However the distribution and expression of cell cycle markers within the IPF lung tissue samples revealed a lack of co-expression of p53/SP-C and $p21^{WAF1}$/SP-C in the hyperplastic ATII cells immediately overlying fibroblastic foci suggests p53-mediated cell stasis or senescence resulting in non-functioning ATII cells rather than variation in cell maturity, a situation where p53 would not be expected to be expressed. My hypothesis of ATII cell stasis or senescence in IPF lung differs from the proposal by Plataki *et al* that these cells are undergoing apoptosis. My reasoning stems from the immunohistochemical expression analysis of an additional marker $p16^{INK4A}$. A study by Chen *et al*, (2005) examined the expression of $p21^{WAF1}$, p53 and $p16^{INK4A}$ in umbilical vein endothelial cells. When $p21^{WAF1}$ and p53 were expressed apoptosis resulted, however when $p16^{INK4A}$ was co-expressed the result was senescence of these cells, as identified by the expression of senescence-associated β-galactosidase (Sen-β-Gal). I propose that this is occurring in IPF lung.

To date the only studies on cellular senescence in IPF have focused on evidence of telomere shortening in two familial cases of the disease, using ancestral genotyping (Alder *et al*, 2011). My findings are the first to report evidence of ATII cell senescence in sporadic cases of IPF. This failure to remove non-functioning ATII cells could lead to a self-perpetuating, non-reparative milieu provoked by as yet unidentified mediators released by these damaged ATII cells. An alternate theory is that these cells are in cell cycle arrest whilst undoing DNA repair processes. Most cells in the body are in cell cycle arrest (quiescent) but are not senescent. Upon stimulation by growth factors a quiescent cell should enter the cell cycle, however this can be blocked by $p21^{WAF1}$ and $p16^{INK4A}$ (Blagosklonny, 2011). $p16^{INK4A}$ is

known to prevent the Cyclin D1/cdk4 complex by binding cdk4 (Sherr and Roberts, 1999; Cheng *et al*, 1999). This then leads to $p21^{WAF1}$ down regulating cdk2/Cyclin E complexes blocking the exit of the cell from G1 (Ortega *et al*, 2002). When cell division is blocked in this way but has continued stimulation by growth factors the cell becomes hypertrophic, as is seen by the ATII cells in the IPF lung tissue samples in my study. Further support for a senescent theory comes from investigations in fibroblast cell culture studies where senescent cells, when stimulated by growth factors, exhibit high levels of Cyclin D1 (Dulic *et al*, 1993, Riabowol, 1996). My study suggests that in ATII cells the continued stimulation by TGF-β conflicts with the blocking of the cell cycle by cdks. This leads to inappropriate S-phase entry to the cell cycle and/or loss of proliferative potential (Blagoskonny *et al*, 2011).

As hyperplastic ATII cells overlying fibroblastic foci did consistently express p53, $p21^{WA1}$, Cyclin D1 and $p16^{INK4A}$, it is plausible to hypothesise that the direct contact/cross-talk in this 'ATII-fibroblastic foci' niche may induce factors/signals, possibly via myofibroblast activation that induces cell stasis in the overlying ATII cells. These findings together with the observation of upregulated TGF-β expression by myofibroblasts and overlying ATII cells (as shown in chapter 3) implicates a possible TGF-β mediated contact inhibition mechanism. In contrast, those hyperplastic ATII cells not in direct contact with fibroblastic foci were shown to express SP-C indicating they may be normal functioning ATII cells. To investigate interactions between cell cycle markers in ATII cells and fibroblastic foci Pearson correlations were performed. Moderate positive correlations were identified for Cyclin D1 and SOCS3 in ATII cells; SOCS3 promotes Cyclin D1 whose levels depend on the rate of cell growth or on growth promoting signals rather than indicating the stage of the cell cycle (Morgan 2007). My data suggests that the growth promoting signals are from TGF-β protein

expressed by increasing numbers of fibroblastic foci. This does not rule out the involvement of alternate growth factors that have previously been shown to be implicated in IPF pathogenesis; tumour necrosis factor alpha (TNF-α) (Piguet *et al*, 1993), platelet derived growth factor (PDGF) (Homma *et al*, 1995), endothelin-1 (ET-1) (Saleh *et al*, 1997) and connective tissue growth factor (CTGF) (Allen *et al*, 1999). Although $p16^{INK4A}$ and $p21^{WAF1}$ can prevent the binding of Cdk4 to Cyclin D1 this has no effect on Cyclin D1 expression levels. This may explain why although Cyclin D1 expression in ATII cells had a moderate positive correlation with increased number of fibroblastic foci but $p21^{WAF1}$ and $p16^{INK4A}$ demonstrated only a weak correlation making it difficult to determine if aberrant cell cycle regulation on its own can affect IPF disease activity. This does not rule out the possibility that cell senescence may reflect the stage of disease progression rather than disease activity.

As mentioned above the altered functionality of the hyperplastic ATII cells, identified by p53, $p21^{WAF1}$ and $p16^{INK4A}$ expression appears to be driven by their close proximity to the fibroblastic foci. Chapter 3 reported TGF-β protein expression by fibroblastic foci. TGF-β-induces hypermethylation of the promoter of SOCS3 in healthy fibroblasts and reduces the expression of SOCS3 (Dees *et al*, 2009). This reduction has been shown to increase mRNA and protein levels of collagen in fibroblast cell culture studies (Dees *et al*, 2010). My combined findings of extensive collagen and TGF-β protein expression (chapter 3) in the presence of low levels of SOCS3 within fibroblastic foci are consistent with previous findings by Dees *et al*, and provide the first evidence for this mechanism in human IPF lung tissue samples. These results suggest, when combined with expression of TRAIL, DR4 and DR5, that myofibroblasts within these niche areas are undergoing apoptosis likely driven by TGF-β.

This concept is supported by Lu *et al* (2006) who observed that fibroblasts from SOCS3 knockout mice have prolonged STAT3 activation, leading to a switch from their anti-apoptotic role, in normal wild type SOCS3 producing cells, to prolonged apoptosis/growth arrest. This net result of niche areas of apoptotic fibroblastic foci with overlying ATII cell senescence, combined with proliferation of ATII cells in diseased areas away from the foci, and intertwined with conserved areas of lung tissue, is a distortion of the delicate lung architecture. This may then lead to mechanical stress on the tissues. A recent study by Cabrera-Benitez *et al* (2012) examined mechanical stress in lung epithelial cell culture and murine models with stress induced via mechanical ventilation. They reported findings of increased TGF-β and α-SMA with decreased expression of surfactant protein B (SP-B) and a slight decrease in E-cadherin. My results of increased expression of TGF-β, continued expression of E-cadherin and no cytoplasmic expression of α-SMA within ATII cells, do not correspond to findings of mechanical stress playing a significant role in the pathogenesis of IPF.

In chapter 3 I identified a moderate positive correlation of Twist and collagen I expression within the fibroblastic foci with number of fibroblastic foci. Twist promotes the proliferation of myofibroblasts within these foci (Kida *et al*, 2007); while it follows that an increase in myofibroblasts would result in increased deposition of collagen I and therefore increased disease activity. Conflicting with this finding was the moderate correlation of TRAIL within the fibroblastic foci, suggesting that in more active disease increased apoptosis of myofibroblasts is occurring. However, my results also identified a moderate positive correlation between myofibroblast expression of p53, despite negligible levels of this marker expressed within the foci. To attempt to confirm the presence of apoptosis within

fibroblastic foci I propose that immunohistochemical markers for transglutaminase may be performed to identify cells in the effector stage (Stevens and Lowe, 2000), along with the identification of DNA laddering by gel electrophoresis (Williamson, 1970).

The correlation of decreased TRAIL, increased numbers of fibroblastic foci and subsequent increased extracellular matrix production may provide a novel target for IPF treatment strategies. Indeed as TRAIL has no effect on normal functioning cells within the body, any mechanism of administering TRAIL could have targeted affects on the niche areas of diseased lung, whilst preserving the functionality of the conserved alveolar epithelia.

In summary my results of increased $p16^{INK4A}$, $p21^{WAF1}$, Cyclin D1 and p53 in hyperplastic ATII cells, are the first to reveal that ATII cells may become senescence and resistant to apoptosis when in direct contact with TGF-β expressing myofibroblasts in IPF lung.

Further studies on a larger sample population including markers of senescence, such as Sen-β-Gal**,** are needed to confirm if the hyperplastic ATII cells in IPF lung tissue are in a state of cell cycle arrest or senescence. Proposed contact inhibition via TGF-β producing fibroblastic foci may be investigated via co-culture studies of IPF myofibroblasts and ATII cells. Additional investigations are also needed to determine why hyperplastic IPF ATII cells are not undergoing apoptosis despite expression of TRAIL and its death receptors DR4/DR5. It may be that these cells are expressing more decoy receptors such as DcR1. However, decoy receptors are usually found on normal cells, whereas DR4/DR5 are mainly expressed by transformed cells (Kim *et al*, 2000). Another plausible hypothesis is that survival factors, such as the protein kinase B (also known as Akt), may be activated in IPF ATII cells, preventing the release of cytochrome C and subsequent apoptosis (Song *et al*, 2005). These

theories require further immunohistochemical expression analysis of DcR1 receptors and protein kinase B, to determine if there is variability in the various niche areas of diseased and conserved areas of IPF lung tissue samples to explore the temporal heterogeneity observed in IPF.

I recognise that whilst this chapter has provided novel information regarding cell senescence and proliferation in IPF, the sample population is relatively small, compared to published studies of apoptosis and cell senescence in liver and renal fibrosis. A larger, multi centre study exploring markers used in my study, with the addition of Sen-β-Gal, DcR1 and protein kinase B would increase statistical validity. Also, biopsy samples do not reveal markers expressed in the very early stages of the disease, and ideally longitudinal studies of biopsy samples taken at intervals from early stage disease would provide more insight into the dynamic development of the disease. However this is not ethically or practicably possible. Despite these shortcomings, findings from my study have provided a better understanding of the pathogenesis of IPF, furthering information reported in cell culture and animal model studies. These results could provide clues to IPF therapeutic modalities. Variation in marker expression between IPF lung tissue samples may identify those individuals with more rapidly progressing disease.

Chapter 5

General discussion

5.1 Messages of thesis

Findings from this study have provided fresh insights into lung tissue remodelling in IPF, advancing previous investigations performed in ATII and IPF fibroblast cell cultures and bleomycin-induced animal models of pulmonary fibrosis. In addition, novel putative immunohistochemical markers have been identified which may allow for better prediction of disease activity in patients with IPF.

5.1.1 Data questions the role of EMT in the pathogenesis of IPF

Chapter 3 revealed little evidence of EMT at the time of biopsy, with only four tissue samples expressing low-moderate to extensive levels of N-cadherin. In addition no samples demonstrated significant loss of cell-cell adhesion; although this does not preclude EMT occurring at a different time-point in the progression of the disease. This contrasts to previous published reports by Willis *et al* (2005) and Kim *et al* (2006) who reported the presence of EMT in IPF lung tissue samples. This conflict in findings may be due to limited sample size in these previous investigations (Willis n=3, Kim n=5), and also the limited selection of markers used failing to provide a complete picture of the process of EMT. Kim *et al* (2006) examined the Wnt signalling pathway to assess the response of ATII cells in IPF patients to TGF-β signalling complexing with α3β1 integrin linkage to β-catenin in the process of EMT (Figure 5.1A), however there was no analysis of cell-cell adhesion markers, crucial to determining EMT presence. In wild type ATII cells α3 integrin links β-catenin to form a complex with TGF-β receptor and E-cadherin thus preventing E-cadherin degradation (Borok, 2009, Kim *et al*, 2009). Immediately following binding of the TGF-β ligand the TGF-β receptor becomes internalised into one of two different cellular compartments; calveolin-1 or early endosome antigen (EEA-1) (Del Galdo *et al*, 2008). In normal ATII cells localisation to

calveolae leads to ubiquitination of TGF-β. A decrease in calveolin-1 has been reported in IPF patients resulting in a shift to the EEA-1 compartment responsible for downstream Smad-2/3 activation, subsequent nuclear translocation of the Smad-2/3-Smad-4 complex (Del Galdo *et al*) and EMT (Figure 5.1a). My results of E-cadherin, TGF-βR and TGF-β protein expression build on this research and provide evidence of a possible attenuated response to TGF-β signalling via disruption of the integrin complex (Figure 5.1b). In the four cases where N-cadherin was expressed I hypothesise that a normal response to TGF-β protein is demonstrated (Figure 5.1a), accentuated by reduced calveolin-1. This corresponds to reports of only a small number of ATII cells in IPF lung tissue showing nuclear accumulation of βY654-β-catenin (Kim *et al*, 2009) and subsequent EMT. My hypothesis implies a concept-change in focus from EMT as a major source of fibroblasts in IPF lung tissue remodelling. Molecular profiling of IPF fibroblasts is needed to identify their source as either bone marrow-derived or residential fibroblasts, leading to the subsequent development of targeted therapies discussed in section 5.2.

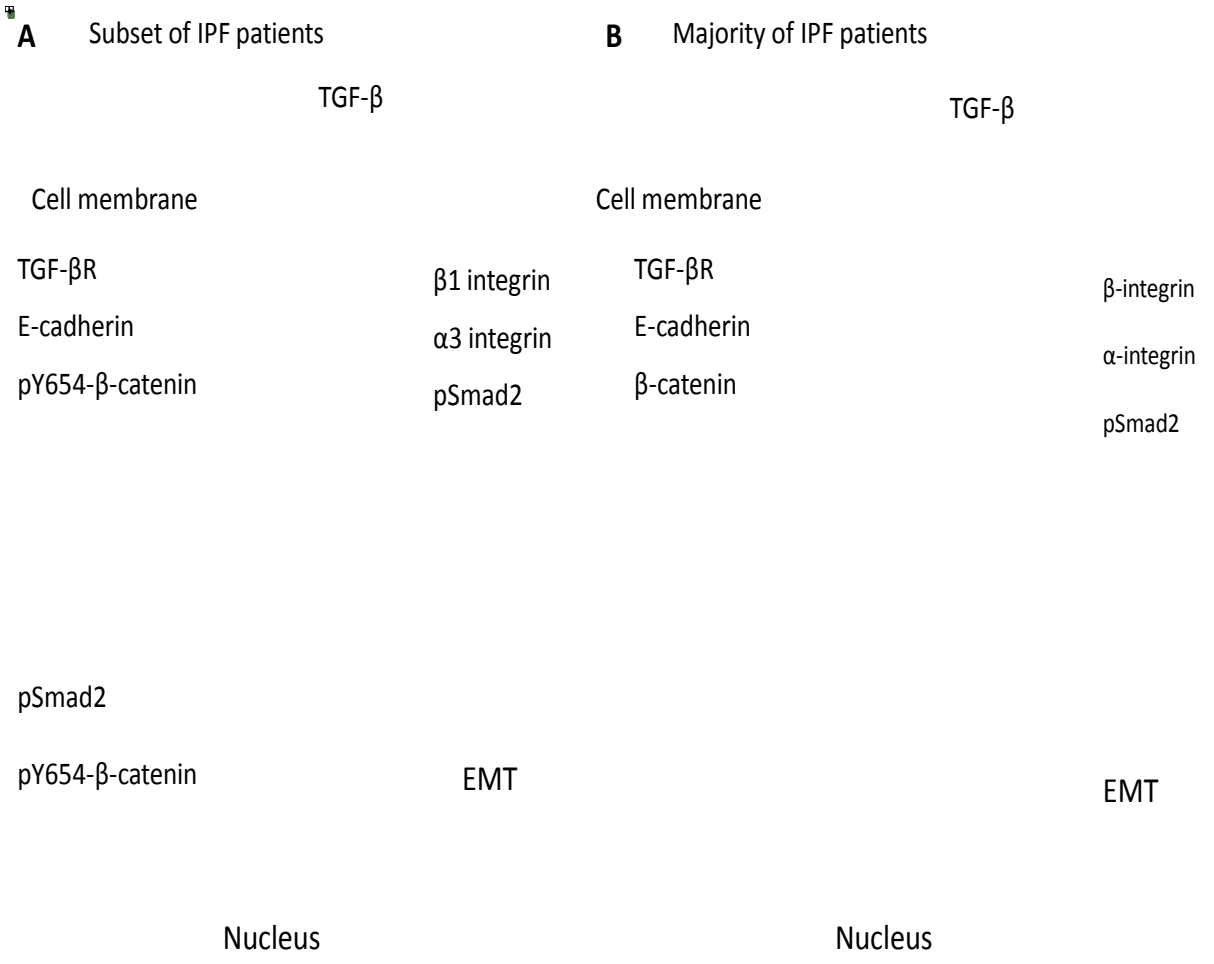

Figure 5.1 Adaptation of a model depicting the inducement of EMT via TGF-β signalling (Borok, 2009). A) In a subset of patients normal TGF-β signalling pathways results in degradation of E-cadherin when complexed to integrins. β-catenin becomes detached from E-cadherin and is localised to the nucleus resulting in the degradation of E-cadherin, upregulation of N-cadherin and EMT. α3 integrin is required for tyrosine phosphorylation (P) of β-catenin. B) In the majority of IPF patients I propose disruption of the integrin complex results in β-catenin remaining complexed to E-cadherin protecting it from degradation.

5.1.2 Findings provide evidence of contact inhibition and inducement of cell senescence in ATII cells overlying fibroblastic foci.

One novel finding of chapter 3 was the identification of variability in the expression of SP-C by ATII cells within the fibrotic areas in IPF biopsies, with temporally spared areas resembling healthy control lungs with normal functioning alveolar epithelium. My identification of apparent non-functioning ATII cells within IPF lung tissue, particularly overlying fibroblastic foci, builds upon *in vitro* and animal model work of Vega *et al* (2004) and Robson *et al* (2006) who proposed that cells undergoing EMT are resistant to apoptosis. By examining a broad panel of markers of proliferation, apoptosis, senescence and cell cycle regulators in IPF lung tissue, I am able to provide the first evidence of potential p53-mediated cell senescence in hyperplastic ATII cells overlying fibroblastic foci. These data, when associated with the expression of TGF-β by the myofibroblasts and ATII cells in IPF lungs provides evidence of potential TGF-β-mediated contact inhibition, leading to prolonged cell stasis and subsequent senescence.

The net result of ATII cell senescence is a reduction in the lung tissue remodelling capacity of IPF epithelium within the micro-niche areas surrounding fibroblastic foci. It is my belief that this inability of ATII cells to transform into Type I pneumocytes exacerbates hypoxaemia in IPF patients. Fibroblast cell culture studies have demonstrated a variable response to levels of hypoxia; moderate hypoxia stimulates proliferation and enhanced collagen production whilst severe hypoxia induces cell cycle arrest via p53 and $p21^{WAF1}$ pathways (Mizuno *et al*, 2009). Based on these cell culture investigations my results in chapter 3, showing low levels of the proliferation marker Ki-67 within fibroblastic foci, would suggest severe hypoxia in these areas; however further investigations in chapter 4

demonstrated negligible expression of p53 and $p21^{WAF1}$ within the same areas contradicts this. This discrepancy may be because, according to the manufacturer of the antibody, in normal cells the level of p53 expression may be below the detection level of immunohistochemistry. A technique currently in development using nanobiosensor based on localized surface plasmon resonance (LSPR) has been shown to detect and distinguish between wild type and mutated p53 (Duan *et al*, 2012). This technique could be used on laser dissected cells within the fibroblastic foci to confirm wild type p53 expression and support the theory of hypoxia induced fibroblast cell cycle arrest. In addition a more accurate detection of hypoxia within my sample population may be made using specific immunohistochemical markers of hypoxia; carbonic anhydrase IX (CA IX) and glucose transport-1 protein (GLUT-1). GLUT-1 mediates cellular glucose uptake, facilitating anaerobic glycolysis and is largely undetectable in normal epithelium (De Shutter *et al*, 2005). A recently developed non-invasive *in vivo* alternative to immunohistochemical analysis is the visualisation of nitroimidazole compounds by positron emission tomography (PET) (Smeland *et al*, 2012). 18F-fluoroazomycin arabinoside (18F-FAZA) gets trapped in hypoxic cells and can be detected by PET scan to allow for assessment of cellular hypoxia throughout the whole lung.

5.1.3 Novel putative markers for predicting disease activity in patients with IPF.

Current methods used for predicting disease activity in IPF patients include the monitoring of FVC, DL_{CO} and progression of fibrosis on HRCT. The reliability of FVC may be limited by co-morbidities such as emphysema (ATS/ERS/JRS/ALAT statement, 2010). The ATS/ERS/JRS/ALAT statement concluded by commenting that prognosis in IPF remains difficult and that the development of a multivariable predictive model is critically important

to inform staging of the disease. By combining my correlation data with case note analysis of imaging and pulmonary function testing in a retrospective study of the patients examined in this thesis, it may be possible to identify markers linked to disease progression and acute exacerbations. Information from these findings may allow for pre-emptive changes in disease management.

Improvements in imaging quality over the past decade have resulted in fewer patients requiring open lung biopsy, therefore limiting the usefulness of an immunohistochemical marker panel for predicting disease activity. However, my data has identified potential targets for the development of blood biomarkers for use in all IPF patients.

5.2 Clinical implications

Currently there are no effective treatments for patients suffering from IPF with drug therapy focused on stabilising the condition of patients, preventing further decline in lung function. Lung transplantation may be considered in suitable candidates aged 65 or under.

My proposal of fibroblastic foci contraction leading to mechanical stresses on the surrounding alveolar epithelium identifies a potential target for drug therapy. Prostacyclin analogs such as iloprost and beraprost, acting via the cAMP-PKA pathway, have been shown in cell culture models to inhibit the contractile properties of fibroblasts (Kamio *et al*, 2007) and could therefore be developed to reduce distortion of wound remodelling within the fibroblastic foci. However, accurate targeting of these drugs is required to avoid impingement of normal wound closure and effective repair processes by fibroblasts in areas away from these foci. One possible mechanism of targeting diseased areas whilst conserving the unaffected areas may be via the use of autologous mesenchymal stem cell transplant.

Bone marrow mesenchymal stem cells (BMMSC) preferentially migrate to sites of inflammation, tissue damage and repair (Vancheri *et al*, 2010) and have been shown to reduce fibrosis in animal models of pulmonary fibrosis (Moodley *et al*, 2009). BMMSC have also been used as vectors in the delivery of chemotherapeutic agents including apoptosis inducing proteins (Vogler *et al*, 2009), such as AT-101 and GX-070 noted below.

The possibility of cell senescence and apoptotic resistance in ATII cells, reported in my thesis, warrants further investigations. The tumour suppressor marker p53, shown in my experiments to be expressed within ATII cells, can induce the anti-apoptotic molecule Bcl-2 (Haldar *et al*, 1995). Studies in drug resistant cancer cells have revealed increased expression of Bcl-2, with trials being performed targeting Bcl-2 as a way of overcoming drug resistance (Kang and Reynolds, 2009). Drugs identified as inhibiting Bcl-2 and therefore promoting apoptosis and having a potential therapeutic role in IPF include; Oblimersen sodium (Herbst and Frankel, 2004), AT-101 (Zerp *et al*, 2009) and GX15-070 (Nguyen *et al*, 2007).

5.3 Critical review of experimental analysis and further work

My study examined lung tissue samples from 21 patients with a confirmed histological diagnosis of IPF from one hospital. In comparison with other studies equally exploring lung tissue remodelling in IPF, my study population is relatively large. However, the sample size and therefore statistical validity could be increased by the use of centralised biobanks containing IPF lung tissue samples from around the world. Only around 7.5-12% of patients with clinical symptoms of IPF and indeterminate or overlapping features with other ILDs have biopsy (Johnston *et al*, 1993) and, with the advent of HRCT this number is decreasing further (Noth *et al*, 2007). This decline in lung tissue availability highlights the

need for tissue banks, such as the European IPF biobank (Jusrus-Liebig University, Germany) to collect, store and make available human biopsy samples with linked access to patient health data for future investigations. In addition to tissue samples these banks collect blood, bronchoalveolar lavages, exhaled breath condensates and urine samples which are more readily obtainable from *all* IPF patients. These fluidic samples could be used to compare markers, noted in my study to be increased in IPF lung tissue samples, compared to control patients, with the potential to search for biomarkers of the disease that can be monitored over the course of the disease.

Immunohistochemistry provides a useful tool in the localisation of markers of interest, with dual immunohistochemistry allowing for interactions between markers to be examined *in vivo*. This capability was particularly important in my investigation where the cellular localisation of α-SMA can indicate or rule out EMT. However, as discussed in section 1.3, when investigating p53 expression, the technique depends on production of a protein with a longer half-life to be identified and, in the absence of this, would provide a negative result (Yemelyanova *et al*, 2011). Molecular techniques, such as RT-PCR, are able to identify smaller quantities of the genes producing proteins; however, identifying a gene product does not imply that the protein product is being expressed thus requiring subsequent confirmation via immunohistochemistry. This is exemplified by my investigations into viral involvement in IPF. Although I found evidence of EBV viral protein in only one IPF lung tissue sample I think it would be of value to attempt detection of a broader range of viruses via a variety of molecular techniques such as Southern blot, DNA sequencing and massively parallel sequencing to ensure reliability of results (Zheng *et al*, 2007, Moore *et al*, 2011).

5.4 Conclusion

This thesis has investigated lung tissue remodelling in IPF lung. My findings suggest the ability of ATII cells to divide and transform into ATI cells is inhibited when in contact with fibroblast foci, and has gone some way towards enhancing our understanding of the temporal heterogeneity seen in IPF lung tissue samples. This study confirms previous findings and contributes additional evidence that suggest EMT does not play a significant role in fibroblastic foci and therefore directs attention towards circulating fibrocytes and residential fibroblasts. The most important limitation of this research lies in the fact that lung biopsy is just a snap shot in the development of IPF lung wound remodelling and that biopsy samples are only obtained in a subset of individuals for whom atypical or overlapping features with other ILDs are found at imaging. Questions are therefore raised as to how representative these biopsy samples are of the whole IPF population. Further experimental investigations are needed to determine the source of fibroblasts within the foci and the factors responsible for the observed contact inhibition of overlying ATII cells. In addition it would be interesting to correlate markers tested in this study with clinical information on lung function and acute exacerbations with the possibility of developing blood biomarkers to predict disease activity and progression.

Information derived from this study may be used to develop targeted interventions aimed at reducing the number of fibroblastic foci and therefore improving ATII cell regeneration of the alveolar epithelium. Correlations of markers with clinical data may lead to the development of additional tools to allow clinicians to provide more accurate prognostic information to their patients and possibly identify those individuals in greater clinical need of lung transplant.

References

1. Alder, JK. Chen. JJ. Lancaster, L. Danoff, S. Su, S. Cogan, JD. Vulto, I. Xie, M. Qi, X. Tuder, RM. Phillips, JA. Lansdorp, PM. Loyd, JE. Armanios, MY. (2008) Short telomeres are a risk factor for idiopathic pulmonary fibrosis. *Proceedings of the National Academy of Science*. 105 (35), pp. 12051-13056.
2. Alder, JK. Cogan, JD. Brown, AI. Anderson, CJ. Lawson, WE. Lansdorp, PM. Phillips III, JA. Loyd, JE. Chen, JJ. Armanios, M. (2011) Ancestral mutation in telomerase causes defects in repeat addition processivity and manifests as familial pulmonary fibrosis. *PLoS Genetics*, 7 (3), pp. e1001352.
3. Allen, JT. Knight, RA. Bloor, CA. Spiteri, MA. Enhanced insulin-like growth factor binding protein-related protein 2 (connective tissue growth factor) expression in patients with idiopathic pulmonary fibrosis and pulmonary sarcoidosis. (1999) *American Journal of Respiratory Cell and Molecular Biology*, 21 (6), pp. 693-700.
4. American Cancer Society (2012) *Cancer Facts and Figures 2012*. www.cancer.org [Accessed June 2012].
5. Arakawa, H and Honma, K. (2011) Honeycomb lung: history and current concepts. *American Journal of Roentgenology*, 196, pp. 773-782.
6. Arase, Y. Suzuki, F. Suzuki, Y. Akuta, N. Kobayashi, M. Kawamura, Y. Sezaki, H. Hosaka, T. Hirakawa, M. Saito, S. Ikeda, K. Kumada, H. (2008) Hepatitis C virus enhances incidence of idiopathic pulmonary fibrosis. *World of Gastroenterology*, 14 (38), pp. 5880-5996.
7. Armanios, MY. Chen, JJ. Cogan, JB. Alder, JK. Ingersoll, RG. Markin, C. Lawson, WE. Xie, M. Vulto, I. Phillips, JA 3rd. Lansdorp, PM. Greider, CW. Loyd, JE. (2007) Telomerase mutations in families with idiopathic pulmonary fibrosis. *New England Journal of medicine*, 356 (13), pp. 1317-1326.
8. Azuma, A. Nukiwa, T. Tsubo, E. Suga, M. Abe, S. Nakata, K. Taguchi, Y. Nagai, S. Itoh, H. Ohi, M. Sato, A. Kudoh, S. Raghu, G. (2005) Double-blind, placebo-controlled trial of prifenidone in patients with idiopathic pulmonary fibrosis. *American Journal of Respiratory and Critical Care Medicine*, 171, pp. 1040-1047.

9. Baker, SJ. Fearon, ER. Nigro, JM. Hamilton, SR. Preisinger, AC. Jessup, M. VanTuinen, P. Ledbetter, DH. Barker, DF. Nakamura, Y. White, R. Vogelstein, B. (1989) Chromosome 17 deletions and p53 gene mutations in colorectal carcinomas. *Science*, 244, pp. 217-221.
10. Barbas-Filho, JV. Ferreira, MA. Sesso, A. Kairalla, RA. Carvalho, CRR. Copelozzi, VL. (2001) Evidence of type II pneumocyte apoptosis in the pathogenesis of idiopathic pulmonary fibrosis (IPF)/usual interstitial pneumonia (UIP). *Journal of Clinical Pathology*, 54, pp. 132-138.
11. Bartram, U. And Speer, CP. (2004) The role of transforming growth factor beta in lung development and disease. *Chest*, 125 (2), pp. 754-765.
12. Baumgartner, KB. Samet, JM. Coultas, DB. Stidley, CA. Hunst, WC. Colby, TV. Waldron, JA. (2000) Occupational and environmental risk factors for idiopathic pulmonary fibrosis: a multicenter case control study. *American Journal of Epidemiology*, 152, pp. 307-315.
13. Belinsky, SA. Nikula, KJ. Palmisano, WA. Michels, R. Saccomanno, G. Gabrielson, E. Baylin, SB. Herman, JG. (1998) Aberrant methylation of p16INK4A is an early event in lung cancer and a potential biomarker for early diagnosis. *Proceedings of the National Academy of Science*, 95, pp. 11891-11896.
14. Behr, J. Maier, K. Degenkolb, B. Krambach, F. Vogelmeier, C. (1997) Anti-oxidative and clinical effects of high-dose N-acetylcysteine in fibrosing alveolitis: adjunctive therapy to maintenance immunosuppression. *American Journal of Respiratory and Critical Care Medicine*, 156, pp. 1897-1901.
15. Bensadoun, ES. Burke, AK. Hogg, JC. Roberts, CR. (1996) Proteoglucan deposition in pulmonary fibrosis. *American Journal of Respiratory and Critical Care Medicine*, 154 (6), pp. 1819-1828.
16. Bhatnagar, J. De Leon-Carnes, M. Kellar, KL. Bandyopadhyay, K. Antoniadou, Z. Shieh,W. Paddock, CD. Zaki, SR. (2012) Rapid simultaneous detection of *clostridium sordellii* and *clostridium perfringens* in archived tissue by a novel PCR-based microsphere assay: diagnostic implications for pregnancy associated viral toxic shock syndrome cases. *Infectious Diseases in Obstetrics and Gynaecology*, 2012, ID 972845.

17. Bhattacharyya, P. Acharya, A. Roychowdhury, S. (2007) Role of matrix metalloproteinases in the pathophysiology of idiopathic pulmonary fibrosis. *Lung India*, 24 (2), pp. 61-65.
18. Blagosklonny, MV. (2006) Cell senescence:hypertrophic arrest beyond restriction point. *Cell Physiology*, 209, pp. 592-597.
19. Blagosklonny, MV. (2011) Cell cycle arrest is not cell senescence. *Aging*, 3 (2), pp. 94-101.
20. Boland, S. Boisvieux-Ulrich, E. Houcine, O. Baeza-Squilban, A. Pouchete, M. Marano, F. (1996). TGF beta 1 promotes actin cytoskeleton reorganization and migratory phenotype in epithelial tracheal cells in primary culture. *Journal of Cell Science*, 109, pp. 2207-2219.
21. Bova, RJ. Quinn, DI. Nankervis, JS. Cole, IE. Sheridan, BF. Jensen, MJ. Morgan, GJ. Hughes, CJ. Sutherland, RL. (1999) Cyclin D1 and p16INK4A expression predict reduced survival in carcinoma of the anterior tongue. *Clinical Cancer Research*, 5, pp. 2810-2819.
22. Bullwinkel, J. Baron-Luhr, B. Ludemann, A. Wohlenberg, C. Gerdes, J. Scholzen, J. (2006) Ki67 protein is associated with ribosomal RNA transcription in quiescent and proliferating cells. *Journal of Cell Physiology*, 206, pp. 624-635.
23. Cabrera-Benitez, NE. Parotto, M. Post, M. Han, B. Spieth, PM. Cheng, WE. Valladares, F. Villar, J. Liu, M. Sato, M. Zhang, H. Slutsky, AS. (2012) Mechanical stress induces lung fibrosis by epithelial mesenchymal transition. *Critical Care Medicine*, 40 (2), pp. 510-517.
24. Cantin, AM. Hubbard, RC. Crytsal, RG. (1989) Glutathione deficiency in the epithelial lining fluid of the lower respiratory tract in idiopathic pulmonary fibrosis. *American Review of Respiratory Diseases*, 139, pp. 370-372.
25. Chamber, RC. Leoni, P. Kaminski, N. Laurent, GJ. Heller, RA. (2003) Global expression profiling of fibroblast responses to transforming growth factor beta 1 reveals the induction of inhibitor of differentiation-1 and provides evidence of smooth muscle cell phenotype switching. *American Journal of Pathology*, 162, pp. 533-546.
26. Cao, B. Guo, Z. Shu, Y. Xu, W. (2000) The potential role of PDGF, IGF-1, TGF-beta expression in idiopathic pulmonary fibrosis. *Chinese Medical Journal*, 113 (9), pp. 776-782.

27. Caraci, F. Gili, E. Calafiore, M. Failla, M. La Rosa, C. Crimi, N. Sortino, MA. Nicoletti, F. Copani, A. Vancheri, C. (2008) TGF-β1 targets the GSK-3β/β-catenin pathway via ERK activation in the transition of human lung fibroblasts into myofibroblasts. *Pharmacological Research*, 57, pp. 274-282.
28. Checa, M. Ruiz, V. Montano, M, Velázquez-Cruz, R., Selman, M. Pardo, A. (2008) MMP-1 polymorphisms and the risk of idiopathic pulmonary fibrosis. *Human Genetics*, 124 (5), pp. 465-472.
29. Chen, J. Huang, X. Halicka, D. Brodsky, S. Avram, A. Eskander, J. Bloomgarden, NA. Darzynkeiwicz, Z. Goligorsky, MS. (2006) Contribution of p16INK4A and p21CIP1 pathways to induction of premature senescence of human endothelial cells: permissive role of p53. *American Journal of Physiology – Heart and Circulatory Physiology*, 290 (4), pp. H1575-H1586.
30. Cheng, M. Oliver, P. Diehl, JA. Fero, M. Roussel, MF. Roberts, JM. Sherr, CJ. (1999) The $p21^{cip1}$ and $p27^{kip1}$ cdk 'inhibitors' are essential activators of cyclin D-dependent kinases in murine fibroblasts. The EMBO Journal, 18 (6), pp. 1571-1583.
31. Chilosi, M. Poletti, V. Murer, B. Lestani, M. Cancellieri, A. Montagna, L. Piccoli, P. Cangi, G. Semenzato, G. Doglioni, C. (2002) Abnormal re-repithelialization and lung remodelling in Idiopathic Pulmonary Fibrosis: The role of ΔN-p63. *Laboratory Investigation*, 82, pp. 1335-1345.
32. Cohen, J. (2003) Applied multiple regression/correlation analysis for the behavioral sciences. United Kingdom. Routledge Academic.
33. Collard, HR. King, TE. Bartelson, BB. Vourelkis, JS. Schwarz, MI. Brown, KK. (2003) Changes in clinical and physiological variables predict survival in idiopathic pulmonary fibrosis. *American Journal of Respiratory and Critical care Medicine*, 168 (5), pp. 538-542.
34. Collard, HR. Ryu, JH. Douglas, WW. Schwarz, MI. Curran-Everett, D. (2004) Combined corticosteroid and cyclophosphomide therapy does not alter survival in idiopathic pulmonary fibrosis. *Chest*, 125, pp. 2169-2174.
35. Collard, HR. Moore, BD. Flaherty, KR. Brown, KK. Kaner, RJ. King Jr, TE. Lasky, JA. Loyd, JE. Noth, I. Olman, MA. Raghu, G. Roman, J. Ryu, JH. Zisman, DA. Hunninghake, GW. Colby, TV. Egan, JJ. Hansell, DM. Johkoh, T. Kaminski, N. Kim, DS. Kondoh, Y. Lynch, DA. Müller-Quernheim, J. Myers, JL. Nicholson,

AG. Selman, M. Toews, GB. Wells, AU. Martinez, FJ. (2007) Idiopathic Pulmonary Fibrosis Clinical Research Network Investigators. Acute exacerbations of idiopathic pulmonary fibrosis. *American Journal of Respiratory and Critical care Medicine*, 176, pp. 636-643.

36. Corrin, B. Butcher, D. McAnulty, BJ. Du Bois, RM. Black, CM. Laurent, GJ. Harrison, NK. (1994) Immunohistochemical localization of transforming growth factor-beta 1 in the lungs of patients with systemic sclerosis, cryptogenic fibrosing alveolitis and other lung disorders. *Histopathology*, 24 (2), pp. 145-150.
37. Cronkhite, JT. Xing, C. Raghu, G. Chin KM. Torres, F. Rosenblatt, RL. Garcia, CK. (2008) Telomere shortening in familial and sporadic pulmonary fibrosis. *American Journal of Respiratory and Critical care Medicine*, 178 (7), pp. 729-737.
38. Crosby, L. and Waters, CM. (2010) Epithelial repair mechanisms in the lung. *American Journal of Physiology Lung and Cell Molecular Physiology*, 298, pp. 715-731.
39. Danowski, BA> and Harris, AK. (1988) Changes in fibroblast contractility, morphology and adhesion in response to a phorbol ester tumour promoter. *Experimental Cell Research*, 177, pp. 47-59.
40. Dees, C. Akhmetshina, A. Busch, N. Horn, A. Gusinde, J. Jünge, A. Gay, S. Distler, O. Schett, G. Distler, J. (2009) Inhibitors of DNA methylotranferases exert potent anti-fibrotic effects via re-activation of SOCS3. *Annals of the Rheumatic Diseases*, 68 (suppl), pp. 94.
41. Dees, C. Akhmetshina, A. Busch, N. Horn, A. Gusinde, J. Jünge, A. Gay, S. Distler, O. Schett, G. Distler, J. (2010) Promoter hypermethylation of the anti-fibrotic gene SOCS-3 by TGF-β as novel mechanism in the pathogenesis of SCC. *Annals of the Rheumatic Diseases*, 69 (suppl 2), pp. A26.
42. Del Galdo, F. Lisanti, MP. Jimenez, SA. (2008) Caveolin-1, TGF-β receptor internalization, and the pathogenesis of systemic sclerosis. *Current Opinion in Rhumatology*, 20 (6), pp. 713-719.
43. Demidenko, ZN and Blagosklonny, MV. (2008) Growth stimulation leads to cellular senescence when the cell cycle is blocked. *Cell Cycle*, 7, pp. 3355-3361.

44. Derycke, LDM. and Bracke, ME. (2004) N-cadherin in the spotlight of cell-cell adhesion, differentiation, embryogenesis, invasion and signalling. *International Journal of Developmental Biology*, 48, pp. 463-476.
45. De Shutter, H. Landuyt, W. Verbeken, E. Goethals, L. Hermans, R. Nuyts, S. (2005) The prognostic value of the hypoxia markers CA IX and GLUT 1 and the cytokines VEGF and IL 6 in head and neck squamous cell carcinoma treated by radiotherapy ± chemotherapy. *BMC Cancer*, 5 (42).
46. Desmouliere, A. Geinoz, A. Gabbiani, F. (1993) Transforming growth factor-beta 1 induces alpha –smooth muscle actin expression in granulation tissue myofibroblasts and in quiescent and growing cultured fibroblasts. *Journal of Cell Biology*, 122 (1), pp. 103-111.
47. Detre, S. Saclani Jotti, G. Dowsett, M. (1995) A 'quickscore' method for immunohistochemistry semiquantification validation for oestrogen receptor in breast carcinoma. *Journal of Clinical Pathology*, 48 (9), pp. 876-878.
48. De Wever, O. Westbroek, W. Verloes, A. Bloemen, N.Bracke, M.Gespach, C. Bruyneel, E. Mareel, M. (2004) Critical role of N-cadherin in myofibroblast invasion and migration in vitro stimulated by colon-cancer-cell-derived TGF-β or wounding. *Journal of Cell Science*, 117, pp. 4691-4703.
49. Duan, RQ. Yuan, JL. Yang, H. Luo, XG. Xi, MR. (2012) Detection of p53 gene mutation by using a novel biosensor based on localized surface plasmon resonance. *Neoplasma*, 59 (3), pp. 348-352.
50. Du Bois, RM. Weycker, D. Albera, C. Bradford, WZ. Costabel, E. Kartashov, A. Lancaster, L. Noble, PW. Sahn, SA. Szwarcberg, J. Thomeer, M. Valeyre, D. King, TE Jr. (2011) Six-minute-walk test in idiopathic pulmonary fibrosis: test validation and minimal clinically important difference. *American Journal of Respiratory and Critical Care Medicine*, 183 (9), pp. 1231-1237.
51. Dulic, V. Drullinger, LF. Lees, E. Reed, SI. Stein, GH. (1993) Altered regulation of G1 cyclins in senescent human diploid fibroblasts: Accumulation of inactive cyclin E-cdk2 and cyclin D1-cdk2 complexes. *Proceedings of the National Academy of Science*, 90, pp. 11034-11038.

52. Eccles, DM. Brett, L. Lessells, A. Gruber, L. Lane, D. Steel, CM. Leonard, RCF. (1992) Overexpression of the p53 protein and allele loss at 17p13 in ovarian carcinoma. *British Journal of Cancer*, 65, pp. 40-44.
53. Egan, JJ. Stewart, JP. Hasleton, PS. Arrand, JR. (1995) Epstein-Barr virus replication within pulmonary epithelial cells in cryptogenic fibrosing alveolitis. *Thorax*, 50, pp. 1234-1239.
54. Eickelberg, O and Laurent, GJ. (2010) The quest for the initial lesion in idiopathic pulmonary fibrosis: gene expression differences in IPF fibroblasts. *American Journal of Respiratory and Critical care Medicine*, 42, pp. 1-2.
55. Elliot, J. Johnston, JA. (2004) SOCS: role in inflammation, allergy and homeostasis. *Trends in Immunology*, 25 (8), pp. 434-440.
56. El-Zammar, O. Rosenbaum, P. Katzenstein, ALA. (2009) Proliferative activity in fibrosing lung disease: a comparative study of Ki-67 immunoreactivity in diffuse alveolar damage, bronchiolitis obliterans - organising pneumonia, and usual interstitial pneumonia. *Human Pathology*, 40, pp. 1182-1188.
57. Enomoto, N. Suda, T. Kato, M. Kaida, Y. Nakamura, Y. Imokawa, S. Ida, M. Chida, K. (2006) Quantitative analysis of fibroblastic foci in usual interstitial pneumonia. *Chest*, 130, pp. 22-29.
58. Evans, MJ. Cabral, LJ. Stephens, RJ. Freeman, G. (1975) Transformation of alveolar type 2 cells to type I cells following exposure to NO_2. *Experimental Molecular Pathology*, 22 (1), pp. 142-150.
59. Fahim, A. Crooks, M. Hart, SP. (2011) Gastro-oesophageal reflux and idiopathic pulmonary fibrosis: a review. *Pulmonary Medicine*, 2001, article ID 634613, 7 pages.
60. Figueroa, S. Gerstenhaber, B. Welch, L. Klimstra, D. Walker-Smith, GJ. Beckett, W. (1992) Hard metal interstitial pulmonary disease associated with a form of welding in a metal parts coating plant. *American Journal of Industrial Medicine*, 21 (3), pp. 363-373.
61. Finesmith, TH. Broadley, KN. Davidson, JM. (1990) Fibroblasts from wounds of different stages of repair vary in their ability to contract a collagen gel in response to growth factors. *Journal of Cell Physiology*, 144, pp. 99-107.
62. Flaherty, KR. Toews, GB. Lynch, JB. Kazerooni, EA. Gross, GB. Strawderman, RL. Hariharan, K. Flint, A. Martinez, FJ. (2001) Steroids in idiopathic pulmonary fibrosis: a

prospective assessment of adverse reactions, response to therapy and survival. *American Journal of Medicine*, 110, pp. 278-282.

63. Flaherty, KR. Mumford, JA. Murray, S. Kazerooni, EA. Gross, BH. Colby, TV. Travis, WD. Flint, A. Toews, GB. Lynch, JP 3rd. Martinez, FJ. (2003) Prognostic implications of physiologic and radiographic changes in idiopathic interstitial pneumonia. *American Journal of Respiratory and Critical Care Medicine*, 168 (5), pp. 543-548.
64. Flaherty, KR. Thwaite, EL. Kazerooni, EA. Gross, BH. Toews, GB. Colby, TV. Travis, WD. Mumford, JA. Murray, S. Flint, A. Lynch, JP 3rd. Martinez, FJ. (2003) Radiological versus histological diagnosis in UIP and NSIP: survival implications. *Thorax*, 58, pp. 143-148.
65. Flanders, K. Sato, M. Ooshima, A. Russo, A. Roberts, A. (2004) Smad-3 as a mediator of the fibrotic response. *International Journal of Experimental Pathology*, 85 (1), pp. A13.
66. Fritschy, JM. (2008) Is my antibody-staining specific? How to deal with pitfalls of immunohistochemistry. *European Journal of Neuroscience*, 28 (12), pp. 2365-2370.
67. Fritz, P. Wu, X. Tuczek, H. Multhaput, H. Schwarzmann, P. (1995) Quanitification in immunohistochemistry. A research method or a diagnostic tool in surgical pathology? *Pathologica*, 87, pp. 300-309.
68. Fukuda, Y. Basset, F. Ferrans, VJ. Yamanaka, N. (1995) Significance of early intra-alveolar fibrotic lesions and integrin expression in lung biopsy specimens from patients with idiopathic pulmonary fibrosis. *Human Pathology*, 26 (1), pp. 53-61.
69. Gartel, AL. Tyner, AL. (2002) The role of the cyclin-dependent kinase inhibitor p21 in apoptosis. *Molecular Cancer Therapeutics*, 1 (8), pp. 639-649.
70. Gauldie, J. (2002) Inflammatory mechanisms are a minor component of the pathogenesis of idiopathic pulmonary fibrosis. *American Journal of Respiratory and Critical Care Medicine*, 165 (9), pp. 1205-1206.
71. Giaid, A. Yanagisawa, M. Langleben, D. Michel, RP. Levy, R. Shennib, H. Kimura, S. Masaki, T. Duguid, WP. Stewart, DJ. (1993) Expression of endothelin-1 in the lungs of patients with pulmonary hypertension. *New England Journal of Medicine*, 328 (24), pp. 1732-1739.

72. Godin, I. Whlie, CC. (1991) TGF beta 1 inhibits proliferation and has a chemotropic effect on mouse primordial germ cells in culture. *Development*, 113 (4), pp. 1451-1457.
73. GREAT BRITAIN (2010) Department of Health/Digital Information Policy (2010) The Caldecott Guardian Manual.
74. Gribbin, J. Hubbard, RB. Le-Jeune, I. Smith, CJ. West, J. Tata, LJ. (2006) Incidence and mortality of idiopathic pulmonary fibrosis and sarcoidosis in the UK. *Thorax*, 61, pp. 980-985.
75. Grinnell, F. (1994) Fibroblasts, myofibroblasts and wound contraction. *Journal of Cell Biology*, 124 (4), pp. 401-404.
76. Haldar, S. Jena, N. Croce, CM. (1995) Inactivation of BCL-2 by phosphorylation. *Proceedings of the National Academy of Sciences*, 92, pp. 4507-4511.
77. Harada, T. Nabeshima, K. Hamasaki, M.Uesugi, N. Watanabe, K. Iwasaki, H. (2010) Epithelial-mesenchymal transition in human lungs with usual interstitial pneumonia: quantitative immunohistochemistry. *Pathology International*, 60 (1), pp. 14-21.
78. Harari, S. Caminati, A. (2010) IPF: New insight on pathogenesis and treatment. *Allergy*, 65, pp. 537-553.
79. Hardy, MA. (1989) The biology of scar formation. *Physical Therapy*, 69 (12), pp. 1014-1024.
80. Hartwell, LH. Weinert, TA. (1989) Checkpoints: controls that ensure the order of cell cycle events. *Science*, 246 (4930), pp. 629-634.
81. Harvey, JM. Clark, GM. Allred, DC. (1999) Estrogen receptor status by immunohistochemistry is superior to the ligand-binding assay for predicting response to adjuvant endocrine therapy in breast cancer. *Journal of Clinical Oncology*, 17 (5), pp. 1474-1481.
82. Hashimoto, N. Phan, SH. Imaizumi, K. Matsuo, M. Nakashima, H. Kawabe, T. Shimokata, K. Hasegawa, Y. (2010) Endothelial-mesenchymal transition in bleomycin-induced pulmonary fibrosis. *American Journal of Respiratory, Cell and Molecular Biology*, 43 (2), pp. 161-172.
83. Hay, ED. (1995) An overview of epithelial-mesenchymal transition. *Acta Anatomica (Basel),* 154, pp. 8-20.

84. Herbst, RS. Frankel, SR. (2004) Oblimersen sodium (Genasence bcl-2 antisense oligonucleotide) A rational therapeutic to enhance apoptosis in therapy of lung cancer. *Clinical Cancer Research*, 10, pp. 4245s.
85. Hinz, B. Pittet, P. Smith-Clerc, J. Chaponnier, C. Meister, J-J. (2004) Myofibroblast development is characterized by specific cell-cell adherens junctions. *Molecular Biology of the Cell*, 15, pp. 4310-4320.
86. Homma, S. Nagaoka, I. Abe, H. Takahashi, K. Seyoma, K. Nukiwa, T. Kira, S. (1995) Localisation of platelet-derived growth factor and insulin-like growth factor I in the fibrotic lung. *American Journal of Respiratory and Critical Care Medicine*, 152 (6), pp. 2084-2089.
87. Horowitz, JC. Lee, DY. Waghray, M. Keshamouni, VG. Thomas, PE. Zhang, H. Cui, Z. Thannickal, VJ. (2004) Activation of the pro-survival phosphatidyl-inositol 3-kinase/AKT pathway by transforming growth factor-beta1 in mesenchymal cells is mediated by P38 MAPK-dependent induction of an autocrine growth factor. *Journal of Biological Chemistry*, 279, pp. 1359-1367.
88. Horowitz, JC. And Thannickal, VJ. (2006) Epithelial mesenchymal interactions in pulmonary fibrosis. *Seminars in Respiratory and Critical Care Medicine*, 27, pp. 600-612.
89. Hubbard, R. Venn, A. Lewis, S. Britton, J. (1990) Lung cancer and cryptogenic fibrosis alveolitis. A population based cohort study. *American Journal of Respiratory and Critical Care Medicine*, 161 (1), pp. 5-8.
90. Hubbard, R. Lewis, S. Richards, K. Johnston, I. Britton, J. (1996) Occupational exposure to metal or wood dust and aetiology of cryptogenic fibrosing alveolitis. *The Lancet*, 347, pp. 284-289.
91. Hubbard, R. Baoku, Y. Kalsheker, N. Britton, J. Johnston, I.(1997) Alpha-1-antitrypsin phenotypes in patients with cryptogenic fibrosing alveolitis: a case-control study. *European Respiratory Journal*, 10, pp. 2881-2887.
92. Hunnunghake, GW. (2005) Antioxidant therapy for idiopathic pulmonary fibrosis. *New England Journal of Medicine*, 353, pp. 2285-2287.
93. Inoshima, I. Kuwano, K. Hamada, N. Yoshimi, M. Maeyama, T. Hagimoto, N. Nakanishi, Y. Hara, N. (2004) Induction of CDK inhibitor p21 gene as a new

therapeutic strategy against pulmonary fibrosis. *American Journal of Physiology-Lung Physiology*, 286 (4), pp. L727-L733.

94. International Health Terminology Standards Development Organisation. *SNOMED CT* [WWW] International Health Terminology Standards Development Organisation. Available from www.ihtsdo.org/snomed-ct/ [Accessed 09/05/2012].
95. Iwai, K. Mori, T. Yamada, N. Yamaguchi, M. Hosoda, Y. (1994). Idiopathic pulmonary fibrosis: epidemiologic approaches to occupational exposure. *American Journal of Respiratory and Critical Care Medicine*, 150, pp. 670-675.
96. Johnston, ID. Gomm, SA. Kalra, S. Woodcock, AA. Evans, CC. Hind, CR. (1993) The management of cryptogenic fibrosing alveolitis in three regions of the United Kingdom. *European Respiratory Journal*, 6, pp. 891-893.
97. Joint Photographic Experts Group (1986) ISO/IEC IS 10918-1|ITU-T Recommendation T.81. Available from: http://www.jpeg.org/jpeg/index.html [Accessed 08/12/2012].
98. Kajstura, J. Rota, M. Hall, SR. Hosoda, T. D'Amario, D. Sandana, F. Zheng, H. Ogórek, B. Rondon-Clavo, C. Ferreira-Martins, J. Matsuda, A. Arranto, C. Goichberg, P. Giordano, G. Haley, K. Bardelli, S. Rayatzadeh, H. Liu, X. Quaini, F. Liao, R. Leri, A. Perella, MA. Loscalzo, J. Anversa, P. (2011) Evidence for human lung stem cells. *New England Journal of Medicine*, 364 (19), pp. 1795-1806.
99. Kalina, M. Mason, RJ. Shannon, JM. (1992) Surfactant protein C is expressed in alveolar type II cells but not clara cells of rat lung. *American Respiratory Journal*, 6, pp. 594-600.
100. Kamei, J. Toyofuku, T. Hori, M. (2003) Negative regulation of p21 by β-catenin/TCT signaling: a novel mechanism by which cell adhesion molecules regulate cell proliferation. *Biochemistry and Biophysical Research Communications*, 312, pp. 380-387.
101. Kamio, K. Liu, X. Suqiura, H. Togo, S. Kobayashi, T. Wang, X. Mao, L. Ahn, Y. Hogaboam, C. Toews, ML. Rennard, SI. (2007) Prostacyclin analogs inhibit fibroblast contraction of collagen gels through the cAMP-PKA pathway. *American Journal of Respiratory Cell and Molecular Biology*, 37 (1), pp. 113-120.
102. Kang, MH. Reynolds, CP. (2009) Bcl-2 inhibitors: targeting mitochondrial apoptotic pathways in cancer. *Clinical Cancer Research*, 15 (4), pp. 1126-1132.

103. Kasper, M. Haroske, G. (1996) Alterations in the alveolar epithelium after injury leading to pulmonary fibrosis. *Histology and Histopathology*, 11 (2), pp. 463-483.

104. Katzenstein, AA and Myers, JL. (1998) Idiopathic pulmonary fibrosis. Clinical relevance of pathological classification. *American Journal of Respiratory and Critical care Medicine*, 157 (4), pp. 1301-1315.

105. Keane, DA. Arenbers, DA. Lynch, SP. Whyte, RI. Lannettoni, MD. Burdick, MD. Wilke, CA. Morris, CB. Glass, MC. DiGiovine, B. Kunkel, SL. Strieter, RM. (1997) The CXC chemokines, IL-8 and IP-10, regulate angiogenic activity in idiopathic pulmonary fibrosis. *Journal of Immunology*, 159 (3), pp. 1437-1443.

106. Kelly, BG. Lok, SS. Hasleton, PS. Egan, JJ. Stewart, JP. (2002) A rearranged form of Epstein-Barr virus DNA is associated with Idiopathic Pulmonary Fibrosis. *American Journal of Respiratory and Critical Care Medicine*, 166, pp. 510-513.

107. Kelly, M. Leigh, R. Gllpin, SE. Cheng, E. Martin, GEM. Radford, K. Cox, G. Gauldie, J. (2006) Cell-specific gene expression in patients with usual interstitial pneumonia. *American Journal of Respiratory and Critical Care Medicine*, 174, pp. 557-565.

108. Keogh, BA and Crystal, RG. (1982) Alveolitis: the key to the interstitial lung disorders (editorial). *Thorax*. 37, pp. 1-10.

109. Key, G. Kubbutat, MH. Gerdes, J. (1994) Assessment of cell proliferation by means of an enzyme-linked immunosorbent assay based on the detection of the Ki-67 protein. *Journal of Immunological Methods*, 177, pp. 113-117.

110. Khun, C. Bolat, J. King, TE. Crough, E. Vartio, T. McDonnald, JA. (1989) An immunohistochemical study of architectural remodeling and connective tissue synthesis in pulmonary fibrosis. *American Review of Respiratory Disease*, 140, pp. 1693-1703.

111. Kida, Y. Asahina, K. Teraoka, H. Gitelman, I. Sato, T. (2007) Twist relates to tubular epithelial-mesenchymal transition and interstitial fibrogenesis in the obstructed kidney. *Journal of Histochemistry and Cytochemistry*, 55 (7), pp. 661-673.

112. Kim, JH. Jang, YS. Eom, KS. Hwang, Y. Kang, HR. Jang, SH. Kim, CH. Park, YM. Lee, MG. Hyun, IG. Jung, KS. Kim, DG. (2007). Transforming growth factor β1

induces epithelial-to-mesenchymal transition of A549 cells. *Journal of Korean Medical Science,* 22, pp. 898-904.

113. Kim, K. Fisher, MJ. Xu, S. El-Deiry, WS. (2000) Molecular determinants of response to TRAIL in killing of normal and cancer cells. *Clinical cancer Research*, 6, pp. 335-346.

114. Kim, KK. Kulger, MC. Wolters, PJ. Robillard, L. Galvez, MG. Brumwel, AN. Sheppard. D. Chapman, HA. (2006) Alveolar epithelial cell mesenchymal transition develops *in vivo* during pulmonary fibrosis and is regulated by the extracellular matrix. *Proceedings of the National Academy of Science of the United States of America.* 103, pp. 13180-13185.

115. Kim, KK. Wei, Y. Szekeres, C. Kugler, MC. Wolters, PJ. Hill, ML. Frank, JA. Brumwell, AN. Wheeler, SE. Kreidberg, JA. Chapman, HA. (2009) Epithelial cell α3β1 integrin links β-catenin and Smad signaling to promote myofibroblast formation and pulmonary fibrosis. *Journal of Clinical Investigation*, 119, pp. 213-224.

116. King, AG. Fulford, LG. Colby, TV. Du Bois, RM. Hansell, DM. Wells, AU. (2002) The relationship between individual histologic features and disease progression in idiopathic pulmonary fibrosis. *American Journal of Respiratory and Critical care Medicine*, 164, pp. 173-177.

117. King, TE, Costabel, U. Cordier, J. DoPico, GA. Du Bois, RM. Lynch, D. Lynch, JP. Myers, J. Panos, R. Raghu, G. Schwartz, D. Smith, CM. (2000) Idiopathic pulmonary fibrosis: Diagnosis and treatment. International Consensus Statement. *American Journal of Respiratory and Critical Care Medicine*, 161, pp. 646-664.

118. King, TE. Schwarz, MI. Brown, K. Tooze, JA. Colby, TV. Waldron, JA Jr. Flint, A. Thurlbeck, W. Cherniack, RM. (2001) Idiopathic pulmonary fibrosis: relationships between histopathologic features and mortality. *American Journal of Respiratory and Critical Care Medicine*, 164 (6), pp. 1025-1032.

119. Kluck, RM. Bossy-Wetzel, E. Green, DR. Newmeyer, DD. (1997) The release of cytochrome c from mitochondria: a primary site for Bcl-2 regulation of apoptosis. *Science*, 275, pp. 1132-1136.

120. Königshoff, M. Balsara, N. Pfaff, E. Kramer, M. Chrobak, I. Seeger, W. Eickelberg, O. (2008) Functional Wnt signalling is increased in idiopathic pulmonary fibrosis. *PLOS ONE*, 3 (5), pp. e2142

121. Kreating, D. Levvey, B. Kotsimbos, T. Whitford, H. Westall, G. Williams, T. Snel, G. (2009) Lung transplantation in pulmonary fibrosis: Challenging early outcomes counterbalanced by surprisingly good outcomes beyond 15 years. *Transplantation Proceedings*, 41 (1), pp. 289-291.

122. Krieg, T. Abraham, D. Lafyatis, R. (2007) Fibrosis in connective tissue disease: the role of the myofibroblast and fibroblast-epithelial cell interaction. *Arthritis Research and Therapy*, 9 (supplement 2), pp. S4.

123. Krizhanovsky, V. Yon, M. Dickins, RA. Hearn, S. Simon, J. (2008) Senescence of activated stellate cells limits liver fibrosis. *Cell*, 134 (4), pp. 657-667.

124. Kubo, H. Nakayama, K. Yanai, M. Suzuki, T. Yamaya, M. Watanabe, M. Sasaki, H. (2005) Anticoagulant therapy for idiopathic pulmonary fibrosis, *Chest*, 128, pp. 1475-1482.

125. Kwok, WK. Ling, M. Yuen, HF. Wong, Y. Wang, X. (2007) Role of p14ARF in TWIST-mediated senescence in prostate epithelial cells. *Carcinogenesis*, 28 (12), pp. 2467-2475.

126. Lama, VN. Phan, SH. (2006) The extra pulmonary origin of fibroblasts: stem/progenitor cells and beyond. *Proceedings of the American Thoracic Society*, 3, pp. 373-376.

127. Latsi, PI. du Bois, RM. Nicholson, AG. Colby, TV. Bisirtzoglou, D. Nikdakopoulau, A. Veeraraghavan, S. Hansell, DM. Wells, AU. (2003) Fibrotic idiopathic interstitial pneumonia: the prognostic value of longitudinal functional trends. *American Journal of Respiratory and Critical Care Medicine*, 168 (5), pp. 531-537.

128. Lawson, WE. Grant, SW. Ambrosini, V. Womble, KE. Dawson, EP. Lane, KB. Markin, C. Renzoni, E. Lympany, P. Thomas, AQ. Roldan, J. Scott, TA. Blackwell, TS. Phillips, JA. 3rd. Loyd, JE. du Bois, RM. (2004) Genetic mutations in surfactant protein C are a rare cause of sporadic cases of IPF. *Thorax*, 59, pp. 977-980.

129. Lawson, WE. Polosukhin, VV. Stathopoulos, GT. Zoia, O. Han, W. Lane, KB. Li, B. Donnelly, EF. Holburn, GE. Lewis, KG. Collins, RD. Hull, WM. Glasser, SW. Whitsett, JA. Blackwell, TS. (2005) Increased and prolonged pulmonary fibrosis in surfactant protein C-deficient mice following intratracheal bleomycin. *American Journal of Pathol*ogy, 167 (5), pp. 1267-1276.

130. Lee, JS. Song, JW. Wolters, PJ. Elicker, BM. King, TE. Kim, DS. Collard, HR. (2012) Bronchoalveolar lavage pepsin in acute exacerbations of idiopathic pulmonary fibrosis. *European Respiratory Journal*, 39 (2), pp. 352-358.

131. Leontieva, OV. Blagosklonny, MV. (2010) DNA damaging agents and p53 do not cause senescence in quiescent cells, while consecutive re-activation of mTOR is associated with conversion to senescence. *Aging*, 2, pp. 924-935.

132. Leslie, KO. (2011) Idiopathic pulmonary fibrosis may be a disease of recurrent, tractional injury to the periphery of the aging lung. *Archives of pathology and Laboratory Medicine*, 136, pp. 591-600.

133. Lettieri, CJ. Nathan, SD. Barnett, SD. Ahmad, S. Shorr, AF. (2006) Prevalence and outcomes of pulmonary arterial hypertension in advanced idiopathic pulmonary fibrosis. *Chest*, 129, pp. 746-752.

134. Lippmann, M. Eckert, HL. Hahan, N. Morgan, WKC. (1973) The prevalence of circulating anti-nuclear and rheumatoid factors in United States coal miners. *Annals of Internal Medicine*, 79 (6), pp. 807-811.

135. Liu, T. Hu, B. Chung, MJ. Ullenbruch, M. Jun, H. Phan, SH. (2006) Telomerase regulation of myofibroblasts differentiation. *American Journal of Respiratory Cell and Molecular Biology*, 34, pp. 625-633.

136. Lu, Y. Fukuyama, S. Yoshida, R. Kobayaski, T. Saeki, K. Shiraishi, H. Yoshimura, A. Takaesu, G. (2006) Loss of SOCS3 gene expression converts STAT3 function from anti-apoptotic to pro-apoptotic. *Journal of Biological Chemistry*, 281 (48), pp. 36683-36690.

137. Luzina, IG. Tod, NW. Iacono, AT. Atamas, SP. (2008) Roles of T lymphocytes in pulmonary fibrosis. *Journal of Leukocyte Biology*, 83 (2), pp. 237-244.

138. Lynch, JB. Wurfel, M. Flaherty, K. White, E. Martinez, F. (2001) Usual interstitial pneumonia. *Seminars in Respiratory and Critical care Medicine*, 22 (4), pp. 357-386.

139. Lynch, DA. (2005) Fibrotic idiopathic pulmonary pneumonia: high resolution computered tomography consideration. *Seminars in Respiratory Critical Care Medicine*, 24 (4), pp. 365-376.

140. Ma, C. Chegini, N. (1999) Regulation of matrix metalloproteinases (MMPs) and their tissue inhibitors in human myometrial smooth muscle cells by TGF-β1. *Molecular Human Reproduction*, 5 (10), pp. 950-954.

141. Maestro, R. Dei Tos, AP. Hamamori, Y. Krasnokutsky, S. Sartorelli, V. Kedes, L. Doglioni,C. Beach, DH. Hannon, GJ. (1999) Twist is a potential oncogene that inhibits apoptosis. *Genes and Development*, 13, pp. 2207-2217.

142. Maeyama, T. Kuwano, K. Kawasaki, M. Kunitake, R. Hagimoto, N. Matsuba, T. Yoshimi, M. Inoshima, I. Yashida, K. Hara, N. (2001) Upregulation of Fas-signaling molecules in lung epithelial cells from patients with idiopathic pulmonary fibrosis. *European Respiratory Journal*, 17, pp. 180-189.

143. Maher, TM. Wells, AU. Laurent, GJ. (2007) Idiopathic pulmonary fibrosis: multiple causes and mechanisms? *European Respiratory Journal,* 30 (5), pp. 835-839.

144. Martinez, FJ. And Flaherty, K. (2006) Pulmonary function testing in idiopathic interstitial pneumonias. *Proceedings of the American Thoracic Society*, 3 (4), pp. 315-321.

145. Mason, RJ. And Williams, MC. (1977) Type II alveolar cells: defender of the alveolus. *American Review of Respiratory Disease*, 115, pp. 81-91.

146. Massova, I. Kotra, LP. Fridman, R. Mabashery, S. (1998) Matrix metalloproteinases: structures, evolution and diversification. *The Journal of the Federation of American Societies for Experimental Biology*, 12, pp. 1075-1095.

147. Matsuo, N. Shiraha, H. Fujikawa, T. Takaoka, N. Ueda, N. Tanaka, S. Nishina, S. Nakanishi, Y. Uemura, M. Takaki, A. Nakamura, S. Kobayashi, Y. Nouso, K. Yagi, T. Yamamoto, K. (2009) Twist expression promotes migration and invasion in hepatocellular carcinoma. *BioMed Central Cancer*, 9, 240.

148. Mattey, DL. Dawes, PT. Nixon, NB. Slater, H. (1997) Transforming growth factor β1 and interleukin 4 induced α-smooth muscle actin expression and myofibroblast *in vitro*: modulation by basic fibroblast growth factor. *Annals of Rheumatoid Disease*, 56, pp. 426-431.

149. McCluggae, WG. Connolly, LE. McGregor, G. Hall, PA. A strategy for defining biologically relevant levels of p53 protein expression in clinical samples with reference to endometrial neoplasia. *International Journal of Gynecological Pathology*, 24 (4), pp. 307-312.

150. McGrath, EE. Lawrie, A. Marriot, H. Mercer, PF. Cross, SS. Chambers, RC. Dockrell, DH. Whyte, MKB. (2011) S111 the role of TNF-related apoptosis inducing ligand (TRAIL) in pulmonary fibrosis. *Thorax*, 66, pp. A51-A52.

151. McGrath, EE. Millar, AB. (2012) Hot off the breath: triple therapy for idiopathic pulmonary fibrosis-hear the PANTHER roar. *Thorax*, 67, pp. 97-98.

152. Medical Research Council Working Party (1981) Long term domiciliary oxygen therapy in chronic hypoxic cor pulmonale complicating chronic bronchitis and emphysema: report of the Medical Research Council Working Party. *Lancet*, 1, pp. 681-686.

153. Mehra, A. and Wrana, JL. (2002) TGF-β and the Smad signal transduction pathway. *Biochemistry and Cell Biology*, 80 (5), pp. 605-622.

154. Mitas, M. Mikhitarian, K. Walters, C. Baron, PL. Elliott, BM. Brothers, TE. Robison, JG. Metcalf, JS. Palesch, YY. Zhang, Z. Gillanders, WE. Cole, DJ. (2001) Quantitative real-time RT-PCR detection of breast cancer micro-metastasis using a multigene marker panel. *International Journal of Cancer*, 93 (2), pp. 162-171.

155. Miyake, Y. Sasaki, S. Yokoyama, T. Chida, K. Azuma, A. Suda, T. Kudoh, S. Sakamoto, N. Okamoto K. Kobashi, G, Washio M, Inaba, Y. Tanaka, H. (2005) Occupational and environmental factors and idiopathic pulmonary fibrosis In Japan. *The Annals of Occupational Hygiene*, 49, pp. 259-265.

156. Mizuno, S. Bogaard, HJ. Voelkel, NF. Umeda, Y. Kadowaki, M. Ameshima, S. Miyamori, I. Ishizaki, T. (2009) Hypoxia regulates human lung fibroblast proliferation via p53-dependent and –independent pathways. *Respiratory Research*, 10, pp. 17.

157. Moodley, UP. Caterina, P. Scaffidi, AK. Misso, NL. Papadimitriau, JM. (2004) Comparison of the morphological and biochemical changes in normal human lung fibroblasts and fibroblasts derived from lungs of patients with idiopathic pulmonary fibrosis during FasL-induced apoptosis. *Journal of Pathology*, 202, pp. 486-495.

158. Moodley, Y. Atienza, D. Manuelpillai, U. Samuel, CS. Tchongue, J. Ilancheran, S. Boyd, R. Trounson, A. (2009) Human umbilical cord mesenchymal stem cells reduce fibrosis of bleomycin-induced lung injury. *American Journal of Pathology*, 175 (1), pp. 303-313.

159. Moore, BB. Murray, L. Das, A. Wilke, CA. Herrygers, AB. Toews, GB. (2006) The role of CCL12 in the recruitment of fibrocytes and lung fibrosis. *American Journal of Respiratory Cell and Molecular Biology*, 35, pp. 175-181.

160. Moore, RA. Warren, RL. Freeman, JD. Gustavensen, JA. Chenard, C. Friedman, JM. Suttle, CA. Zhao, Y. Holt, RA. (2011) The sensitivity of massively parallel sequencing for detecting candidate infectious agents associated with human tissue. *PLOS ONE*, 6 (5), pp. e19838.

161. Mora, AL. Torres-Gonzalez, E. Rojas, M. Xu, J. Ritzenthaler, J. Speck, SH. Roman, J. Brigham, K. Stecenko, A. (2007) Control of virus reactivation arrests pulmonary herpes virus induced fibrosis in IFN-gamma receptor-deficient mice. *American Journal of Respiratory and Critical Care medicine*, 175, pp. 1139-1150.

162. Moreira, JN. Santos, A. Simões, S. (2006) Bcl-2-targeted antisense therapy (oblimersen sodium): Towards clinical reality. *Reviews on recent clinical trials*, 1, pp. 217-235.

163. Morgan, DO. (2007) *The cell cycle*. London: Oxford University Press

164. Muller, NL. Staples, CA. Miller, RR. Vedal, S. Thurbeck, WM. Osbrow, DN. (1987) Disease activity in idiopathic pulmonary fibrosis. *Radiology*, 165, pp. 731-734.

165. Nagai, S. Kitaich, M. Hamada, K. Nago, T. Hoshino, Y. (1999) Hospital-based historical cohort study of 234 histologicaly proven Japanese patients with IPF. *Sarcoidosis Vascular Diffuse Lung Disease*, 16 (2), pp. 209-214.

166. Nakayama, S. Mukae, H. Sakamoto, N. Kakugawa, T. Yoshioka, S. Soda, H. Oku, H. Urata, Y. Kondo, T. Kubota, H. Nagata, K. Kohno, S. (2008) Pirfenidone inhibits the expression of HSP47 in TGF-beta1 simulated human lung fibroblasts. *Life Sciences*, 82 (2-4), pp. 210-217.

167. Nathan, SD. Noble, PW and Truder, RM. (2007) Idiopathic pulmonary fibrosis and pulmonary hypertension: connecting the dots. *American Journal of Respiratory and Critical Care Medicine*, 175, pp. 785-880.

168. National Health Service (2012) NHS National research ethics guidelines [WWW] NHS Health Research Authority. Available from: www.nres.nhs.uk [Accessed May 2012].

169. Navaratnam, V. Flemming, KM. West, J. Smith, CJ. Jenkins, RG (2011) The rising incidence of idiopathic pulmonary fibrosis in the UK. *Thorax*, 66, pp. 462-467.

170. Nemery, B. (1990) Metal toxicity and the respiratory tract. *European Respiratory Journal*, 3 (2), pp. 202-219.

171. Ng, YH. Zhu, H. Leung, PCK. (2012) Twist modulates human trophoblastic cell invasion via regulation of N-cadherin. *Endocrinology*, 153, pp. 925-936.

172. Nguyen, M. Marcellus, RC. Roulston, A. Watson, M. Serfass, L. Murthy Madiraju, SR. Goulet, D. Viallet, J. Bélec, L. Billot, X. Acoca, S. Purisima, E. Wiegmans, A. Cluse, L. Johnstone, RW. Beauparlant, P. Shore, GC. (2007) Small molecule obtatoclax (GX15-070) antagonizes MCL-1 and overcomes MCL-1-mediated resistance to apoptosis, *Proceedings of the National Academy of Sciences*, 104 (49), pp. 19512-19517.

173. Nicholson, AG. Fulford, LG. Colby, TV. du Bois, RM. Hansell, DM. Wells, AU. (2002) The relationship between individual histologic features and disease progression in IPF. *American Journal of Respiratory and Critical Care Medicine*, 166, pp. 173-177.

174. Nishiyama, O. Taniguchi, H. Kondah, Y. Kimura, T. Kato, K. Kataoka, K. Ogawa, T. Watanabe, F. Arizono, S. (2010) A simple assessment of dyspnoea as a prognostic indicator in idiopathic pulmonary fibrosis. *European Respiratory Journal*, 36 (5), pp. 1067-1072.

175. Noble, PW. Albera, C. Bradford, WZ. Costabel, U. Glassberg, MK. Kardatzke, D. King, TE. Lancaster, L. Sahn, SA. Szwarcberg, J. Valevre, D. du Bois, RM. (2011) Pirfenidone in patients with idiopathic pulmonary fibrosis (CAPACITY): two randomized trials. *Lancet*, 377 (9779), 1760-1769.

176. Noth, I. and Martinez, FJ. (2007) Recent advances in idiopathic pulmonary fibrosis. *Chest*, 132 (2), pp. 637-650.

177. Nozaki, Y. Liu, T. Hatano, K. Gharaee-Kermani, M. Phan, SH. (2000) Induction of telomerase activity in fibroblasts from bleomycin-injured lungs. *American Journal of Respiratory Cell Molecular Biology*, 23 (4), pp. 460-465.

178. Okami, K. Reed, AL. Cairns, P. Koch, WM. Westra, WH. Wehage, S. Jen, J. Sidransky, D. (1999) Cyclin D1 amplification is independent of p16 inactivation in head and neck squamous cell carcinoma. *Oncogene*, 18 (23), pp. 3541-3545.

179. Ohtsubo, M. Theodoras, AM. Schumacher, J. Roberts, JM. Pagano, M. (1995) Human cyclin E, a nuclear protein essential for the G1 to S phase transition. *Molecular Cell Biology*, 15 (5), pp. 2612-2624.

180. Oliver, CL. Bauer, A. Wolter, KG. Ubell, ML. Narayan, A. O-Connell, KM. Fisher, SG. Wang, S. Wu, X. Ji, M. Carey, TE. Bradford, TW. (2004) In vitro effects of the BH3 mimetic (-)-gossypol on head and neck squamous cell carcinoma cells. *Clinical cancer Research*, 10 (22), pp. 7757-7763.

181. Ortega, S. Malumbres, M. Barbacid, M. (2002) Cyclin D-dependent kinases. INK4 inhibitors and cancer. *Biochemica et Biophysica Acta (BBA)-Reviews on cancer*, 1602 (1), pp. 73-87.

182. Paakko, P. Kaarteenaho-Wiik, R. Pollanen, R. Soini, Y. (2000) Tenascin mRNA expression at the foci of recent injury in usual interstitial pneumonia. *American Journal of Respiratory and Critical Care Medicine*, 161, pp. 967-972.

183. Papiris, AS. Kollintaz, A. Kitsanta, P. Kapotsis, G. Karatze, M. Milic-Emilli, J. Roussos, C. (2005) Relationship of BAL and lung tissue CD4+ and CD8T T lymphocytes and their ratio in Idiopathic pulmonary fibrosis. *Chest*, 128 (4), pp. 2971-2971.

184. Pardo, A. Selman, M. (2002) Idiopathic pulmonary fibrosis: new insights in its pathogenesis. *International Journal of Biochemical Cell Biology,* 34 (12), pp. 1534-1538.

185. Patel, RM. Goldblum, JR, His, ED. (2004) Immunohistochemical detection of human herpes virus-8 latent nuclear antigen-1 is useful in the diagnosis of Karposi sarcoma. *Modern Pathology*, 17, pp. 456-460.

186. Patel, NM. Lederer, DJ. Burczuk, AC. Kawat, SM. (2007) Pulmonary hypertension in idiopathic pulmonary fibrosis. *Chest*, 132 (2), pp. 998-1006.

187. Phan, SH. (2002) The myofibroblast in pulmonary fibrosis. *Chest*, 122 (6 suppl), pp. 286s-289s.

188. Pickart, CM. (2001) Mechanisms underlying ubiquitination. *Annual Review of Biochemistry*, 70, pp. 503-533.

189. Piguet, PF. Ribaux, C. Karpuz, V. Grau, GE. Kapanci, Y. (1993) Expression and localization of tumour necrosis factor-alpha and its mRNA in idiopathic pulmonary fibrosis. *American Journal of Pathology*, 143, pp. 651-655.

190. Plataki, M. Koutsopoulos, AV. Darivianaki, K. Delides, G. Siafakas, NM. Bouros, D. Expression of apoptotic and antiapoptotic markers in epithelial cells in idiopathic pulmonary fibrosis. *Chest*, 127, pp. 266-274.

191. Potenta, S. Zeisberg, E. Kalluri, R. (2008) The role of endothelial-to-mesenchymal transition in cancer progression. *British Journal of Cancer,* 99, pp. 1275-1279.

192. Powell, DW. Mifflin, RC. Valentich, JD. Crowe, SE. Saada, JI West, AB. (1999) Myofibroblasts. Paracrine cells important in health and disease. *American Journal of Physiology-Cell Physiology*, 277 (1), pp. C1-C19.

193. Pozharskaya, V. Torres-Gonzalez, E. Rojas, M. Gal, A. Amin, M. Dollard, S. Roman, J. Stecenko, AA. Mora, AL. (2009) TWIST: A regulator of epithelial-mesenchymal transition in lung fibrosis. *PLos ONE,* 4 (10), e7559.

194. Quan, TE. Cowper, S. Wu, S. Bockensteadt, LK. Bucala, R. (2004) Circulating fibrocytes: collagen-secreting cells of the peripheral blood. *International Journal of Biochemistry and Cell Biology*, 36 (4), pp. 598-600.

195. RadRounds Radiology Network (2009) www.radrounds.com. [Accessed May 2012].

196. Raghu, G. Mageto, Y. Lockhart, D. Schmidt, RA. Wood, DE. Godwin, JD. (1999) The accuracy of the clinical diagnosis of new-onset idiopathic pulmonary fibrosis and other interstitial lung disease. *Chest*, 116, pp. 1168-1174.

197. Raghu, G. Weycker, D. Edelsberg, J. Bradford, WZ. Oster, G. (2006) Incidence and prevalence of idiopathic pulmonary fibrosis. *American Journal of Respiratory and Critical Care Medicine*, 174 (7), pp. 810-816.

198. Raghu, G. Collard, HR. Egan, JJ. Martinez, FJ. Behr, J. Brown, KK. Colby, TV. Cordier, JF. Flaherty, KR. Lasky, JA. Lynch, DA. Ryu, JH. Swigris, JJ. Wells, AU. Ancochea, J. Bouros, D. Carvalho, C. Costabel, U. Ebina, M. Hansell, DM. Johkoh, T. Kim, DS. King, TE. Kondoh, Y. Myers, J. Mu¨ller, NL. Nicholson, AG. Richeldi, L. Selman, M. Dudden, RF. Griss, BS. Protzko, SL. Schunemann, HJ. (2011) An official ATS/ERS/JRS/ACAT statement: Idiopathic Pulmonary Fibrosis: Evidence-based guidelines for diagnosis and management. *American Journal of Respiratory and Critical Care Medicine,* 183, pp. 788-824.

199. Raghu, G. and Meyer, KC. (2012) Silent gastro-oesophageal reflux and microaspiration in IPF: mounting evidence for anti-reflux therapy? *European Respiratory Journal*, 39, pp. 242-245.

200. Ramos, C. Montano, M. Garcia-Alvarez, J. Ruiz, V. Uhal, BD. Selman, M. Pardo, A. (2001) Fibroblasts from idiopathic pulmonary fibrosis and normal lungs differ in growth rate, apoptosis and tissue inhibitor of metalloproteinases expression. *American Journal of Respiratory Cell and Molecular Biology*, 24, pp. 591-598.

201. Raskar, VS. and Coultas, DB. (2006) Is Idiopathic pulmonary fibrosis and environmental disease? *Proceedings of the American Thoracic Society*, 3, pp. 293-298.

202. Reynolds, SD and Malkinson, AM. (2010) Clara cell: progenitor for the bronchiolar epithelium. *International Journal of Biochemistry and Cell Biology*, 42 (1), pp. 1-4.

203. Robson, EJ. Khaled, WT. Abell, K. Watson, CJ. (2006) Epithelial-to-mesenchymal transition confers resistance to apoptosis in three murine mammary epithelial cell lines. *Differentiation*, 74 (5), pp. 254-264.

204. Rønn, SG. Billestrup, N. Mandrup-Poulsen, T. (2007) Diabetes and suppressor of cytokine signaling protein. *Diabetes*, 56, pp. 541-548.

205. Rudd, RM. Haslam, PL, Turner-Warwick, M. (1981) Cryptogenic fibrosing alveolitis relationships of pulmonary physiology and bronchoalveolar lavage to treatment and prognosis. *American Review of Respirator Disease*, 124, pp. 1-8.

206. Sabattini, E. Bisgaard, K. Ascani, S. Poggi, S. Picciolli, M. Ceccarelli, C. Pieri, F. Fraternali-Orcioni, G. Pileri, SA. (1998) The EnVision ++ system: a new immunohistochemical method for diagnostics and research. Critical comparison with the APAAP, ChemMate, CSA, LABC and SABC techniques. *Journal of Clinical Pathology*, 51 (7), pp. 506-511.

207. Saini, KS. And Walker, NI. (1998) Biochemical and molecular mechanisms regulating apoptosis. *Molecular and Cellular Biochemistry*, 178, pp. 9-25.

208. Saleh, D. Furukawa, K. Tsao, MS. Maghazachi, A. Corrin, B. Yanagisawa, M. Barnes, PJ. Giaid, A. (1997) Elevated expression of endothelin-1 and endothelin-converting enxyme-1 in idiopathic pulmonary fibrosis: possible involvement of pro-

inflammatory cytokines. *American Journal of Respiratory Cell and Molecular Biology*, 16 (2), pp. 187-193.

209. Santini, MT. Rainaldi, G. Indovina, PL. (2000) Apoptosis, cell adhesion and the extracellular matrix in the three-dimensional growth of multicellular tumour spheroids. *Clinical Reviews in Oncology/Haematology*, 26, pp. 75-87.

210. Schmidt, M. Sun, G. Stacey, MA. Mori, L. Mattoli, S. Identification of circulating fibrocytes as precursors of bronchial myofibroblasts in asthma. *Journal of Immunology*, 171, pp. 380-389.

211. Scott, J. Johnston, I. Britton, J. (1990) What causes cryptogenic fibrosing alveolitis? A case –control study of environmental exposure to dust. *British Medical Journal*, 301, pp. 1015-1017.

212. Selman, M. Pardo, A. (2006) Role of epithelial cells in idiopathic pulmonary fibrosis: from innocent targets to serial killers. *Proceedings of the American Thoracic Society*, 3, pp. 364-372.

213. Serrano, M. Hannon, GJ. Beach, D. (1993) A new regulatory motif in cell-cycle control causing specific inhibition of cyclin D/CDK4. *Nature*, 336, pp. 704-707.

214. Sherr, CJ. Roberts, JM. (1999) CDK inhibitors: positive and negative regulators of G1-phase progression. *Genes and Development*, 13, pp. 1501-1512.

215. Shintani, Y. Maeda, M. Chaika, N. Johnson, KR. Wheelock, MJ. (2008) Collagen 1 promotes epithelial-to-mesenchymal transition in lung cancer cells via Transforming Growth Factor-β signaling. *American Journal of Respiratory Cell and Molecular Biology,* 38, pp. 95-104.

216. Sides, MD. Klingsberg, RC. Shan, B. Gordon, KA. Nguyen, HT. Lin, Z. Takahashi, T. Flemington, EK. Lasky, JA. (2011) The Epstein-Barr virus latent membrane protein 1 and transforming growth factor-β1 synergistically induce epithelial-mesenchymal transition in lung epithelial cells. *American Journal of Respiratory Cell and Molecular Biology,* 44, pp. 852-862.

217. Smeland, E. Kilvaer, TK. Sorbye, S. Valkov, A. Andersen, A. Bremnes, RM. Busund, L. Donnem, T. (2012) Prognostic impacts of hypoxic markers in soft tissue sarcomas. *Sarcoma*, 2012, ID 541650.

218. Song, K. Chen, Y. Goke, R. Wilmen, A. Seidal, C. Göke, A. B, Hilliard. Chen, Y. (2000) Tumour necrosis factor-related ligand (Trail) is an inhibitor of autoimmune

inflammation and cell cycle progression. *Journal of Experimental Medicine*, 191 (7), pp. 1095-1104.

219. Souza, CA. Muller, NL. Flint, J. Wright, JL. Churg, A. (2005) Idiopathic pulmonary fibrosis spectrum of high-resolution CT findings. *American Journal of Roentgenology*, 183, pp. 1531-1539.

220. Steele, MP. Speer, MC. Loyd, JE. Brown, KK. Herron, A. Sllfer, SH. Burch, LH. Wahidi, MM. Phillips, JA. Sporn, TA. McAdams, P. Schwarz, MI. Schwartz, DA. (2005) Clinical and pathologic features of familial interstitial pneumonia. *American Journal of Respiratory and Critical care Medicine*, 172, pp. 1146-1152.

221. Stein, GH. Drullinger, LF. Soulard, A. Dilic, V. (1999) Differential roles for Cyclin-dependent kinase inhibitors p21 and p16 in the mechanisms of senescence and differentiation in human fibroblasts. *Molecular and Cellular Biology*, 19 (3), pp. 2109-2117.

222. Stevens, A. and Lowe, J. (2000) *Pathology*. 2nd ed. London. Mosby

223. Strange, C. and Highland, KB. (2004) Interstitial lung disease in the patient who has connective tissue disease. *Clinical Chest Medicine*, 25, pp. 549-559.

224. Strip BR, Reynolds, SD. (2008) Maintenance and repair of the bronchiolar epithelium. *Proceedings of the American Thoracic Society*, 5, pp. 328-333.

225. Suigris, JJ. Wambildt, FS. Behr, J. du Bois, RM. King, TE. Raghu, G. Brown, KK. (2010) The 6 minute walk test in idiopathic pulmonary fibrosis: longitudinal changes and minimal important difference. *Thorax*, 65 (2), pp. 173-177.

226. Sumikawa, H. Johkoh, T. Colby, TV. Ichikado, K. Suga, M. Taniguchi, H. Kondoh, Y. Ogura, T. Arakawa, H. Fujimoto, K. Inoue, A Mihara, N. Honda, O. Tomiyama, N. Nakamura, H. Müller, NL. (2008) Computed tomography findings in pathological usual interstitial pneumonia. *American Journal of Respiratory and Critical Care Medicine*, 177 (4), pp. 433-439.

227. Sun, S. Ning, X. Zhang, Y. Lu, Y. Nie, Y. Han, S. Liu, L., Du, R. Xia, L. He, L. Fan, D. (2009) Hypoxia-inducible factor-1 alpha induces Twist expression in tubular epithelial cells subjected to hypoxia, leading to epithelial-to-mesenchymal transition. *Kidney International,* 75 (12), pp. 1278-1287.

228. Sweet, MP. Patti, MG. Leard, LE. Golden, JA. Hays, SR. Hoopes, C. Theodore, PR. (2007) Gastroesophageal reflux in patients with idiopathic pulmonary fibrosis

referred for lung transplantation. *Journal of Thoracic and Cardiovascular Surgery*, 133 (4), pp. 1078-1084.

229. Swigris, JJ. Wamboldt, FS. Behr, J. du Bois, RM. King, TE. Raghu, G. Brown, KK. (2010) The 6 minute walk in idiopathic pulmonary fibrosis: longitudinal changes and minimum important difference. *Thorax*, 65, pp. 173-177.

230. Taille, C. Grootenboer-Mignot, S. Boursier, C. Michel, L. Debray, M. fagart, J. Barrientos, L. Mailleux, A. Cigna, N. Tubach, F. Marchal-Somme, J. Soler, P. Chollet-Martin, S. Crestani, B. (2011) Identification of periplakin as a new target for autoreactivity in idiopathic pulmonary fibrosis. *American Journal of Respiratory and Critical care Medicine*, 183, pp. 759-766

231. Tang, Y. Johnson, JE. Browning, PJ, Cruz-Gerus, RA. Davis, A. Graham, BS. Brigham, KL. Oates, JA Jr. Loyd, JE. Stecenko, AA. (2003). Herpes virus DNA is consistently detected in lungs of patients with idiopathic pulmonary fibrosis. *Journal of Clinical Microbiology*, 41 (6), pp. 2633-2640.

232. Tauille, C. Grootenboer-Mignot, Boursier, C. Michel, L. Debray, MP. Fagart,J. Barrientos, L. Mailleux, A. Cigna, N. Tubach, F. Marchal-Sommé, J. Soler, P. Chollet-Martin, S. Crestani, B. (2011) Periplakin: A new antigenic target in idiopathic pulmonary fibrosis. *American Journal of Respiratory and Critical Care Medicine*, 183 (6), pp. 759-766.

233. Tarnavski, O. Zeisberg, M. (2007) Endo-to-mesenchymal transition contributes to cardiac fibrosis. *Nature Medicine*, 13 (8), pp. 952-961.

234. Taskar, VS. and Coultas, DB. (2006) Is idiopathic pulmonary fibrosis and environmental disease? *Proceedings of the American Thoracic Society*, 3, pp. 293-298.

235. Taylor, CR. Levenson, RM. (2006) Quantification of immunohistochemistry – issues concerning methods, utility and semiquantitative assessment II. *Histopathology*. 49, pp. 411-424.

236. Thabut, G. Christie, JR. Porcher, R. Cashier, Y. Dauriat, G. Jebrak, G. Fournier, M. Lesèche, G. Porcher, R. Mal, H. (2009) Survival after bilateral versus single-lung transplant for idiopathic pulmonary fibrosis. *Annals of Internal Medicine*, 151, pp. 767-774.

237. Thannickal, VJ. Horowitz, JC. (2006) Evolving concepts of apoptosis in idiopathic pulmonary fibrosis. *Proceedings of the American Thoracic Society*, 3, pp. 350-356.

238. Titto, L. Bloigu, R. Heiskanen, U. Paakkoo, P. Kinnula, P. Kaarteenaho-Wiik, R. (2006) Relationship between histopathological features and the course of idiopathic pulmonary fibrosis. *Thorax*, 61, pp. 1091-1095.

239. Tobin, RW. and Raghu, G. (1998) Increased gastro-esophageal reflux in patients with idiopathic pulmonary fibrosis. *American Journal of Respiratory and Critical Care Medicine*, 158, pp. 1804-1808.

240. Triantafyllidou, C. Manali, ED. Magkou, C. Sotiropoulau, C. Kololekas, LF. Kagouridis, K. Rontogianni, D. Papiris, SA. (2011) Medical Respiratory Council dyspnea scale does not relate to fibrotic profusion in IPF. *Diagnostic Pathology*, 6, pp. 28.

241. Tsai, C. Chen. T. Yeq, T. Chen, L. Wang, J. Chiu, C. Hung, S. (2011) Hypoxia inhibits senescence and maintains mesenchymal stem cell properties through down-regulation of E2A-p21 by HIF-TWIST. *Blood*, 117, pp. 459-469.

242. Tsakiri, KD. Cronkhite, JT. Kuan, PJ. Xing, C. Raghu, G. Weissler, JC. Rosenblatt, RL. Shay, JW. Garcia, CK. (2007) Adult-onset pulmonary fibrosis caused by mutations in telomerase. *Proceedings of the National Academy of Science*, 104 (18), pp. 7552-7557.

243. Tsantes, A. Tassiopoulas, S. Papadhimitriou, SI. Bonovas, S. Kavalierou, L. Vaiopoulos, G. Meletis, I. (2003) Suboptimal erythropoietic response to hypoxemia in idiopathic pulmonary fibrosis. *Chest*, 124, pp. 548-553.

244. Tsuji, T. Aoshiba, K. Nagai, A. (2006) Alveolar cell senescence in patients with pulmonary emphysema. *American Journal of Respiratory and Critical Care Medicine*, 174, pp. 886-893.

245. Turner-Warwick, M. Burrows, B. Johnson, A. (1980) Cryptogenic fibrosing alveolitis: response to corticosteroid treatment and its effect on survival. *Thorax*, 35, pp. 593-599.

246. Tzilas, V. Kpti, A. Papandrinopoulas Martalits, D. Tsoukalas, G. (2009) Prognostic factors in idiopathic pulmonary fibrosis. *American Journal of the Medical Sciences*, 338 (6), pp. 481-485.

247. Tzouvelekis, A. Koliakos, G. Ntolios, P. Baira, I. Bouros, E. Oikonomou, A. Zissimopoulos, A. Kolios, G. Kakagia, D. Paspaliaris, V. Kotsianidis, I. Froudarakis, M. Bouros, D. (2011) Stem cell therapy for idiopathic pulmonary fibrosis: a protocol proposal. *Journal of Translational Medicine*, 9, pp. 182.

248. Vancheri, C. Failla, M. Crimi, N. Raghu, G. (2010) Idiopathic pulmonary fibrosis: a disease with similarities and links to cancer biology. *European Respiratory Journal*, 35, pp. 496-504.

249. Vega, S. Morales, AV. Ocana, OH. Valdes, F. Fabregat, I. Nieto, MA. (2004) Snail blocks the cell cycle and confers resistance to cell death. *Genes and Development*, 18 (10), pp. 1131-1143.

250. Vogler, M. Walczak, H. Stadel, D. Haas, TL. Genze, F. Jovanovic, M. Bhanot, U. Hasel, C. Möller, P. Gschwend, JE. Simmet, T. Debatin, CM. Fulda, S. (2009) Small molecule XIAP inhibitors enhance TRAIL-induced apoptosis and antitumor activity in preclinical models of pancreatic carcinoma. *Cancer Research*, 69 (6), pp. 2425-2434.

251. Wahl, GM. Carr, AM. (2001) The evolution of diverse biological responses to DNA damage: insights from yeast and p53. *Nature Cell Biology*, 4 (4), pp. 328.

252. Walker, RA. (2006) Quantification of immunohistochemistry – issues concerning methods, utility and semiquantitative assessment I. *Histopathology*, 49, pp. 406-410.

253. Wallace, WAH. Howie, SEM. Lamb, D. Salter, DM. (1995) Tenascin immunoreactivity in cryptogenic fibrosing alveolitis. *Journal of Pathology*, 174, pp. 415-420.

254. Wang, S. and El-Deiry, WS. (2003) TRAIL and apoptosis induction by TNF-family death receptors. *Oncogene*, 22, pp. 8628-8633.

255. Watts, KL. Sampson, EM. Schultz, GS. Spiteri, MA. (2005) Simvistatin inhibits growth factor expression and modulates profibrogenic markers in lung fibroblasts. *American Journal of Respiratory Cell and Molecular Biology*, 232 (4), pp. 290-300.

256. Wells, AU. Desai, SR. Rubens, MB. Goh, NSL. Cramer, D. Nicholson, AG. Colby, TV. du Bois, RM. Hansell, DM. (2003) Idiopathic pulmonary fibrosis: a composite physiologic index derived from disease extent observed by computed tomography. *American Journal of Respiratory and Critical Care Medicine*, 167, pp. 962-969.

257. Wells, AU. and Hirani, N. (2008) Interstitial lung disease guidelines: The British Thoracic Society in collaboration with the Thoracic Society of Australia and New Zealand and the Irish Thoracic Society. *Thorax*, 63, pp. v1-v58.

258. Wells, AU. Behr, J. Costabel, U. Cottin, V. Poletti, V. (2012) Triple therapy in idiopathic pulmonary fibrosis: an alarming press release. *European Respiratory Journal*, 39, pp. 805-806.

259. White, GE. Cotterill, A. Adley, MR. Soilleux, GJ. Greaves, DR. (2011) Suppressor of cytokine signaling SOCS3 expression is increased at sites of acute and chronic inflammation. *Journal of Molecular Histology*, 42 (2), pp. 137-157.

260. Williamson, R. (1970) Properties of rapidly labeled deoxyribonucleic acid fragments isolated from the cytoplasm of primary cultures of embryonic mouse liver cells. *Journal of Molecular Biology*, 51 (1), pp. 157-168.

261. Willis, BC. and Borok, Z. (2007) TGF-β induced EMT: mechanisms and implications for fibrotic lung disease. *American Journal of Physiology Lung Cellular and Molecular Physiology,* 10, pp. 1152.

262. Willis, BL. Liebler, JM. Luby-Phelps, K. Nicholson, AG. Crandall, ED. du Bois, RM. Borok, Z. (2005) Induction of epithelial-mesenchymal transition in alveolar epithelium cells by transforming growth factor-beta 1: potential role in idiopathic pulmonary fibrosis. *American Journal of Pathology*, 166, pp. 1321-1332.

263. Winterbauer, RH. Hammar, SP. Hallman, KO. Hays, JE. Pardee, NE. Morgan, EH. Allen, JD. Moores, KD. Bush, W.Walker, JH. (1978) Diffuse interstitial pneumonitis: Clinicopathologic correlations in 20 patients treated with prednisone/azathioprine. *The American Journal of Medicine*, 65 (4), pp. 661-672.

264. Wong, H. and Riabowol, K. (1996) Differential CDK-inhibitor gene expression in aging human diploid fibroblasts. *Experimental Gerontology*, 31, pp. 311-325.

265. Wootton, SC. Kim, DS. Kondoh, Y. Chen, E. Lee, JS. Song, JW. Huh, JW. Taniguchi, H. Chiu, C. Boushey, H. Lancaster, LH. Wolters, PJ. DeRisi, J. Ganem, D. Collard, HR. (2011). Viral infection in acute exacerbations of idiopathic pulmonary fibrosis. *American Journal of Respiratory and Critical Care Medicine*, 183 (12), pp. 1698-1702.

266. www.legislation.hmso.gov.uk/acts/acts2004/20040030.htm (accessed June 2005).

267. Yamada, M. Kuwano, K. Maeyama, T. (2008) Dual-immunohistochemistry provides little evidence for epithelial-mesenchymal transition in pulmonary fibrosis. *Histochemistry Cell Biology*, 129, pp. 453-462.

268. Yang, A. McKeon, F. (2000) p63 and p73: p53 mimics, menaces and more. *Nature Review Molecular Cell Biology*, 1 (3), pp. 199-207.

269. Yemelyanova, A. Vang, R. Kshirsagar, M. Lu, D. Marks, MA. Shih, IeM. Kurman, RJ. (2011) Immunohistochemical staining patterns of p53 can serve as a surrogate marker for TP53 mutations in ovarian carcinoma: an immunohistochemical and nucleotide sequencing analysis. *Modern Pathology*, 24 (9), pp. 1248-1253.

270. Zanelli, R. Barbic, F. Migliori, M. Michetti, G. (1994) Uncommon evolution of fibrosing alveolitis in a hard metal grinder exposed to cobalt dusts. *Science of the Total Environment*, 150, pp. 225-229.

271. Zeisberg, EM. Potenta, S. Xie, L. Zeisberg, M. Kalluri, R. (2007) Discovery of endothelial to mesenchymal transition as a source for carcinoma associated fibroblasts. *Cancer Research*, 67, pp. 10123-10128.

272. Zeisberg, Em. Tarnavski, D. Zeisberd. M. Dorfman, AL. McMullen, JR. Gustafsson, E. Chandraker, A. Yuan, X. Pu, WT. Roberts, AB. Neilson, AG. Sayegh, MH. Izumo, S. Kalluri, R. (2007) Endothelial-to-mesenchymal transition contributes to cardiac fibrosis. *Nature Medicine*, 13, pp. 952-961.

273. Zeisberg, M. Yang, C. Martino, M. Duncan, MB. Rieder, F. Tanjore, H. Kalluri, R. (2007) Fibroblasts derive from hepatocytes in liver fibrosis via epithelial to mesenchymal transition. *Journal of Biological Chemistry*, 282, pp. 23337-23347.

274. Zerp, SF. Stoter, R. Kuipers, G. Yang, D. Lippmasn, ME. Blitterswjik, WJ. Bartelink, H. Rooswinkel, R. Lafleur, V. Verheij. (2009) AT-101, a small molecule inhibitor of anti-apoptotic Bcl-2 family members, activates the SAPK/JNK pathway and enhances radiation-induced apoptosis. *Radiation Oncology*, 4 (47)

275. Zhang, K. Rekhter, MD. Gorden, D. Phan, SH. (1994) Myofibroblasts and their role in lung collagen gene expression during pulmonary fibrosis: A combined immunohistochemical and *in situ* hybridization study. *American Journal of Pathology*, 145, pp. 114-125.

276. Zheng, H. Murai, Y. Hong, M. Nakanishi, Y. Nomoto, K. Masuda, S. Tsuneyama, K. Takano, Y. (2007) Jamestown Canyon virus detection in human tissue specimens. *Journal of Clinical Pathology*, 60, pp. 787-793.

277. Zhou, L. Lim, L. Costa, RH. Whitsett, JA. (1994) Thyroid transcription factor-1 hepatocyte nuclear fctor-3 beta, surfactant protein B, C and Clara cells secretory protein in developing mouse lung. *American Journal of Pathology*, 145, pp. 114-125.

Appendix

Appendix 1

2% acid alcohol

600ml industrial methylated spirits (Genta Medical, UK)

400ml distilled water

10mls acetic acid (VWR International, UK)

Appendix 2

Scotts alkaline tap water substitute

100g sodium bicarbonate (VWR International, UK)

1 crystal of thymol (VWR International, UK)

5 litres distilled water

Appendix 3

Eosin working solution

100g calcium formate (VWR International, UK)

300mls 1% eosin (VWR International, UK)

700mls distilled water

Appendix 4

Protocols for target markers in routine use at the University Hospital of North Staffordshire. Developed by Miss Deborah Latham, Lead Biomedical Scientist, Immunohistochemistry.

Antibody; E-cadherin (Vector Labs, UK), clone 36B5, product code VP-E601

Control; membrane staining of breast endothelial cells

Antigen retrieval	Microwave in citrate buffer pH6 for 10 minutes at 100% power, 10 minutes at 70% power, cool solution and slides for 20 minutes.
Dilution	1:50
Incubation time and temperature	60 minutes at room temperature

Antibody; α-SMA (Dako, Denmark), clone 1A4, product code M0851.

Control; Smooth muscle cells of normal colon tissue.

Antigen retrieval	Microwave in citrate buffer pH6 10 minutes at 100% power, 10 at minutes 70% power, cool solution and slides for 20 minutes.
Dilution	1:800
Incubation time and temperature	30 minutes at room temperature

Antibody; Ki-67 (Dako, Denmark), clone MIB-1, product code M7240.

Control; Lung cancer tissue. Nuclear expression of proliferating tumour cells.

Antigen retrieval	Microwave in citrate buffer pH6 10 for minutes at 100% power, 10 minutes at 70% power, cool for 20 minutes.
Dilution	1:50
Incubation time and temperature	30 minutes at room temperature

Antibody; Epstein Barr Virus (EBV) (Vector labs, UK), clone CS1, CS2, CS3 and CS4, product code VP-E609.

Control; Hodgkin's disease affected lymph node. Cytoplasmic expression of Reed Sternberg cells.

Antigen retrieval	Trypsin enzymatic digestion at 37^{o}C for 10 minutes
Dilution	1:40
Incubation time and temperature	60 minutes at room temperature

Antibody; Anti-Cytomegalovirus (Dako, Denmark), clones CCH2 and DDG9, product code M0854.

Control; Kidney with CMV expression. Nuclear expression in CMV infected cells.

Antigen retrieval	Trypsin enzymatic digestion at 37^{o}C for 40 minutes
Dilution	1:25
Incubation time and temperature	30 minutes at room temperature

Appendix 5

Citrate buffer pH6

42g citric acid (VWR International, UK)

20 litres distilled water

260mls 2M sodium hydroxide (VWR International, UK)

Appendix 6

EDTA (1mM disodium salt) pH8

10 litres distilled water

3.76g EDTA (VWR International, UK)

17mls 0.5M sodium hydroxide (VWR International, UK)

Appendix 7

DAB enhancing solution

16g sodium chloride (VWR International, UK)

2 litres distilled water

10g copper sulphate (VWR International, UK)

Appendix 8

TRIS buffered saline TBS pH7.6

162g sodium chloride (VWR International, UK)

12g TRIS (VWR International, UK)

20 litres distilled water

70mls 1M hydrochloric acid (VWR International, UK)